

UNCLASSIFIED

AD NUMBER

ADB029256

LIMITATION CHANGES

TO:

Approved for public release; distribution is unlimited.

FROM:

Distribution authorized to U.S. Gov't. agencies only; Proprietary Information; FEB 1978. Other requests shall be referred to Air Force Materials Lab., Wright-Patterson AFB, OH 45433.

AUTHORITY

AFML ltr 27 Feb 1987

THIS PAGE IS UNCLASSIFIED

AD 30 29256

AUTHORITY:

SERIAL / Inst etc.

27 Feb 27



1 OF 3
ADB
0292561



AD 110.
DDC FILE COPY AD B029256

AFML-TR-78-13

LEVEL

2

**RESEARCH TO CONDUCT AN EXPLORATORY
EXPERIMENTAL AND ANALYTICAL INVESTIGATION
OF ALLOYS**

*GOVERNMENT PRODUCTS DIVISION
PRATT & WHITNEY AIRCRAFT
WEST PALM BEACH, FLORIDA*

MARCH 1978

TECHNICAL REPORT AFML-TR-78-18
For Period February 1975 - April 1977



Distribution limited to U. S. Government agencies only. Proprietary information; 9 February 1978. Other requests for this document must be referred to AFML/LLM, Wright-Patterson Air Force Base, Ohio 45433.

AIR FORCE MATERIALS LABORATORY
AIR FORCE WRIGHT AERONAUTICAL LABORATORIES
AIR FORCE SYSTEMS COMMAND
WRIGHT-PATTERSON AIR FORCE BASE, OHIO 45433


78 08 10 02 5

NOTICE

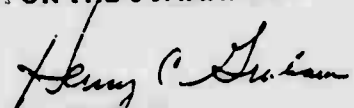
When Government drawings, specifications, or other data are used for any purpose other than in connection with a definitely related Government procurement operation, the United States Government thereby incurs no responsibility nor any obligation whatsoever; and the fact that the government may have formulated, furnished, or in any way supplied the said drawings, specifications, or other data is not to be regarded by implication or otherwise as in any manner licensing the holder or any other person or corporation, or conveying any rights or permission to manufacture, use, or sell any patented invention that may in any way be related thereto.

Distribution limited to U.S. Government agencies only. Proprietary information; 9 February 1978
Other requests for this document must be referred to AFML/LLM, Wright-Patterson Air Force Base, Ohio 45433.

This technical report has been reviewed and is approved.


HARRY A. LIPSITT
Project Engineer
High Temperature Materials Group

FOR THE COMMANDER


HENRY C. GRAHAM
Acting Chief, Processing and
High Temperature Materials Branch
Metals and Ceramics Division
Air Force Materials Laboratory

"If your address has changed, if you wish to be removed from our mailing list, or if the addressee is no longer employed by your organization please notify AFML/LLM, W-P AFB, OH 45433 to help us maintain a current mailing list".

Copies of this report should not be returned unless return is required by security considerations, contractual obligations, or notice on a specific document.

AIR FORCE/56780/6 July 1978 - 200

REPRODUCTION QUALITY NOTICE

This document is the best quality available. The copy furnished to DTIC contained pages that may have the following quality problems:

- **Pages smaller or larger than normal.**
- **Pages with background color or light colored printing.**
- **Pages with small type or poor printing; and or**
- **Pages with continuous tone material or color photographs.**

Due to various output media available these conditions may or may not cause poor legibility in the microfiche or hardcopy output you receive.

☐ **If this block is checked, the copy furnished to DTIC contained pages with color printing, that when reproduced in Black and White, may change detail of the original copy.**

Unclassified
SECURITY CLASSIFICATION OF THIS PAGE (When Data Entered)

REPORT DOCUMENTATION PAGE		READ INSTRUCTIONS BEFORE COMPLETING FORM
1. REPORT NUMBER AFML-TR-78-181	2. GOVT ACCESSION	RECIPIENT'S CATALOG NUMBER
4. TITLE (and Subtitle) RESEARCH TO CONDUCT AN EXPLORATORY EXPERIMENTAL AND ANALYTICAL INVESTIGATION OF ALLOYS.		5. TYPE OF REPORT & PERIOD COVERED February 1975-June 1977, Interim Report
7. AUTHOR(s) M. J. Blackburn, D. L. Ruckle and C. E. Bevan		6. PERFORMING ORG. REPORT NUMBER
9. PERFORMING ORGANIZATION NAME AND ADDRESS United Technologies Corporation Pratt & Whitney Aircraft Group Government Products Division West Palm Beach, Florida 33402		8. CONTRACT OR GRANT NUMBER(s) F33615-75-C-1167
11. CONTROLLING OFFICE NAME AND ADDRESS Air Force Materials Laboratory/LLM Air Force Systems Command Wright-Patterson Air Force Base, Ohio 45433		10. PROGRAM ELEMENT PROJECT, TASK AREA & WORK UNIT NUMBERS 7021-01-68
14. MONITORING AGENCY NAME & ADDRESS (if different from Controlling Office)		12. REPORT DATE March, 1978
		13. NUMBER OF PAGES 201
		15. SECURITY CLASS. (of this report) Unclassified
		15a. DECLASSIFICATION DOWNGRADING SCHEDULE
16. DISTRIBUTION STATEMENT (of this Report) Distribution limited to U.S. Government agencies only. Proprietary information; 9 February 1978. Other requests for this document must be referred to AFML/LLM, WPAFB, OH 45433.		
17. DISTRIBUTION STATEMENT (of the abstract entered in Block 20, if different from Report)		
18. SUPPLEMENTARY NOTES		
19. KEY WORDS (Continue on reverse side if necessary and identify by block number) Titanium Aluminides, Alloy Development, Mechanical Properties, Powder Metallurgy, Forging, Joining, Machining		
20. ABSTRACT (Continue on reverse side if necessary and identify by block number) A new class of alloys based on intermetallic compounds in the titanium aluminum system has shown the potential for application in the tempera- ture range of 1000-1500°F. This program was undertaken to investigate alloys of this type based on the compound Ti ₃ Al (alpha two). The pro- gram has been divided into three parts, Alloys Development, Alloy Characterization and Processing Methods. The objective of the Alloy		

DD FORM 1473 EDITION OF 1 NOV 65 IS OBSOLETE

SECURITY CLASSIFICATION OF THIS PAGE (When Data Entered)

372 117 78 08 10 02 5

Unclassified

SECURITY CLASSIFICATION OF THIS PAGE (When Data Entered)

Development program was to identify alloys which exhibited ductility at low and intermediate temperatures. A large number of alloys have been prepared and examined, and as a result of this screening program, alloys meeting the ductility requirements have been identified in the Ti-Al-Nb system. It has been found that the elevated temperature properties of these alloys are somewhat lower than anticipated and methods of eliminating this problem through the use of alloying additions such as silicon are described. The importance of heat treatment and structure on mechanical properties is documented and the most effective treatments identified. Powder metallurgy preforms and castings have been used to prepare larger isothermally forged sections of selected alloys. Material from these forgings was used to generate tensile, creep, stress rupture and fatigue properties over a range of temperatures. In addition, physical properties were determined on one alloy. The results of these tests are presented and are considered sufficiently promising to warrant considerations of these alloys for use in gas turbine engine components. Manufacturing and processing procedures that have been studied include casting, forging, welding, diffusion bonding, brazing and machining. The results indicate that for the new alloy compositions many of the practices currently used for conventional titanium alloys are applicable to the aluminides.

SECURITY CLASSIFICATION OF THIS PAGE (When Data Entered)

LEVEL

2

FOREWORD

This interim report covers work performed on Contract F33615-75-C-1167, Project No. 7021-01-68, in the period February, 1975 to April, 1977.

The investigation was conducted by the Commercial Products Division, Pratt & Whitney Aircraft, East Hartford, Connecticut, under the technical direction of Dr. H. A. Lipsitt, AFML/LLM, Wright-Patterson Air Force Base, Ohio.

Mr. D. L. Ruckle was program manager for the first year and Dr. M. J. Blackburn for the second year of the program. Mr. S. Z. Hayden and Mr. C. E. Bevan were the responsible engineers. The experimental assistance of Mr. D. Haase is gratefully acknowledged.

X	
BY _____	
DATE _____	
BY _____	
DATE _____	
B	

TABLE OF CONTENTS

SECTION	PAGE
I. INTRODUCTION	1
II. ALLOY DEVELOPMENT	5
1. Introduction	5
2. Program Goals	6
3. Background	7
4. Alloy Formulation	14
5. Experimental Methods	17
6. Results and Discussion	22
A. Forging	34
B. Bend Test Results	39
C. Heat Treatment and Structure	56
7. Mechanical Properties	64
A. Hardness	64
B. Tensile Testing	64
C. Creep Rupture	67
8. Summary and Conclusions	71
III. ALLOY SCALE-UP AND CHARACTERIZATION	75
1. Introduction	75
2. Experimental Techniques and Results - <u>First Year Program</u>	76
A. Material Procurement and Consolidation	76
B. Forging	85
C. Screening Program	85
D. Test Program	93
1) Tensile Testing	98
2) Charpy Impact	100
3) Creep Rupture	106
4) High Cycle Fatigue (HCF)	111
5) Strain Controlled Low Cycle Fatigue (LCF)	114

TABLE OF CONTENTS (Cont'd)

SECTION	PAGE
6) Notched (K_t 2.0) Low Cycle Fatigue	121
7) Crack Growth Rate Testing	126
8) Physical Properties	126
9) Thermal Fatigue	131
<u>Second Year Program</u>	131
A. Characterization of Ti-13.5Al-21.5Nb Alloy	134
B. Additional Heat Treatment Studies	145
3. Discussion	148
IV. MANUFACTURING FEASIBILITY STUDIES	152
1. Introduction	152
2. Joining Studies	157
A. Brazing	157
B. Diffusion Bonding	166
C. Weldment Evaluation	170
D. Forging Studies	173
E. Machining Studies	180
F. Casting Studies	194
3. Summary and Conclusions	197
V. REFERENCES	200

LIST OF ILLUSTRATIONS

FIGURE NUMBER		PAGE
1	Ternary Schematics	8
2	Periods III-VB Transition Elements Showing Crystal Structure of AB_3 Compound Formation with Group IIIA Elements	18
3	Tensile and Creep Rupture Specimens	20
4	Alloy Development	21
5	Photomicrographs of Hardness Impressions in Ti_3Al Base Alloys	29
6	An Example of a Distorted Hardness Impression Observed in Some Alpha Two Base Alloys (Ti-25Al-5Nb-2.5Sn- 0.25Si, As-Cast)	30
7	Coarse Acicular (Colony) Structure Found in Alpha Two Alloys With Low Solute Contents in the As-Cast Condition (Ti-25Al-1Fe)	30
8	The Fine Acicular (Widmanstätten) Structures Observed in Alpha Two Alloys with an Intermediate Concentration of Transition Elements in the As-Cast Condition (Ti-26.4Al-4.8Nb-0.8Fe)	31
9	The Coarsened Acicular Structure in the Alloy Ti-24Al-11Nb After Homo- genization at 1830°F for 96 Hours	31
10	The Equiaxed Alpha Two Structure Formed in the Ti-28Al-5Nb Alloy After Homogenization at 1830°F for 96 Hours	32
11	Oxide Particles (Scandia) Formed in the Ti-25Al-18.3Zr-1Sc Alloy (As-Cast)	35
12	Bend Ductility as a Function of Temperature in Ti-Al-Nb Alloys	55
13	Schematic Phase Section Along the Composition Line $(TiNb)_3Al$	57

LIST OF ILLUSTRATIONS (Cont'd)

FIGURE NUMBER		PAGE
14	"Recrystallization" Reaction Produced by Tempering Some Martensitic Struc- tures in Alpha Two Alloys	59
15	The Influence of Alpha-Beta Working on Alpha Two Alloy Structure	61
16	The Influence of Cooling Rate from the Beta Phase Field on Structure of Alpha Two Alloys	62
17	Transmission Electron Micrograph Illustrating the Heavily Faulted DO ₁₉ :L1 ₂ Phase Mixture Observed in Alloy Ti-12.5Al-37.5Zr-12.5In, (Ti ₃ Al) _{0.5} (Zr ₃ In) _{0.5}	63
18	Structure:Heat Treatment Effect on Ti-24Al-11Nb	68
19	Schematic Presentation of Creep Resistance and RT Tensile Ductility in the Ti-Al-Nb System	72
20	Process Selection	77
21	Property Characterization	78
22	Photograph Showing Titanium Hot Isostatic Press (HIP) Container After Can Filling and Sealing - Note "Dished" End Cover	81
23	Photograph Showing HIP Container After Hot Isostatic Press at 2250°F/3 Hours/15 ksi	83
24	Microstructure of Material Exposed at 2250°F/4 Hours Thermally Induced Porosity Test	84
25	Effect of Solution Treatment Temperature on Microstructure of Ti-16Al-10Nb W/O After HIP at 2250°F/3 Hours/15 ksi - Etchant: Kroll's Etch	86
26	Isothermal Forgings Produced for Screening Evaluation	87

LIST OF ILLUSTRATIONS (Cont'd)

FIGURE NUMBER		PAGE
27	Effect of Solution Treatment Temperature and Cooling Rate on Microstructure of Ti-16Al-10Nb W/O After HIP and Beta Forging - Etchant: Kroll's Etch	91
28	Microstructure of Ti-16Al-10Nb Alloy, Beta Forged + 2200°F/1 Hour/OQ + 1200°F/87 Hours/AC Showing Instability of Quenched Martensitic Phase	92
29	Microstructure of Ti-16Al-10Nb Alloy, Beta Forged + 2200°F/1 Hour/OQ + 1500°F/87 Hours/AC Showing Instability of Quenched Martensitic Phase	93
30	Pancake Forging Configuration Produced for Ti-16Al-10Nb Alloy Characterization	96
31	As-Forged Microstructure of Ti-16Al-10Nb Pancake Forging	97
32	Microstructure of Ti-16Al-10Nb Pancakes Heat Treated at 2200°F/1 Hour/Rapid Air Cool + 1600°F/8 Hours/Air Cool	99
33	Yield Strength, Ultimate Strength, Elongation for Ti-16Al-10Nb W/O	102
34	Charpy Impact Toughness vs. Temperature for Ti-16Al-10Nb	105
35	Larson-Miller Plot of Creep Rupture Data	108
36	Longitudinal Cross Sections of Ti-16Al-10Nb W/O Creep Specimens Showing Alpha Case on Specimen Surface	110
37	Longitudinal Cross Sections of Ti-16Al-10Nb W/O Creep Specimens Showing Alpha Case on Specimen Surface	112
38	Westinghouse HCF Data for Ti-16Al-10Nb W/O	115
39	Strain Controlled Low Cycle Fatigue Specimens	116

LIST OF ILLUSTRATIONS (Cont'd)

FIGURE NUMBER		PAGE
40	Longitudinal Strain Range vs. Cycles to Failure for Ti-16Al-10Nb (Strain Controlled)	118
41	Load Range vs. Cycle Number for Ti-16Al-10Nb - Test Temperature: 800°F	119
42	Load Range vs. Cycle Number for Ti-16Al-10Nb Strain Controlled LCF - Test Temperature: 1200°F	120
43	(a) Typical Low Cycle Fatigue Fracture of Ti-16Al-10Nb (b) Fatigue Striations Observed on Ti-16Al-10Nb Low Cycle Fatigue Fracture	122
44	Stress vs. Cycles to Failure for Ti-16Al-10Nb - K_t 2.0 Load Controlled LCF	124
45	(a) Fracture Surface of Ti-16Al-10Nb Low Cycle Fatigue Specimen (b) Longitudinal Cross Section Showing Microstructure in Notch with Recrystallized Grains Adjacent to Specimen Surface	125
46	Center Notched Panel for Fatigue Crack Growth Measurement	127
47	Crack Growth Rate for Ti-16Al-10Nb	128
48	Comparison of the Thermal Expansion of Titanium Aluminides and Conventional Materials	132
49	Pancake Forging Configuration Produced for the 20-Pound Nominal Ti-13.5Al-21.5Nb Alloy	138
50	Microstructure of the 20-Pound Nominal Ti-13.5Al-21.5Nb Alloy	140
51	0.2% Offset Yield Strength, Ultimate Tensile Strength and % Elongation vs. Temperature for the Nominal Ti-13.5Al-21.5Nb 20-Pound Ingot in the 2200°F (1200°C)/1 Hour/AC Condition	142

LIST OF ILLUSTRATIONS (Cont'd)

FIGURE NUMBER		PAGE
52	S-N Curve for Ti-13.5Al-21.5Nb at 800°F	147
53	Ti-16Al-10Nb Process Developments	153
54	(a) Au-Ni Brazed Ti-16Al-10Nb W/O Joint Showing Wetting and Erosion of Base Metal (b) Micrograph of Joint Showing Phases Formed During Braze Note Porosity and Oxides in Joint	161
55	Results of Ti-16Al-10Nb W/O Brazing Trials	163
56	Results of Ti-16Al-10Nb W/O Brazing Trials	164
57	(a) Ti-18Cu-10Ni Brazed Ti-16Al-10Nb (b) Ti-47Cr-5Be-6Al Brazed Ti-16Al- 10Nb Note Both Brazed Trials Conducted at 1750°F	165
58	Longitudinal Cross Section of Diffusion Bonded Ti-16Al-10Nb W/O Specimens - Note Bond Line in (a) and Recrystal- lized Layer of Grains in (b) at Prior Bond Line	170
59	Results of Ti-16Al-10Nb Welding Trials	172
60	Ti-16Al-10Nb W/O Forging Trials (Left to Right) Top: 1900°F, 0.01 inch/inch/minute 1900°F, 0.05 inch/inch/minute Middle: 2000°F, 0.1 inch/inch/minute 2000°F, 0.5 inch/inch/minute Bottom: 2200°F, 0.1 inch/inch/minute 2200°F, 0.5 inch/inch/minute	177
61	Flow Stress as a Function of Percent Reduction for Subscale Isothermal Forgings Produced from Ti-16Al-10Nb W/O Ingot	179

LIST OF ILLUSTRATIONS (Cont'd)

FIGURE NUMBER		PAGE
62	Smooth High Cycle Fatigue Specimen Used in Machining Studies Program (MDL 2329)	183
63	Effect of Peening on the Surface Condition and Microstructure of Ti-16Al-10Nb W/O - (a) 10N, (b) 15N, (c) 18N and (d) 33N	187
64	Effect of Elevated Temperature Exposure on the Microstructure of Peened Ti-16Al-10Nb W/O	188
65	Westinghouse HCF Data for Ti-16Al- 10Nb W/O	191
66	Surface Condition After Machining of Alloys	195
67	Results of Electron Beam Casting Experiments Left : Ti-6Al-4V - Baseline Trial Center: Ti-16Al-10Nb - Baseline Trial Right : Ti-16Al-10Nb - Increased Electron Beam Power Com- pared to Center	196
68	Surface Reaction of Alloy Ti-16Al- 10Nb with (a) Zirconia, (b) Alumina and (c) Graphite Mold Materials	198

LIST OF TABLES

TABLE NUMBER		PAGE
1	List of α_2 Alloy Compositions Melted	23
2	Microstructural, Hardness and Qualitative Evaluation of α_2 Alloy	25
3	Isothermal Forging Results for α_2 Alloy Compositions	36
4	Forged Plus Heat Treatment Results for α_2 Alloy Compositions	40
5	Three Point Bend Test Results for α_2 Alloy Compositions	42
6	Tensile Results for α_2 Alloy Compositions	65
7	Creep Rupture Results for α_2 Alloy Compositions	69
8	Chemical Composition of Titanium Aluminide Alloy	79
9	Nuclear Metals Reported REP Titanium Aluminide Powder Size Distribution	80
10	Phase I, Task I Process Screening Mechanical Properties of Ti-16Al-10Nb	88
11	Isothermal Forging Results	95
12	Summary of Phase I, Task II - Characterization Property Testing	101
13	Tensile Properties for Ti-16Al-10Nb	103
14	Charpy Impact Toughness of Ti-16Al-10Nb	104
15	Creep Rupture Properties of Ti-16Al-10Nb	107
16	Notched Stress Rupture Properties for Ti-16Al-10Nb	109
17	Westinghouse High Cycle Fatigue Data for Ti-16Al-10Nb	113
18	Smooth Low Cycle Fatigue Properties of Ti-16Al-10Nb Strain Controlled	117

LIST OF TABLE (Cont'd)

TABLE NUMBER		PAGE
19	Notched Low Cycle Fatigue Properties of Ti-16Al-10Nb	123
20	Thermal and Electrical Resistivity of Ti-16Al-10Nb	129
21	Specific Heat of Ti-16Al-10Nb	129
22	Coefficient of Linear Thermal Expansion of Ti-16Al-10Nb	130
23	Thermal Fatigue Results for Ti-16Al- 10Nb	133
24	Chemical Composition of Titanium Aluminide Alloy TMCA Heat V5301, Ti-13.5Al-21.4Nb	135
25	Isothermal Forging Results	137
26	Tensile Results for the Nominal Ti-13.5Al-21.5Nb 20-Pound Ingot	141
27	Creep Results for the Nominal Ti-13.5Al-21.5Nb 20-Pound Ingot	144
28	High Cycle Fatigue Results for the Nominal Ti-13.5Al-21.5Nb 20-Pound Ingot	146
29	Parameters Used for the Titanium Aluminide Brazing Study	159
30	Parameters Used for the Titanium Aluminide Diffusion Bonding Study	168
31	Chemical Composition of Titanium Aluminide Alloy TMCA Heat V5123, Ti-16Al-10Nb	175
32	Parameters Used for the Titanium Aluminide Isothermal Forging Study	176
33	Tensile Results for the Titanium Aluminide Isothermal Forging Study	181
34	Parameters Used for the Titanium Aluminide Machining Study	184
35	Westinghouse Cycle Fatigue Data for Ti-16Al-10Nb	190

LIST OF TABLES (Cont'd)

TABLE
NUMBER

PAGE

36

Westinghouse High Cycle Fatigue Data
for Ti-16Al-10Nb

193

I. INTRODUCTION

High performance gas turbine engine designs inherently depend on high strength, lightweight materials. In the past, major advances in engine technology have been associated with the widespread applications of nickel and cobalt base superalloys and the conventional alpha-beta titanium alloys. Recently, intensive development programs have been directed toward the application of both metal and resin matrix composite materials in compressor structure. Significant programs are also being conducted to develop the basic materials and design technology necessary to apply ceramics to the highest temperature turbine blades and vanes. This latter effort is important in that it depends on changes in design philosophy and capability as a result of the brittle nature of ceramic materials, as well as advancement of material capability itself.

A third area of new materials technology has been identified with the potential to work profound changes in engine weight and performance. This is the development and application of intermetallic compounds or ordered alloys. In general, these materials exhibit properties which lie between conventional metallic alloys and ceramics in that they have limited ductility and attractive high temperature strength. Two such compounds of interest for high temperature use have been identified in the titanium-aluminum system, the Ti_3Al (α_2) phase and the $TiAl$ (γ) phase. The former titanium aluminide has been extensively studied in the USSR,^(1,2) and at least one Soviet alloy is reported to be based on Ti_3Al with a use temperature to 1500°F. Some preliminary work on the $TiAl$ type materials in the United States had indicated a potential use temperature up to 1800°F in a non-coated condition; internal work at Pratt & Whitney Aircraft in 1972-73 had verified the properties and potential of both of these ordered materials.

Based on this preliminary evaluation, design analysis and payoff studies were conducted which indicate significant weight savings in a wide range of engine applications, such as an advanced transport engine (ATE), an advanced tactical fighter engine (ATF), or an advanced supersonic transport engine (AST). Turbine rotor weight savings from 30 to 40% (3 to 5% of engine weight) could be achieved with widespread application of the titanium aluminides in rotating hardware, or engine weight savings of up to 16% by application of these materials in static structures such as vanes, cases and bearing supports.

Another major area of benefit in application of these materials relates to the growing problem of availability of strategic materials. The majority of current known reserves of the elements necessary for superalloys are controlled by foreign sources. Although the supply of nickel itself seems stable, U.S. reserves are projected to be less than 500,000 tons of the 45,000,000 world reserves. The supply of chromium, which is a critical requirement in conventional superalloys, depends heavily on sources such as the USSR and Turkey. Mainland China possesses the majority of the world supply of tungsten. The successful use of titanium aluminides would reduce United States dependence on superalloy constituent elements, and would potentially reduce high temperature material costs at the same time.

Current U.S. supply of titanium is largely dependent on Australia and Canada; however, of the estimated world titanium reserves of 123,000,000 tons, over 33,000,000 tons exist within the U.S., and 30,000,000 tons within Canada. The majority of the United States supply of titanium occurs as ilmenite (FeTiO_3), and though it is slightly more expensive to process than rutile (TiO_2), it represents an enormous

domestic reserve of this critical metal.

Thus it was clear that the technical advantages of applying aluminide alloys coupled with the material conservation considerations fully justified a program. A necessary requirement before initiating such a program was a clear definition of anticipated problems coupled with a technical approach to overcome such problems.

The two major areas of concern were the lack of ductility at low temperatures and the processing characteristics of this class of alloys about which little was known. Improved ductility was deemed necessary not only from the standpoint of adequate performance of the materials under service conditions, but also to facilitate component assembly under shop conditions. The development of processing methods for aluminides was obviously necessary in order to produce components and to incorporate sections into a gas turbine engine. Various aspects of the approach, definition and performance of a program aimed at a solution to these problems are described in this report, which covers work on Contract F33615-C-75-1167. However, it should be emphasized that this effort is but one element of an integrated program being performed by the Air Force, through both internal and contractually sponsored work.

This interim summary covers work performed on Ti_3Al or α_2 type alloys from February, 1975 to April, 1977. The effort can be divided into three parts:

- Alloy Development
- Alloy Scale-Up and Characterization
- Processing and Manufacturing Methods

This report will cover each of these areas separately although some overlap exists. It should also be emphasized that work continues on the project; the results obtained in future work could modify some of the conclusions drawn in this report.

II. ALLOY DEVELOPMENT

1. Introduction

The first analyses of the titanium aluminum system showed a wide range of solid solution stability of pure alpha Ti up to the intermetallic phase TiAl (γ). The existence of an intervening phase or phases was recognized by the mid to late fifties and the next decade was spent in, often acrimonious, discussion of the structure, composition and stability field of these phases. (4, 5) It is generally agreed that only one phase occurs, with a composition based on Ti_3Al (often denoted alpha two, α_2). Controversy continues over the stability range of this phase and its structure although for all practical purposes a hexagonal superlattice with a DO_{19} structure is an accurate description. Several of the physical and mechanical properties of this Ti_3Al phase have been determined, although data are rather sparse for non-stoichiometric compositions. In general, the physical properties measurements indicate that bonding tends to be metallic in this alloy although evidence of some covalency has been obtained. The compound shows extensive plasticity at high temperatures, but little or no ductility is observed in tension at room temperature.

Thus, the most significant problem in the development of the titanium aluminide materials is the potential consequences of their limited low temperature ductility on other important design properties. Low ductility in itself is not normally directly related to component failure in conventional metallic components; however, it can function as a secondary cause of failure. For example, the low cycle fatigue behavior of materials is partially a function of ductility as well as microstructure, surface stress state, residual dislocation structure and other factors. In addition, foreign object damage capability of airfoils is also partially a function

of ductility, as well as factors such as fracture initiation energy and fracture toughness.

Ductility can be related to thermal fatigue life although other factors such as modulus of elasticity and thermal coefficient of expansion are also important. Ductility can also dramatically affect load transfer from areas with strong notch concentrations to adjacent areas. Such load transfer is particularly important in dovetail or fir tree turbine blade root design to avoid notched stress rupture failure. The general effects of low temperature ductility on component behavior must be considered in relation to specific component maximum load-temperature sequencing during an engine cycle. For example, it is rare for turbine engine components to achieve maximum load and minimum temperature at the same instant in time. The basic problem in evaluation of new materials is to develop sufficient specific property data under engine related temperature and load conditions to identify the full design capability, as well as to identify specific problem areas where material and design capability improvement is required. Definition of basic environmental effects such as oxidation rates can also be critical in material application; the oxidation testing being conducted by the Air Force is covering this area of characterization.

2. Program Goals

As the program has evolved, the property goals defined for aluminide alloys have both changed and broadened. Early in the program the two major alloy requirements were as follows:

- Ductility of 2-3% tensile elongation at 500°F--which corresponds approximately to the idle temperature in many turbine engines.

- Stress rupture capability equal to the nickel-base alloy INCO 713 (comparison to be made on a density-corrected basis).

3. Background

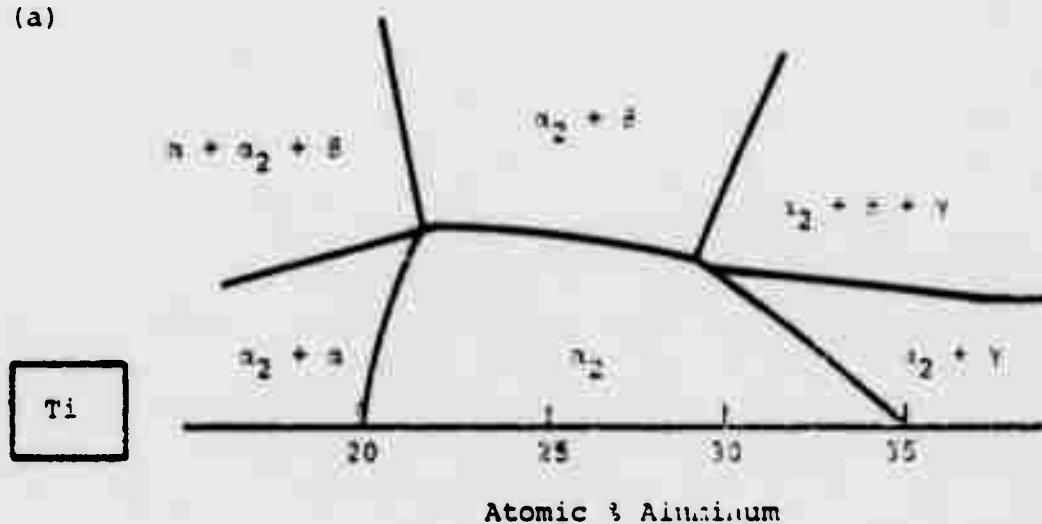
In designing the alloy development program several factors had to be considered, including the previous work performed on Ti_3Al type alloys. The following paragraphs cover aspects of the known characteristics of Ti_3Al at the outset of this program which were deemed useful in defining an approach to alloy development.

Alloying Behavior - In considering the basic alloying characteristics of Ti_3Al , both the extent of solubility and the nature of phase mixtures formed when the solubility is exceeded have to be considered. These features are shown schematically in the phase diagrams in Figures 1(a) and (b), which are constructed for intermediate temperatures (1200-1600°F)--the potential application temperature range for Ti_3Al type alloys. Examples of the bounding phases for the addition of a beta stabilizing element such as niobium are shown in Figure 1(a).

The direction and extent of the single phase (Ti_3Al) field modification is dictated by both the solubility of an element and the atomic site on which substitution occurs in the Ti_3Al lattice. Figure 1(b) illustrates the direction in which the phase field will move for the cases of elements that replace aluminum, titanium and both elements in the Ti_3Al lattice, respectively.

Elements that replace aluminum in Ti_3Al are found in groups IIIA to VA and these elements, coupled with the known solubilities (atomic %), are as follows:

(a)



(b)

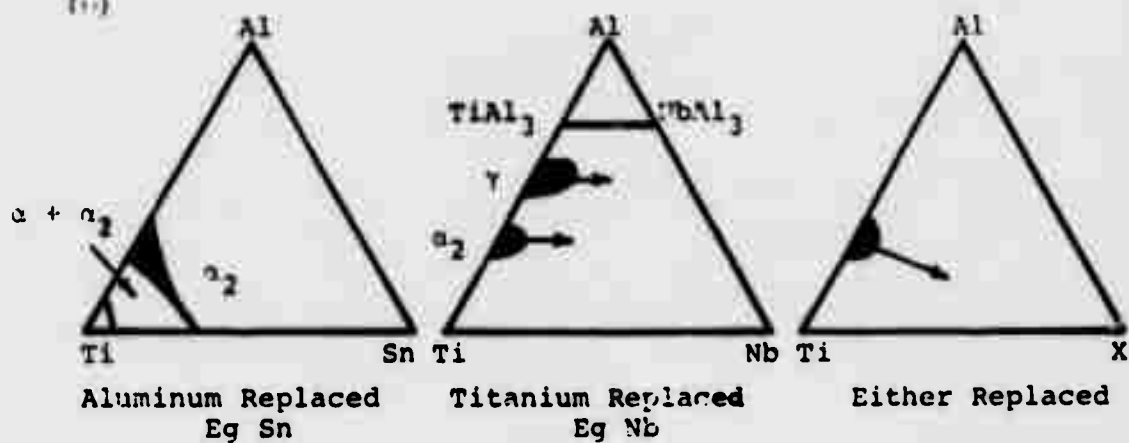


Figure 1. Ternary Schematics

Ga (50-100%)	Ge (>1%)	As (?)
In (High)	Sn (100%)	Sb (>1%)
Ti (?)	Pb (High)	Bi (>1%)

Elements known to replace titanium are found in the B subgroups of the periodic table as follows:

Sc (~5%)	Hf (>5%)	Mo (~1%) (Probably >1%)
Y (<1%)	V (>1%)	W (>1%)
La (?)	Nb (~6%)	Mn, Fe, Co, Ni, Cu (>1%)
Ti	Ta (>1%)	Ag (<1%)
Zr (50%)	Cr (<1%)	

Elements that are of finite solubility but do not fall into the above classification include:

Be (~8%) Carbon, Boron, Silicon, Oxygen and Nitrogen

Structural parameters that may be changed by the addition of solute elements within the single phase regions are the ordering kinetics and critical temperature, T_c . In stoichiometric Ti_3Al , it is impossible to suppress ordering by conventional quenching techniques although a very fine domain size is produced by water quenching. However, on annealing at intermediate temperature, e.g., 1475°F, rapid domain growth occurs and virtually complete elimination of anti-phase domain boundaries (APB's) occurs, resulting in a high degree of long range order.⁽⁵⁾ This is also true in alloys with quite wide deviations from stoichiometry. The influence of specific elements on ordering kinetics has not been studied in any detail. However, niobium additions certainly retard the ordering rate, and quite small domain sizes are retained after quite long aging treatments.⁽⁷⁾ Similar effects have been observed in some hafnium containing alloys.

The bounding phases that can occur when the solid solubility limit of a given element is exceeded will obviously be strongly dependent upon several factors, including composition and temperature. Figure 1(a) is a schematic of bounding phases for an element that replaces titanium, such as Nb, Mo, etc. An additional complication in these systems is the tendency of the β -phase to order to a B2 type structure. Elements from the later transition series, such as Fe, Ni, Co, etc., tend to form intermetallic phases of the form TiX or Ti_2X .

With the aluminum replacing elements, the situation tends to be relatively straightforward at substoichiometric compositions, in that solid solutions (α) and a two-phase region ($\alpha + \alpha_2$) will occur. However, in aluminum-rich alloys, complexities can arise with higher phases from the TiX system; for example, at the composition $Ti_3(Al_{0.5}Ga_{0.5})$, the phase Ti_2Ga is formed within an α_2 matrix.⁽⁸⁾ The number of other possible phases in many of these systems could further complicate potential phase equilibria in these regions of a ternary phase diagram.

Another possibility, which will be developed in more detail later, is to produce mixtures of $Ti_3Al + X_3Al$ phases in which the X_3Al has an ordered face centered cubic structure. This type of structure can occur in the Ti-Al-Zr system.

Structural Modifications - The above paragraphs detail the possible phase structures that could form at intermediate temperatures in systems based on Ti_3Al . At high temperatures the β -phase is stable in all dilute systems and in many more conventional alloys.

Cooling from the region of β -phase stability will result in transformation; in most of the systems of interest, rapid

cooling will lead to a martensitic structure and slower cooling to an acicular structure formed by nucleation and growth. The essential point is that morphologically similar structures to those in conventional titanium alloys can also be produced in these alpha two base systems.

Since we are dealing with a hexagonal structure, a second structural modification, controlled texture, may be possible in these alloys. Solid state processing methods would have to be employed to produce a specific texture, since the lack of suitable mold materials would appear to preclude controlled solidification methods. The advent of successful sheet processing methods could allow the analysis and perhaps exploitation of such effects.

Flow and Fracture - Considering the dearth of mechanical property data (at least in tension), the flow and fracture characteristics of Ti_3Al are reasonably well documented. It has been shown that, at least in compression, \bar{a} type dislocations are mobile at room temperature.⁽⁸⁾ Both basal and prism slip systems can be activated and there is a distinct tendency for rather sharp planar dislocation grouping to occur. The basic problem would therefore appear to be the operation of slip or possibly twinning systems capable of producing displacements normal to the c-axis of the hexagonal structure. One such possibility is the $\bar{c} + \bar{a}$ type dislocation which is apparently readily formed in the ductile alloys from the Ti-Al-Ga system. Apparently, fracture occurs at ambient temperatures by cleavage failure, on the same strange plane of separation observed in stress corrosion failures of conventional alpha-phase titanium alloys. The influence of microstructure and grain size has not been studied. The basic conclusions that can be drawn from the observations to date are that the low temperature brittleness of Ti_3Al seems to

be related to the absence of slip modes capable of producing displacements normal to the basal plane. Heat treatment and grain size control may be possible methods of controlling flow and fracture properties, but no clear-cut directions can be accurately defined at this point.

Lipsitt⁽⁹⁾ has measured the tensile properties of Ti_3Al , manufactured by powder metallurgy methods, over a range of temperatures. It was shown that finite ductility occurs above ~ 1200 F, although specimen yielding occurred below this temperature. This is the only information that quantitatively defines the ductility problem and allows an assessment to be made of ductility changes produced by alloying additions.

Ti-Al-Ga - Early measurements in this system by Hoch and Gegel⁽¹⁰⁾ showed that alloys near the composition $Ti_3(Al_{0.5}Ga_{0.5})$ had quite high tensile ductility at room temperature. Williams and Blackburn⁽⁸⁾ suggested that this occurred due to a particle ductilizing effect of the Ti_2Ga phase that occurs in this alloy. Godden and Roberts⁽¹¹⁾ confirmed that ductility occurs in this system (although over a narrow compositional range) and found that maximum ductility occurred in a single phase (α_2) alloy. The cost of gallium precludes its use in engineering materials, at least at high concentrations. Thus, one of the objectives of any alloy development program is to duplicate this ductilizing effect with more economic alloying additions.

Ti-Al-Nb - Both German⁽¹²⁾ and Russian⁽¹³⁾ work has shown that this system appears an attractive base on which to build an alloy development program. It has been shown that in specific alloy compositions over 4% elongation is observed below $1000^\circ F$.

Ti-Al-Mo - Weissmann and coworkers⁽¹⁴⁾ have recently evaluated alloys from the $\alpha + \alpha_2 + \beta$ phase field in this system. By carefully controlling the microstructure, ductilities of several percents have been obtained at room temperature. However, the specific heat treatments employed would seem incompatible with subsequent use of material at high temperatures; this emphasizes one of the difficulties inherent in this type of system--thermal stability.

Creep Properties - The exact composition of the Russian alloy ST5 is unknown, but assuming it is virtually pure Ti_3Al , a convenient baseline for comparison of creep properties is offered. It has been shown that the creep properties of the alpha two phase and its alloys are considerably better than those of conventional alloys. Alloys from the following systems have been shown to exhibit improved properties over the base compound:

Ti-Al-Nb

Ti-Al-Sn

Ti-Al-Hf

Ti-Al-W

Ti-Al-Mo

In summary, the alloying characteristics of alloys based on Ti_3Al are known in sufficient detail to identify both the elements that are soluble and the phase mixtures that bound the single-phase region. The effect of single component additions on properties, especially in tension, are less well documented; however, at least two systems are known that show some promise for room temperature ductility.

4. Alloy Formulation

Although some definition of useful alloy development directions could be derived from the above discussion, the large number of compositional effects available for study had to be restricted to a smaller number of specific directions. In addition, a methodology had to be established which allowed an assessment of the mechanical property capability of a large number of alloys. The following sections cover the selection and evaluation of alloys studied in the current program.

The alloys selected for evaluation fall into five general groups which are listed below, together with the reasons for choosing the systems.

- Single (substitutional) element additions - to provide some basic solubility and property data and identify useful ternary phase systems.
- Two (or more) substitutional element additions (one element Nb or Zr) - to investigate the potential of modifying properties by two substitutional element additions.
- Two element additions - one substitutional, one interstitial - to study the possibility of amplifying creep resistance by dynamic strain aging processes.
- Additions to produce two-phase structures of the $\alpha_2 + \beta$ type - to control the ordering reaction in the beta phase and then extend the study to modification of the α_2 component of the system.
- Additions to promote a two-phase mixture of ordered hexagonal (DO_{19}) and face centered cubic ($L1_2$) phases - it was hypothesized that in a two-phase mixture, a ductile component, $L1_2$ -phase, may produce some overall ductility in the whole system.

It is inevitable that some overlap between these areas occur. The first three areas may be combined as all relate to the single phase Ti_3Al region and will be discussed as a general group.

Single-Phase Alloys - The additions selected for study included both elements for which no previous information was available (e.g., W, Ta) and also additional studies on systems for which some results had been generated.

The studies of two (or more) additions were confined to systems in which some indication of property improvement for any given three elements had been shown. For example, the Ti-Al-Nb ternary system appeared a useful base upon which to build.

The third group of alloys examined the usefulness of interaction between interstitial and substitutional elements in a Ti_3Al solid solution. It was anticipated that by analogy with conventional titanium alloys containing silicon additions, a dynamic strain aging process may occur and thus improve creep and stress rupture characteristics. Previous exploratory work at P&WA had demonstrated some promise for Hf-C additions.

Alpha Two Plus Beta Systems - The basic problem with the use of the beta phase as a potential ductilizing phase in an $\alpha_2 + \beta$ type alloy is the tendency to ordering in this phase. The product phase, often denoted B2, has an ordered B2 lattice or possibly Heusler structure ($L2_1$). The formation tendency is accentuated by high aluminum content; in fact, it was first detected in Ti-Al-Mo alloys near the composition Ti_2AlMo .⁽¹⁵⁾ This ordering reaction tends to embrittle the beta phase and thus, it has to be eliminated or controlled if

practical use is to be made of the structure. There is the rather remote possibility that a phase similar in nature to NiTi could be produced. NiTi, although possessing the B2 structure, exhibits considerable plasticity at ambient temperatures.⁽¹⁶⁾ The first effort was aimed at controlling the ordering reaction in the beta phase and then attempting to modify the alpha two component of the system. The background for such an approach was rather sparse; it was known that the Ti-Al-Mo and Ti-Al-Nb systems exhibit ordered B2 beta phases. The influence of vanadium and chromium on structure was not as well documented, but Russian and early USA work had not shown much promise in these systems. Addition of the later transition elements, at least as single element additions, tends to produce $\alpha_2 + \beta$ + compound or α_2 + compound type structures; again, these alloys show little evidence of low temperature ductility, although in the case of iron, high temperature ductility is enhanced. The major effort in this segment of the work was on alloys from the Ti-Al-Nb system.

Ordered Hexagonal and (Face Centered) Cubic Mixtures - The basic philosophy behind the study of such a system is that in a two-phase mixture, a ductile component may yield some overall ductility to the whole system. It should be noted that compounds that have an ordered face centered cubic structure ($L1_2$ class), as a group include more examples of ductile intermetallics than any other class of intermetallics.

Specifically, Zr_3Al is the only intermetallic of Group IV element based compounds which exhibit >10% elongation at room temperature.⁽¹⁷⁾ Recent P&WA studies of the Ti-Al-Zr system have shown that, contrary to earlier Russian work, the mixed $L1_2:DO_{19}$ structure does not occur until the zirconium content is approximately 50%. This large concentration, coupled with the rather low beta-transus, would seem to

exclude this system from active consideration for the development of useful engineering materials. However, it may be possible to perturb the phase equilibria based on the crystal chemistry of the early transition elements, as outlined below. The essential aim would be to bring the mixed structure closer to the Ti_3Al composition.

If we examine the alloying behavior of the early transition elements with Group III and IVA elements, Figure 2 can be constructed for AB_3 compounds. It can be seen that four phase stability regions may be delineated, DO_{19} , $L1_2$, $A15$ and systems which do not form AB_3 compounds. Both yttrium and cerium aluminides exist in both the DO_{19} and $L1_2$ structural forms. These aid in positioning the boundaries. As usual, the only theoretical treatment that has been attempted for predicting the relative stability of the $L1_2$ and $A15$ structures does not work for these compounds. Macklin⁽³⁾ calculates that Zr_3Al should have an $A15$ structure and Nb_3Al should have an $L1_2$ structure, when in fact, the reverse is true.

The specific alloy systems studied in the present program were selected from the $Ti-Al-Zr$ system with addition of In , La , etc.

5. Experimental Methods

The basic problem in conducting any meaningful evaluation of alloys, such as those under consideration here, is to measure properties on a restricted amount of material. It is obvious that to melt large amounts of material, process and conduct a screening evaluation program for all alloy compositions was impossible within the confines of the program. Thus, the following sequence of stages was used in the alloy

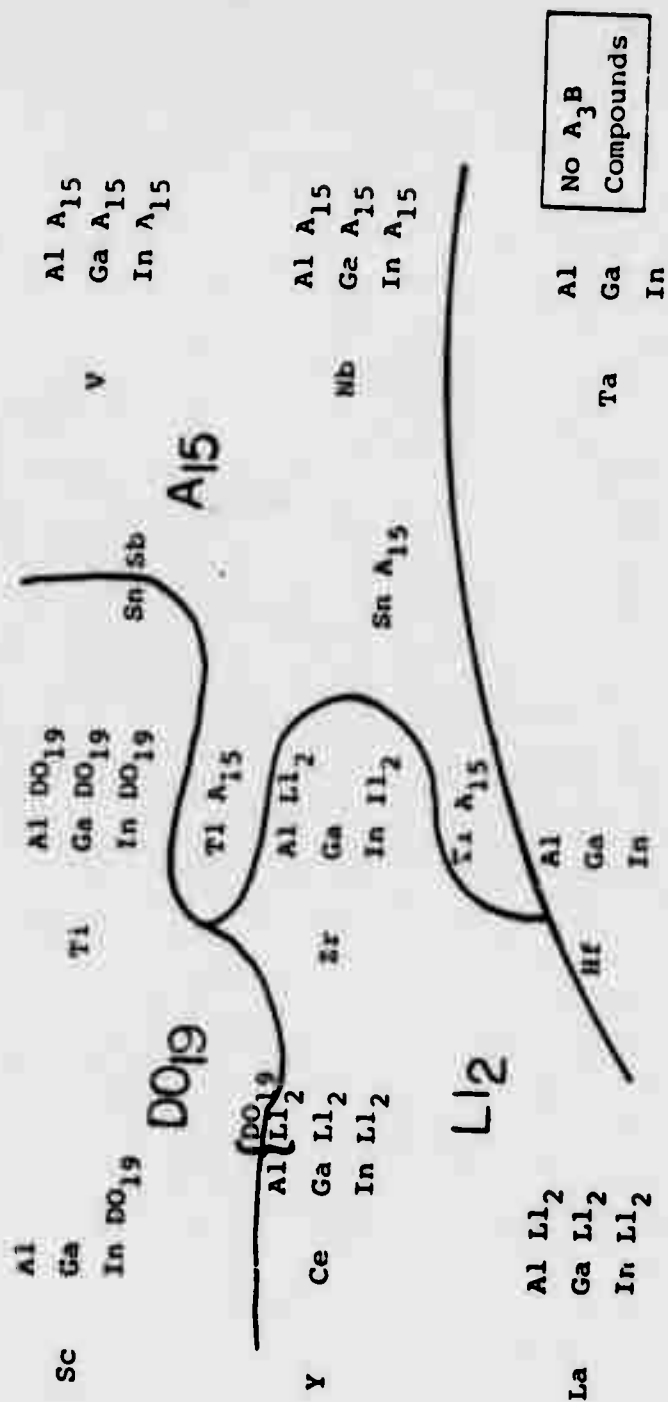


Figure 2. Periods III-VB Transition Elements Showing Crystal Structure of AB₃ Compound Formation With Group IIIA Elements

development program.

- 1) Formulate alloys.
- 2) Melt 100 gram buttons by a non-consumable arc method. High purity materials were used to prepare alloys; for example, electrolytic titanium with an oxygen content of 0.03%. Alloys were melted at least five times to ensure homogeneity.
- 3) Evaluate the structure of the cast alloys and measure hardness. As a check of the flow and fracture characteristics of the alloy, the hardness impressions in unetched sections were examined by optical microscopy. The tendency for the material to crack and the intensity of slip markings around the impressions were recorded.
- 4) Homogenize buttons by thermal treatments at 1800-2000°F for periods of up to one week. Changes in structure and hardness were evaluated after this treatment.
- 5) Isothermally forge buttons to produce thin pancakes. Investigate the structure and hardness produced by this operation.
- 6) Cut bend specimens from the forged section and measure strength and bend ductility over the temperature range of room temperature to 1200°F. A three point bend rig and an Instron Test machine were used for these tests.
- 7) Conduct heat treatment and structural studies on the remainder of the forging and evaluate bend ductility of material after selected heat treatments.

If, at the completion of this screening study, an alloy showed promise, it was scaled up to a two-pound size. Alloys were melted in a non-consumable arc furnace and drop cast into a copper mold approximately 1.5" in diameter. A number of these castings were x-rayed, which revealed the presence of shrinkage porosity. In most cases this porosity did not

influence subsequent forging operations, but a small number of defects were detected after forging (usually in locations in which little flow occurred). Thus, many of the latter ingots were HIP'ed at 2250°F for four hours at 15 ksi, which served to heal shrinkage porosity and also increased the alloy homogeneity. Forging of ingots was performed on isothermal T2M dies. Usually the ingot was split into two pieces which yielded pancakes four inches in diameter and three-tenths of an inch thick. This was a sufficient size to produce about four specimen blanks. As in many cases where more than one heat treatment was studied, these specimen blanks were heat treated individually. Specimens, shown in Figure 3, were then prepared from the heat treated sections and used to measure the tensile and creep rupture properties of the material. Remaining pieces of the forging blank were used for additional heat treatment and bend property determinations. The microstructure and hardness of every alloy was recorded at each stage of the cycle. In a small number of cases more sophisticated techniques, such as x-ray analysis, transmission electron microscopy, etc., were used to elucidate phase structure and flow and fracture processes.

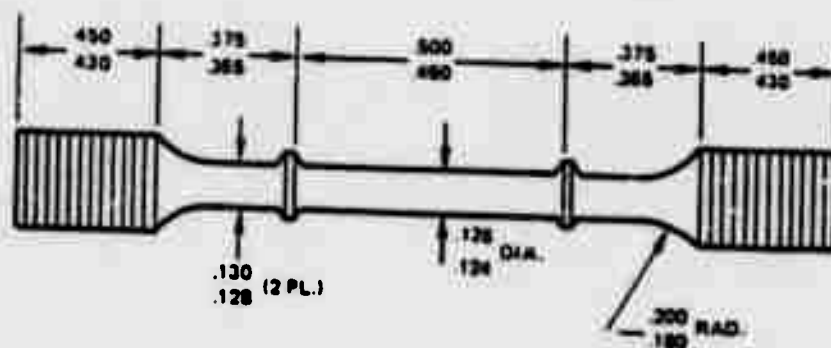


Figure 3. Tensile and Creep Rupture Specimen

A flow chart illustrating the sequence of evaluation steps is shown in Figure 4.

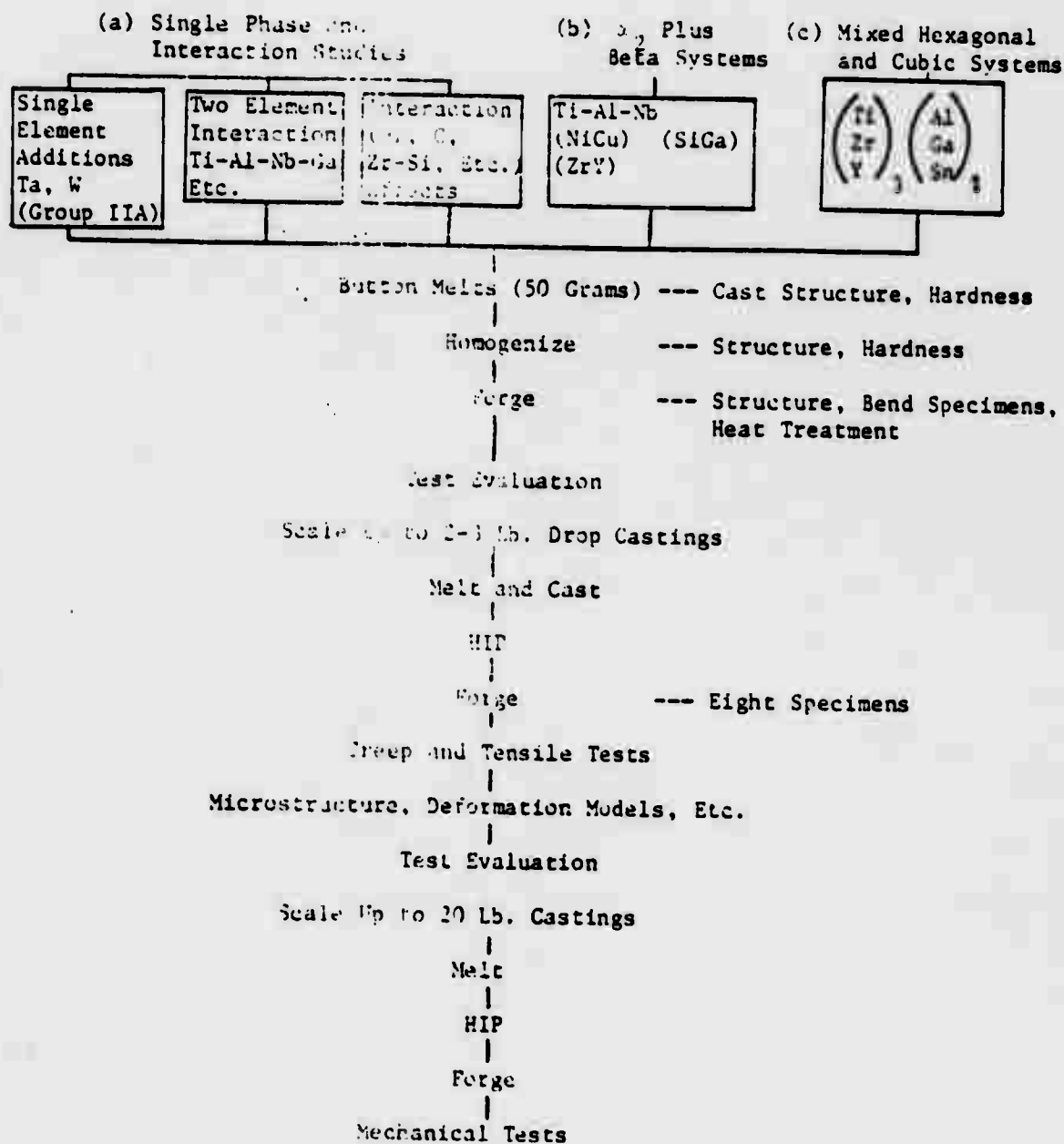


Figure 4. Alloy Development

6. Results and Discussion

In this section the rather extensive results obtained in the Alloy Development part of the program are reviewed. The large amount of information makes detailed discussion of each alloy impossible and thus we shall attempt to give a general summary with emphasis on the more positive aspects. Documentation of microstructures is also a problem as it would take about three thousand micrographs to illustrate all features of each alloy at the various stages of processing. Therefore, again, micrographs typical of groups of alloys or a specific processing or heat treatment will be given. It was noted in the introduction to this section that a logical scale-up sequence had been defined for studying alloys. To aid in the continuity of the story, we shall combine the results obtained on both button and the larger drop castings, for the initial evaluation sequence was the same for both product forms. In some cases alloys have been produced on both forms. Finally, it should be noted that emphasis has shifted several times during the course of the study. To give one example, in early 1976 it appeared that the Ti-Al-Zr system offered the best alloy base for further study, but by the end of the year the Ti-Al-Nb system had supplanted this system. Such factors explain why emphasis may have been placed on a specific alloy at a given point in time which, in retrospect, could be considered not worthy of analysis.

Table 1 lists all alloys melted in the study, compositions are given in both weight and atomic percent; in subsequent discussions, atomic percent will be used to describe alloys. The alloys are arranged in the groupings defined in Section 4, although in some cases overlap occurs. The results of the evaluation of alloys, in both the as-cast and homogenized conditions, are given in Table 2. Assessment of the propensity

TABLE 1

List of α_2 Alloy Compositions Melted

Alloy No.	W/O	A/O
- - -	Ti-15.7 Al	Ti-25Al
Ti-20	Ti-15.8 Al	Ti-25Al
Single Element Additions		
Ti-8	Ti-15.8Al-1.1Sc	Ti-25Al-1Sc
Ti-9	Ti-15.8Al-5.3Sc	Ti-25Al-5Sc
Ti-10	Ti-15.8Al-1.5Cu	Ti-25Al-1Cu
Ti-11	Ti-15.8Al-7.3Cu	Ti-25Al-5Cu
Ti-12	Ti-15.8Al-1.4Ni	Ti-25Al-1Ni
Ti-13	Ti-15.8Al-0.8Ni	Ti-25Al-5Ni
Ti-14	Ti-15.7Al-1.7Ge	Ti-25Al-1Ge
Ti-15	Ti-15.4Al-8.3Ge	Ti-25Al-5Ge
Ti-31	Ti-15.6Al-2.5Ag	Ti-25Al-1Ag
Ti-32	Ti-15.3Al-11.8Ag	Ti-25Al-5Ag
Ti-33	Ti-15.2Al-7.8Bi	Ti-25Al-1Bi
Ti-34	Ti-13.2Al-20.0Bi	Ti-25Al-5Bi
Ti-35	Ti-15.5Al-2.8Sb	Ti-25Al-1Sb
Ti-36	Ti-14.5Al-13.1Sb	Ti-25Al-5Sb
#28	Ti-15.8Al-1.3Fe	Ti-25Al-1Fe
#30	Ti-15.8Al-1.5Co	Ti-25Al-3Co
#35	Ti-15.3Al-1.2W	Ti-25Al-1W
#36	Ti-15.8Al-1.1Ta	Ti-25Al-1Ta
Ti-40	Ti-15.8Al-3.0Be	Ti-25.0Al-2.0Be
Ti-41	Ti-15.8Al-1.1Be	Ti-25.0Al-5.0Be
Ti-42	Ti-14.7Al-1.1Se	Ti-22.5Al-5.0Be
Ti-53	Ti-15.0Al-16.1Nb	Ti-25Al-8Nb
#50	Ti-15.1Al-14.3Zr	Ti-30Al-7Zr
#51	Ti-17.0Al-10.3Zr	Ti-30Al-14Zr
Two or more element additions		
Ti-4	Ti-15.8Al-1.2Nb-3.2Ga	Ti-25Al-2Nb-2Ga
Ti-3	Ti-14.7Al-10.1Nb-7.6Ga	Ti-25Al-5Nb-5Ga
Ti-5, (#34)	Ti-15.0Al-10.3Nb-1.3Ni	Ti-25Al-5Nb-1Ni
Ti-6	Ti-14.2Al-10.2Nb-2.3Pd	Ti-25Al-5Nb-1Pd
Ti-7, (#33)	Ti-15.0Al-10.3Nb-1.4Cu	Ti-25Al-5Nb-1Cu
Ti-16	Ti-8.2Al-12.0Sn-7.3Ge	Ti-15Al-5Sn-5Ge
Ti-25	Ti-14.5Al-1.7In-3.6Sn	Ti-23.75Al-3.75In-1.25Sn
Ti-28	Ti-12.6Al-14.4Nb-6.1Sn	Ti-22.5Al-7.5Nb-2.5Sn
Ti-37	Ti-14.6Al-10.1Nb-3.9HF	Ti-25Al-5Nb-1HF
Ti-38	Ti-14.6Al-10.0Nb-3.9W	Ti-25Al-5Nb-1W
Ti-39	Ti-17.9Al-10.3Nb-4.0W	Ti-30Al-5Nb-1W
Ti-46	Ti-14.6Al-10.2Nb-1.3Ni-2.1Mo	Ti-25Al-5Nb-1Ni-1Mo
#29	Ti-16.0Al-10.0Nb-1.0Fe	Ti-26.4Al-1.8Nb-0.8Fe
#33	Ti-15.0Al-10.3Nb-1.4Cu	Ti-25Al-5Nb-1Cu
#34	Ti-15.0Al-10.3Nb-1.3Ni	Ti-25Al-5Nb-1Ni
#43	Ti-14.6Al-10.0Nb-3.9HF	Ti-25Al-5Nb-1HF
Ti-54	Ti-14.2Al-15.6Nb-3.8W	Ti-25Al-8Nb-1W
Ti-55	Ti-14.4Al-15.9Nb-2.1Mo	Ti-25Al-8Nb-1Mo
Ti-56	Ti-14.2Al-15.6Nb-3.8Ta	Ti-25Al-8Nb-1Ta
Ti-57	Ti-14.2Al-15.6Nb-3.8HF	Ti-25Al-8Nb-1HF
Ti-58	Ti-14.6Al-16.0Nb-1.1V	Ti-25Al-8Nb-1V
#53	Ti-14.6Al-16.0Nb-1.2Fe	Ti-25Al-8Nb-1Fe
#54	Ti-15.0Al-16.0Nb-1.0Fe	Ti-25Al-8Nb-0.8Fe
#56	Ti-14.2Al-15.9Nb-3.8W	Ti-25Al-8Nb-1W
Ti-47	Ti-15.1Al-10.3Nb-1.3Ni-1.1V	Ti-25Al-5Nb-1Ni-1V
#45	Ti-14.1Al-10.0Nb-1.3Ni-4.0W	Ti-25Al-5Nb-1Ni-1W

TABLE 1 (Cont'd)

Alloy No.	W/O	A/O
#57	Ti-14.2Al-15.6Nb-3.8Ta	Ti-25Al-8Nb-1Ta
#58	Ti-14.2Al-15.6Nb-3.8Hf	Ti-25Al-8Nb-1Hf
#59	Ti-14.6Al-16.0Nb-1.1V	Ti-25Al-8Nb-1V
#55	Ti-14.5Al-10.0Nb-0.7Ni-0.0W	Ti-25Al-5Nb-0.5Ni-1W
Interaction Effects		
Ti-1	Ti-13.8Al-18.2Hf-.17C	Ti-28Al-5Hf-0.7C
Ti-30	Ti-12.0Al-34.4Zr-.1CB	Ti-23.1Al-18.7Zr-.46B
#31	Ti-15.0Al-18.0Nb	Ti-25.9Al-9Nb
#32	Ti-15.0Al-18.0Nb-1.5Hf-0.55Si	Ti-26Al-9.1Nb-0.4Hf-0.8Si
#46	Ti-13.8Al-9.5Nb-9.4Zr-6.1Sn-0.1Si	Ti-25Al-5Nb-5Zr-2.5Sn-0.25Si
Ti-50	Ti-13.5Al-21.4Nb-0.65Cr-0.15Si	Ti-24Al-11Nb-0.5Cu-0.25Si
Ti-51	Ti-13.5Al-21.4Nb-0.65Ni-0.15Si	Ti-24Al-11Nb-0.5Ni-0.25Si
Ti-52	Ti-13.5Al-21.4Nb-0.6Fe-0.15Si	Ti-24Al-11Nb-0.5Fe-0.25Si
Ti-59	Ti-14.2Al-15.7Nb-3.8Hf-0.1C	Ti-25Al-8Nb-1Hf-0.4C
Ti-60	Ti-14.7Al-16.2Nb-0.2B	Ti-25Al-8Nb-1B
Ti-61	Ti-14.5Al-15.9Nb-0.9B1	Ti-25Al-8Nb-1B1
#60	Ti-13.6Al-21.4Nb-0.3Cb	Ti-24.2Al-11.0Nb-0.15B
#61	Ti-13.6Al-21.4Nb-0.4Al	Ti-24.2Al-11.0Nb-0.1B1
#62	Ti-13.6Al-21.4Nb-0.15Si	Ti-24Al-11Nb-0.25Si
Alpha two plus Beta Systems		
#42	Ti-13.9Al-21.4Nb	Ti-24Al-11Nb
Ti-44	Ti-14.3Al-19.7Nb-1.2Hf	Ti-25.2Al-10.1Nb-0.3Hf
Ti-48	Ti-14.3Al-19.7Nb-1.2Ni	Ti-25Al-10Nb-1Ni
#47	Ti-13.6Al-28.2Nb	Ti-25Al-15Nb
Mixed Hexagonal + Cubic Systems		
Ti-17	Ti-2.0Al-61.4Zr-25.8In	Ti-6.25Al-56.25Zr-13.75In
Ti-18	Ti-4.8Al-48.9Zr-20.5In	Ti-12.5Al-37.5Zr-12.5In
Ti-19	Ti-9.0Al-30.4Zr-12.8In	Ti-18.75Al-18.75Zr-6.25In
Ti-21	Ti-8.0Al-92.0Zr	Ti-22.8Al-77.2Zr
Ti-22	Ti-9.3Al-77.7Zr	Ti-23.5Al-58.0Zr
Ti-23 (#21)	Ti-10.8Al-59.3Zr	Ti-24.0Al-38.8Zr
Ti-24 (#22)	Ti-12.9Al-34.7Zr	Ti-24.5Al-19.5Zr
Ti-26	Ti-14.1Al-7.5Zr-3.3Sn	Ti-23.75Al-3.75Zr-1.25Sn
Ti-27	Ti-12.6Al-14.2Zr-6.1Sn	Ti-22.5Al-7.5Zr-2.5Sn
Ti-29 (#23)	Ti-12.8Al-34.3Zr-0.9Sc	Ti-24.2Al-19.2Zr-1Sc
#24	Ti-13.2Al-32.7Zr-1.8Y	Ti-25Al-18.3Zr-1Y
#25	Ti-13.1Al-32.4Zr-2.7Ta	Ti-25Al-18.3Zr-1Ta
#26	Ti-9.7Al-31.0Zr-10.7Sn	Ti-25Al-18.8Zr-5Sn
Ti-43	Ti-9.8Al-31.1Zr-10.3In	Ti-20.0Al-18.8Zr-5.0In
#22	Ti-12.9Al-34.7Zr	Ti-24.5Al-19.5Zr
#49	Ti-14.4Al-18.3Zr	Ti-25Al-9.38Zr
Ti-49	Ti-13.4Al-33.2Zr-0.2B	Ti-25Al-18.25Zr-1B
75:25/Ti3Al:Zr3In		
50:50/Ti3Al:Zr3In		
75:25/Ti3Al:Zr3In		
25:75/Ti3Al:Zr3Al		
50:50/Ti3Al:Zr3Al		
75:25/Ti3Al:Zr3Al		
95:5/Ti3Al:Zr28Sn		
90:10/Ti3Al:Zr3Sn		
75:25/Ti3Al:Zr3Al+1Sc		
75:25/Ti3Al:Zr3Al+1Y		
75:25/Ti3Al:Zr3Al+1Ta		
75:25/Ti3Al:Zr3Al+5Sn		
75:25/Ti3Al:Zr3Al+5In		
75:25/Ti3Al:Zr3Al		
87.5:12.5/Ti3Al:Zr3Al		
75:25/Ti3Al:Zr3Al+1B		

NOTE: Number designation e.g., #28 identifies drop casting; letter plus number designation e.g., Ti-46 identifies button

TABLE 2

Microstructural, Hardness and Qualitative Evaluation of α_2 Alloy

O = None
S = Slight
M = Moderate
E = Extensive

Composition (a/o)	Alloy Number	Homogenized		Heat Treatment	Slip/Cracking		Phase (a) Present
		HV-10	HV-10		Slip	Cracking	
Ti-20 Ti-3Al	Ti-20	297 276		1000°/144hr 1000°/4d	F/S M/M	F/S F/M	Single Phase Single Phase
SINGLE ELEMENT ADDITIONS							
Ti-25Al-1Sc	Ti-8	307		1000/144	F/O	F/M	Single Phase
Ti-25Al-5Sc	Ti-9	376		1000/144	M/S	F/E	Single Phase
Ti-25Al-10Cu	Ti-10	335		1000/144	F/O	F/M	Single Phase
Ti-25Al-5Cu	Ti-11	370		1000/144	M/O	F/S	2-Phase
Ti-25Al-1Mn	Ti-12	268		1000/144	E/S	M/M	2-Phase
Ti-25Al-5Mn	Ti-13	460		1000/144	S/E	F/E	2-Phase
Ti-25Al-1Ge	Ti-14	281		1000/144	E/E	F/M	Single Phase?
Ti-25Al-5Ge	Ti-15	358		1000/144	M/M	M/M	2-Phase
Ti-25Al-1Ag	Ti-31	323		1000/72	E/S	F/E	2-Phase?
Ti-25Al-5Ag	Ti-32	338		1000/72	E/S	F/M	Single Phase
Ti-25Al-1Bi	Ti-33	302		1000/72	E/S	F/E	Single Phase
Ti-25Al-5Bi	Ti-34	322		1000/72	M/M	E/E	Single Phase
Ti-25Al-1Sb	Ti-35	341		1000/72	E/S	M/M	Segregation + Porosity
Ti-25Al-5Sb	Ti-36	354		1000/88	M/M	M/M	2-Phase
Ti-25Al-2Bz	Ti-40	265		1000/88	S/S	M/M	Segregation + Porosity
Ti-25Al-5Bz	Ti-41	335		1000/88	S/S	M/M	2-Phase?
Ti-22.5Al-5Bz	Ti-42	346		1000/96	M/S-M	M/S	2-Phase
Ti-25Al-1Fe	#28	331		1000/96	S/O	M/S	
Ti-25Al-8Nb	Ti-53	404		1000/96			
Ti-30Al-14Zr	#31	396		1000/96	M/M	S/M	2-Phase
Ti-30Al-7Zr	#50	308		1000/96	M/M	N/E	Single or 2 Phase
Two or more element additions							
Ti-25Al-2Nb-2Cu	Ti-4	405		1000/144	E/O	F/M	Single Phase
Ti-25Al-5Nb-5Cu	Ti-3	538		1000/144	E/O	F/S	
Ti-25Al-5Nb-1Mn	Ti-5 (#34)	281		1000/144	M/M	F/S	2-Phase

TABLE 2 (Cont'd)

Composition (%)	Alloy Number	Hardness HV-10	Slip/ Cracking	Heat Treatment (C/Hrs.)	Hardness HV-10	Slip/ Cracking	Phase(s) Present
Ti-25Al-5Nb-1Pd	Ti-6	394	S/M	1000/144	265	M/S	2-Phase
Ti-25Al-5Nb-1Cu	Ti-7 (#33)	365	M/O	1000/144	269	M/O	2-Phase
Ti-25Al-5Nb-5Ge	Ti-16	314	M/M				Eutectic
Ti-23.75Al-3.75Nb-1.25Sn	Ti-25	377	M/S	1000/72	336	M/S	2-Phase
Ti-27.5Al-7.5Nb-2.5Sn	Ti-28	301	M/S	1000/72	263	M/S	Single Phase
Ti-25Al-5Nb-1Nb	Ti-37	350	M/S	1000/72	291	M/M	
Ti-25Al-5Nb-1W	Ti-38	422	O/C	1000/72	330	Distorted/S	
Ti-25Al-5Nb-1W	Ti-39	414	S/S	1000/72	395	Distorted/S	
Ti-25Al-5Nb-1W	#33	377	S/S	1000/96	290	S/S	2-Phase
Ti-25Al-5Nb-1W	#34	303	S/M	1000/96	253	S/M	2-Phase
Ti-25Al-5Nb-1W	#43	248	E/M	1000/96	223	S/M	
Ti-25.5Al-5.5Nb-1W	#29	400	S/S	1000/96	287	S/S	2-Phase
Ti-25.5Al-5.5Nb-0.8W							
Ti-25.5Al-5.5Nb-1W	Ti-44	337	S/S	1000/96	235	S/O	
Ti-25Al-5Nb-1W	Ti-48	294	S/S	1000/96	262	M/VS	2-Phase
Ti-25Al-5Nb-1W	Ti-54	439	O/O	1000/96	315	M/VS	2-Phase
Ti-25Al-5Nb-1W	Ti-55	476	S/O	1000/96	301	M/VS	2-Phase
Ti-25Al-5Nb-1W	Ti-56	429	S/VS	1000/96	262	M/S	2-Phase
Ti-25Al-5Nb-1W	Ti-57	411	S/S	1000/96	295	M/S	2-Phase
Ti-25Al-5Nb-1W	Ti-58	346	S/S	1000/96	257	M/VS	2-Phase
Ti-25Al-5Nb-1W	#53	266	M/M	1000/96	265	M/S	2-Phase
Ti-25Al-5Nb-0.8W	#54	256	M/S-M	1000/96	280	M/VS	2-Phase
Ti-25Al-5Nb-1W	#56	277	M/M	1000/96	285	S-M/VS	2-Phase
Ti-25Al-5Nb-1W	#57	232	M/M	1000/96	234	S-M/VS	2-Phase
Ti-25Al-5Nb-1W	#58	243	M/S	1000/96	290	M/M	2-Phase
Ti-25Al-5Nb-1W	#59	226	M/S-M	1000/96	238	M/S	2-Phase
Ti-25Al-5Nb-0.5Al-0.5	#55	242	M/S-M	1000/96	301	M/S	2-Phase
Ti-25Al-5Nb-1Nb-1W	Ti-46	362	S/O	1000/96	300	S/VS	2-Phase
Ti-25Al-5Nb-1Nb-1W	Ti-47	366	S/M	1000/96	257	M/S	2-Phase
Ti-25Al-5Nb-1Nb-1W	#5	258	M/M	1000/96	306	M/M	2-Phase
Interaction Effects							
Ti-25Al-5Nb-0.7C	Ti-1	373	M/S	1000/72			Carbides
Ti-23.1Al-18.72Zr-4.68 Ti-30		424	O/O	1000/96			Borides
Ti-25Al-5Nb-5Zr-2.5	#46	294	M/M	1000/96			2-Phase
Sn-25Al							
Ti-25Al-9.1Nb-0.1W-0.01	#32	429	S/S	1000/96			Single + Silicides
Ti-25Al-11Nb-0.05Al	#52	237	M/VS	1000/96			2-Phase

TABLE 2 (Cont'd)

Composition (%)	Alloy Number	Hardness HV-10	Slip/ Cracking	Heat Treatment (C/hrs.)	Hardness HV-10	Slip/ Cracking	Phase(s) present
Ti-2Al-11Nb-0.5Cu-0.25Si	Ti-50	353	0/0	1000/96	259	M/VS	2-Phase
Ti-2Al-11Nb-0.5Ni-0.25Si	Ti-51	337	0/0	1000/96	260	M/VS	2-Phase
Ti-2Al-11Nb-0.5Fe-0.25Si	Ti-52	415	0/0	1000/96	266	M/VS	2-Phase
Ti-25Al-8Nb-1Hf-0.4C	Ti-59	314	S-M/S	1000/96	269	S/VS	2-Phase
Ti-25Al-8Nb-1B	Ti-60	293	S/S	1000/96	233	S-M/S	Single Borides
Ti-25Al-8Nb-0.2B1	Ti-61	415	S/S	1000/96	223	M/S	Complex
Ti-24.2Al-11.0Nb-0.15b	#60*	195	S-M/S	1000/96	243	M/S	2-Phase
Ti-24.2Al-11.0Nb-0.1B1	#61*	218	S/S	1000/96	217	M-E/VS	2-Phase
Alpha two plus Beta Systems							
Ti-24Al-11Nb	#2	468	S/O	1000/96	246	S/VS	2-Phase
Ti-25.2Al-10.1Nb-0.3Hf	Ti-44	337	S/S	1000/96	235	S/O	2-Phase
Ti-25Al-10Nb-1Hf	Ti-48	284	S/S	1000/96	242	M/VS	2-Phase
Ti-25Al-15Nb	#17	224	M/S	1000/96	283	M/S	Single or two phase
Mixed Hexagonal and Cubic Systems							
25:75/Ti3Al:Zr3In	Ti-17	236	S/O	1000/144	217	S/S	Complex
50:50/Ti3Al:Zr3In	Ti-18	475	M/O	1000/144	327	M/O	Complex
75:25/Ti3Al:Zr3In	Ti-19	525	M/O	1000/144	359	M/S	Complex
Zr3Al	Ti-21	576	0/0	900/170	196		Single Phase
25:75/Ti3Al:Zr3Al	Ti-22	514	0/0	900/170	385		Complex
50:50/Ti3Al:Zr3Al	Ti-23 (#21)	519	0/0	900/170	382		Complex
75:25/Ti3Al:Zr3Al	Ti-24 (#22)	536	0/0	900/170	255		Single Phase
95:5/Ti3Al:Zr3Sn	Ti-26	335	M/S	1000/72	289	E/S	Single Phase
90:10/Ti3Al:Zr3Sn	Ti-27	348	M/S	1000/72	288	E/M	Single Phase
75:25/Ti3Al:Zr3Al	Ti-29 (#23)	554	0/0	1000/72	305		Oxides
75:25/Ti3Al:Zr3Al+1Y	#24	437	S/S	1000/96	306	M/S	Complex + Oxides
75:25/Ti3Al:Zr3Al+5Sn	#26	310	M/S	1000/96	356	S/M	3-Phase (Complex)
75:25/Ti3Al:Zr3Al+5In	Ti-43	420	M/VS	1000/88	314	M/S	Complex + porosity
75:25/Ti3Al:Zr3Al	#22	517	S/VS	1000/96	338	M/S	Complex
75:25/Ti3Al:Zr3Al+1In	#25	438	S/S	1000/96	306	M/S	Complex + oxides
87.5:12.5/Ti3Al:Zr3Al	#29*	254	M/M	1000/96	231	M/M	Complex
75:25/Ti3Al:Zr3Al+1B	Ti-49	306	M/VS	1000/96	331	M/VS	Complex + Borides

*As-HIP'ed at 2250F/15 ksi/3 hours

of a given alloy to flow and fracture was made by analyzing individual hardness impressions. Figure 5 gives examples of such evaluations with varying tendency to cracking. Figure 5(a) shows an alloy which exhibits no cracking; Figure 5(b) shows an example of moderate cracking which is often difficult to distinguish from coarse slip lines; Figure 5(c) shows more extensive cracks; and Figure 5(d) illustrates a cracked section of an alloy not associated with a hardness indentation. Obviously alloys which exhibited such spontaneous cracking were eliminated from the program. The shape of hardness impressions also varied in certain alloys, in some cases very distorted shapes being formed as shown in Figure 6. Such anisotropy may reflect the influence of crystallographic orientation on flow and fracture characteristics.

Many of the alloys exhibited high hardness in the as-cast condition and a low tendency to crack around hardness impressions. Homogenization treatments resulted in reduction in hardness and an increased tendency to crack. These changes can be correlated with structural modifications. In the as-cast condition, alloys usually exhibited an acicular structure not unlike beta transformed structures in conventional titanium alloys. The degree of acicularity has been found to depend on alloy composition. The base Ti_3Al and dilute alloys exhibit irregular plate-like structures, shown in Figure 7, not unlike the massive-type martensite formed in pure titanium. Alloys containing transition elements tend to consist of much finer plates, as illustrated in Figure 8. During homogenization treatments, multiphase alloys retain acicular structure although some coarsening may occur, Figure 9.

In single-phase alloys high temperature exposure results in recrystallized structures of the type shown in Figure 10.

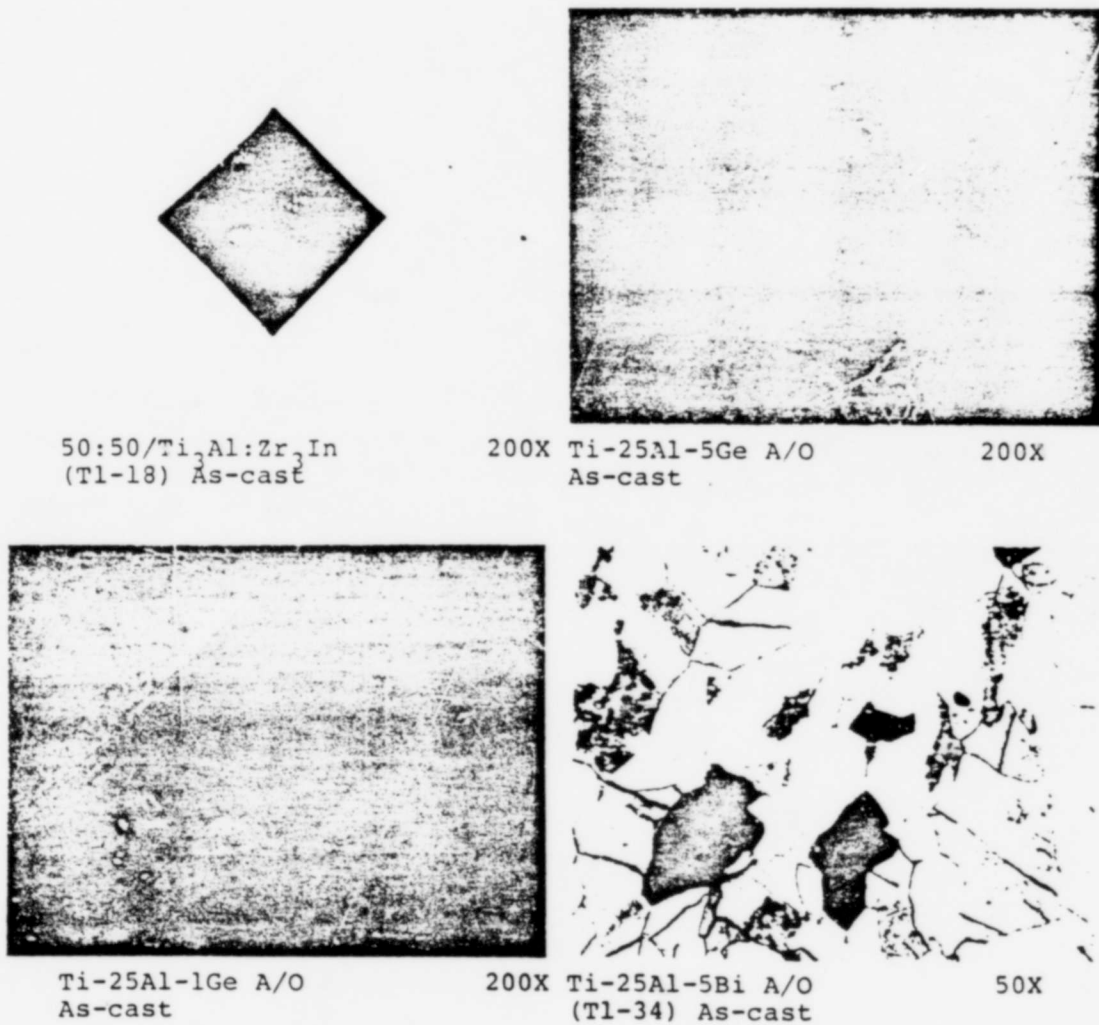


Figure 5. Photomicrographs of Hardness Impressions in Ti₃Al Base Alloys

(a) No Cracking	(b) Slight Cracking
(c) Extensive Cracking	(d) Spontaneous Cracking

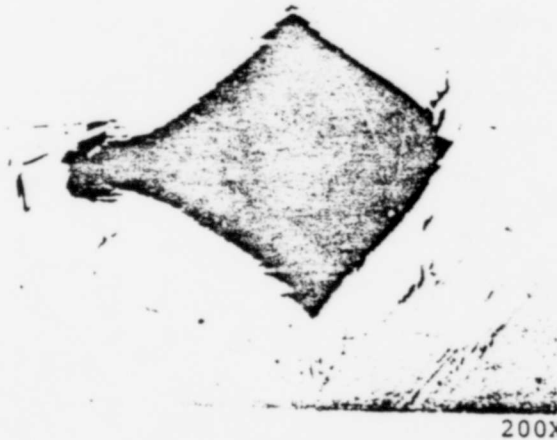


Figure 6. An Example of a Distorted Hardness Impression Observed in Some Alpha Two Base Alloys (Ti-25Al-5Nb-5Zr-2.5Sn-0.25Si, As-Cast)

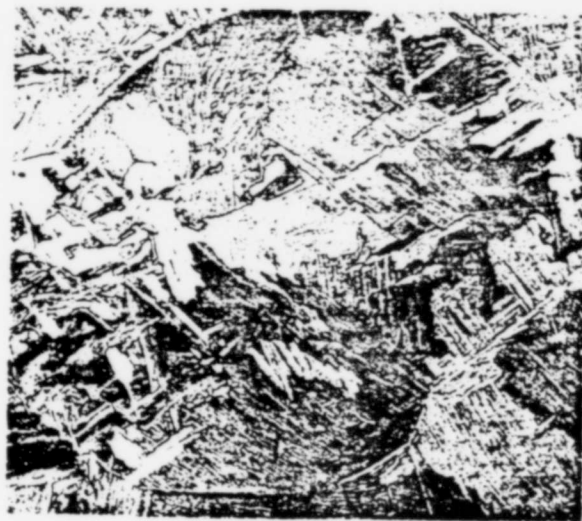


Figure 7. Coarse Acicular (Colony) Structure Found in Alpha Two Alloys With Low Solute Contents in the As-Cast Condition (Ti-25Al-1Fe)



Figure 8. The Fine Acicular (Widmanstätten) Structures Observed in Alpha Two Alloys with an Intermediate Concentration of Transition Elements in the As-Cast Condition (Ti-26.4Al-4.8Nb-0.3Fe)

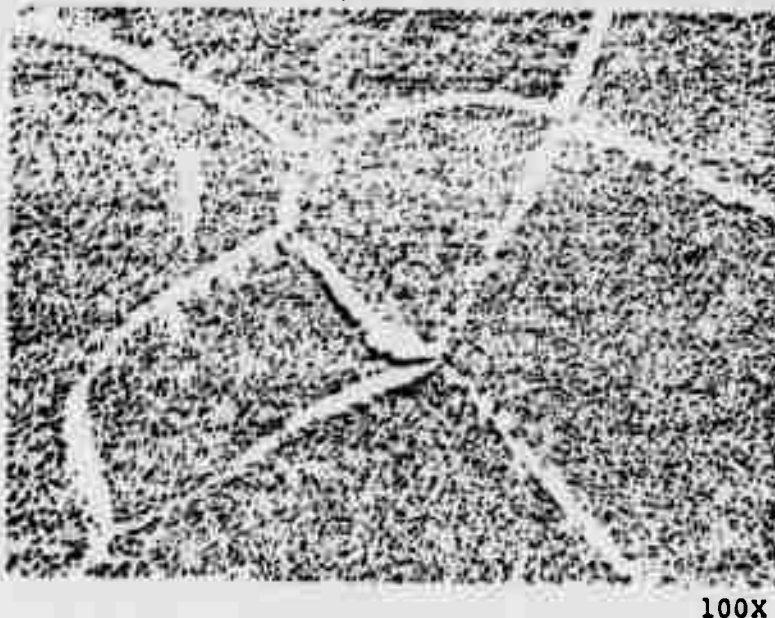


Figure 9. The Coarsened Acicular Structure in the Alloy Ti-24Al-11Nb After Homogenization at 1830°F for 96 Hours

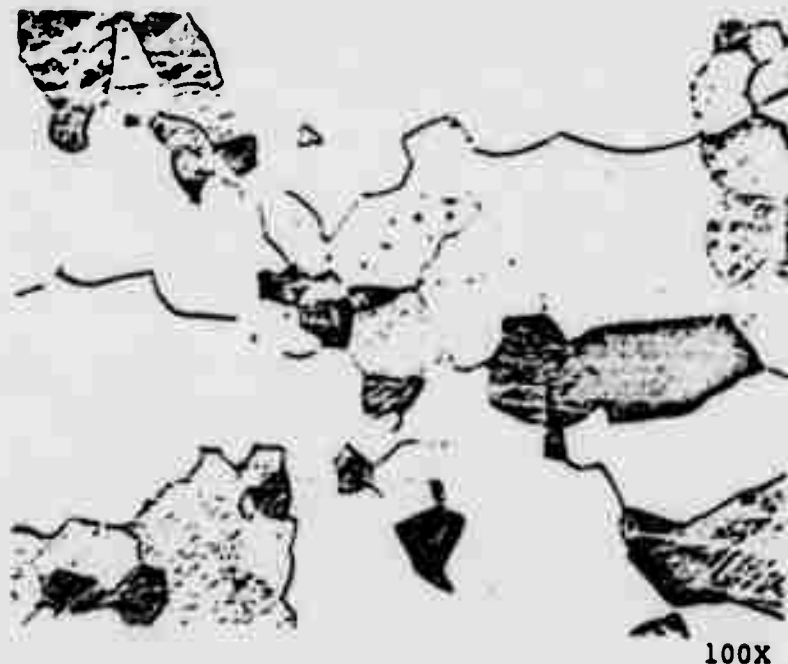


Figure 10. The Equiaxed Alpha Two Structure Formed in the Ti-28Al-5Nb Alloy After Homogenization at 1830°F for 96 Hours

We shall return to a more detailed discussion of the phase and structural relationships in these alloys in a later section.

If the characteristics of individual or groups of alloys are examined, the following trends emerge:

- Most alloys in the Single Element Group appear to offer only a hardness increase over the base Ti_3Al compound. Copper and iron may increase crack resistance. Niobium additions are also beneficial; a point to be expanded upon below. Alloys containing scandium are of interest from both a hardness and phase structure viewpoint. It can be seen that the Ti-25Al-1Sc alloy exhibits the lowest hardness of any alloy in Table 2, after homogenization. If the

scandium content is increased to 5%, oxide particles can be observed which have been shown by microprobe analysis to be scandia. Other elements from Group IIIB show similar behavior (see Alloys #24 and #25). It is possible that the low hardness results from an oxygen scavenging action of scandium. As has been found that oxygen content has a marked effect on ductility of some alpha two alloys, the additions of small amounts of Group IIIB elements could be an effective method of reducing the bulk oxygen content of such alloys.

- All alloys from the Multi-Addition Group contain either niobium or zirconium as the third element. Examination of the slip/cracking relationships for this series indicates more promising trends in that the cracking tendency, even in the homogenized condition, is reduced. A tendency to improve characteristics as the niobium content increases can also be detected, a trend which carries into the alpha two plus beta system discussed below.
- The majority of alloys in the Interactions Group are also based on Ti-Al-Nb base alloys. In several cases the solubility limit of the interstitial elements were exceeded in the alloys leading to the formation of quite large precipitates, which are probably deleterious to mechanical properties. Examination of these results, and assuming the solubility of the interstitial elements is not strongly dependent on composition, can set the solubility ranges for silicon and carbon, based on the criterion of precipitate detectability in optical micrographs, at between 0.4 and 0.7% carbon and between 0.25 and 0.4% for silicon.
- The alpha two plus beta group contains several alloys with attractive characteristics and as we shall discuss

several alloys in considerably more detail below. It appears from these and other Ti-Al-Nb alloys that the limit of stability of alpha two at intermediate temperatures ($\sim 1700^{\circ}\text{F}$) along the $(\text{Ti-Nb})_3\text{Al}$ compositional line is about 10 atomic percent niobium.

- The alloys produced to study the mixed cubic plus hexagonal structures also contain several compositions with attractive characteristics. It can be seen from Table 2 that in the as-cast condition in virtually all alloys, high hardness values are combined with little or no tendency to crack. Upon homogenization, which was usually accompanied by recrystallization to an approximately equiaxed structure, the majority of alloys soften and show an increased propensity to cracking. It may also be noted that the alloys containing Group IIIB elements contain oxide particles and only very low concentrations of these elements are present in the matrix. Figure 11 illustrates this point for these alloys.

A. Forging

In order to increase the homogeneity and produce structural refinement, a large number of alloys were forged on isothermal dies. This process also served to increase the structural integrity of the material and produced shapes compatible with the sectioning of mechanical property specimens from the forged sections. As an additional step, many of the alloys produced in the form of two-pound drop castings were hot isostatically pressed (HIP'ed) before forging. It has been found that the process increases the material yield to virtually 100% after forging. Nearly all alloys were forged at 2000°F (1090°C), which in some alloys is above the beta transus but in most lies in the two phase alpha (two) plus beta phase field. The forging operation coupled with a

relatively slow cooling rate can give rather coarse structures.

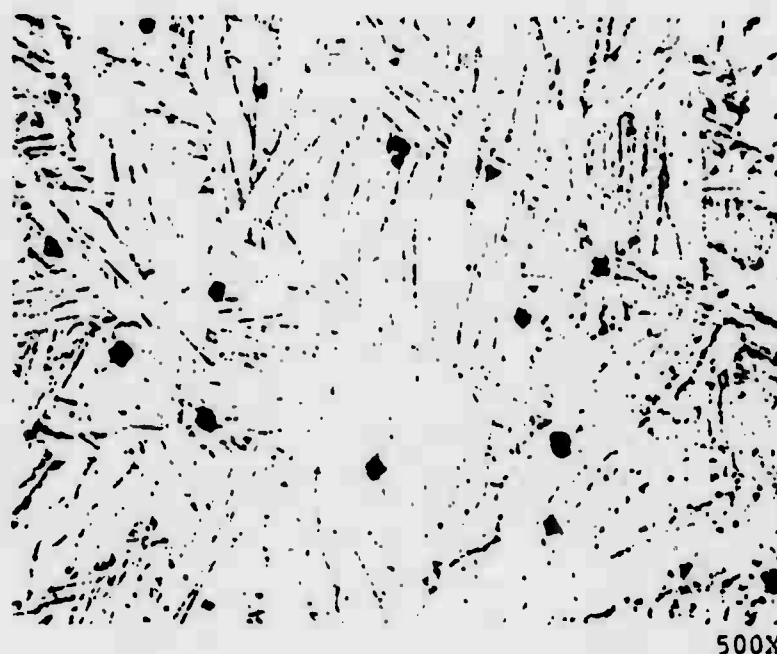


Figure 11. Oxide Particles (Scandia) Formed in the Ti-25Al-18.3Zr-1Sc Alloy (As-Cast)

Over eighty alloys have been forged and an assessment of the forging characteristics together with structural information and hardness values are given in Table 3. It can be seen that a very large number of alloys were forged with no problem, only five alloys showing pronounced cracking tendencies. The latter group included the base compound Ti_3Al , although a second ingot forged with only minor difficulty, alloys containing high concentrations of bismuth and germanium (#T1-34, 15) and an alloy from the Ti_3Al-Zr_3Al series containing yttrium (#24). Forging reduction of >70 percent in height were achieved in most alloys.

The structure of alloys tended to be refined by the forging

TABLE 3

Isothermal Forging Results for α_2 Alloy Compositions

Composition (a/o)	Alloy Number	Forging Temperature ^a	% Reduction	Forging Macroeffects (Cracking)	As Forged Hardness HV-10	Slip/Cracking	Microstructure
Ti ₃ Al	Ti-20	2000°F	--	E	166	--	Single Phase
Single Element Additions							
Ti-25Al-18c	Ti-8	2000°F	64.7	--	229	E/E	2nd Phase at Boundary
Ti-25Al-5Cu	Ti-11	2000	62.1	--	315	E/E	
Ti-25Al-16c	Ti-14	2000	67.9	M	196	M/E	
Ti-25Al-1Fe	#28	2050	83.3	0	338	S/M	
Ti-25Al-3Cu	#30	2000	81.2	0	352	M/S	Single + Oxides
Ti-25Al-1W	#35	2050	83.3	0	317	E/M	
Ti-25Al-1Ta	#36	2050	84.0	M	327	M/M	
Ti-25Al-5Sc	Ti-9	2000	69.2	S	302	S/S	
Ti-25Al-1Cu	Ti-10	2000	63.4	0	213	E/E	Single
Ti-25Al-1Mn	Ti-12	2000	77.8	0	286	M/M	
Ti-25Al-5Mn	Ti-13	2000	66.3	G	308	S/E	
Ti-25Al-5Ge	Ti-15	2000	63.5	0	381	S/S	
Ti-25Al-1Ag	Ti-31	2000	64.2	S	276	E/E	2-Phase
Ti-25Al-5Ag	Ti-32	2000	63.3	G	280	E/E	
Ti-25Al-1B1	Ti-33	2000	77.6	M	279	E/E	
Ti-25Al-5B1	Ti-34	2000	56.6	E	313	M/E	
Ti-25Al-18b	Ti-35	2000	62.0	C	286	S/E	Single Fine GS
Ti-25Al-52b	Ti-36	2000	66.1	S	354	M/M	
Ti-25Al-1Fe	#28	2000	81.2	0	278	M/S	
Ti-25Al-28b	Ti-40	2000	67.1	VS	302	M/M	
Ti-25Al-58b	Ti-41	2000	71.5	0	313	S/M	Segregation
Ti-22.5Al-58b	Ti-42	2000	64.7	0	318	S/M	
Ti-25Al-68b	Ti-53	2000	69.6	0	237	M/S	
Ti-20Al-7Zr	#50	2000	80.5	0	342	M/S	
Ti-30Al-14Zr	#51	2000	80.8	0	407	M/S	2-Phase
Two or More Element Additions							
Ti-25Al-2Nb-2Co	Ti-4	2000	61.9	S	194	M/M	Acicular
Ti-25Al-5Nb-5Co	Ti-3	2000	62.3	-	370	E/M	
Ti-25Al-5Nb-1Mn	Ti-5(#34)	2000	69.1	0	264	M/S	
Ti-25Al-5Nb-1Cu	Ti-7(#33)	2000	65.8	-	219	E/M	
Ti-23.75Al-3.75Nb-1.25Sn	Ti-25	2000	68.0	0	353	O/M	2-Phase

7

0 = None; S = Slight; M = Moderate; E = Extensive

TABLE 3 (Cont'd)

Composition (a/o)	Alloy Number	Forging Temperature	% Reduction	Forging Macroeffects (Cracking)	As Forged Hardness	Slip/ Cracking	Microstructure
Ti-22.5Al-7.5Nb-2.5Sn	Ti-28	2000	67.4	0	HV-10 275	M/S	
Ti-26.4Al-4.8Nb-0.8Fe	#29	2000	81.3	0	298	M/M	2-Phase
Ti-25Al-5Nb-1Pd	Ti-6	2000	60.3	0	253	M/M	2-Phase
Ti-25Al-5Nb-1Hf	Ti-37	2000	72.6	0	298	M/M	2-Phase
Ti-25Al-5Nb-1W	Ti-38	2000	64.1	0	138	?	2-Phase
Ti-30Al-5Nb-1W	Ti-19	2000	65.5	0	184	?	Complex
Ti-25Al-5.5Sn-5Ge	Ti-16	2000	65.9	0	141	M/M	
Ti-25Al-5Nb-1Cu	#33	2000	42.1	0	251	M/M	
Ti-25Al-5Nb-1Ni	#34	2000	81.5	0	227	M/M	
Ti-25Al-5Nb-1Ni-1Mo	Ti-26	2000	65.2	0	200	M/S	
Ti-25Al-5Nb-1Ni-1V	Ti-47	2000	65.4	0	261	M/S	
Ti-25Al-5Nb-1W	Ti-54	2000	71.2	0	207	S/S	2-Phase
Ti-25Al-5Nb-1Mo	Ti-55	2000	71.1	0	278	S/S	2-Phase
Ti-25Al-5Nb-1Ta	Ti-56	2000	71.1	0	239	S-N/V	2-Phase
Ti-25Al-5Nb-1Hf	Ti-57	2000	71.1	0	244	M/V	2-Phase
Ti-25Al-5Nb-1V	Ti-58	2000	69.9	0	235	M/S	2-Phase
Ti-25Al-5Nb-1Fe	#53	2000	87.0	0	272	M/S	Fine - Acicular
Ti-25Al-5Nb-0.8Fe	#54	2000	87.0	0	269	M/S	2-Phase
Ti-25Al-5Nb-1W	#56	2000	80.0	0	283	M/M	2-Phase
Ti-25Al-5Nb-1Ta	#57	2000	80.0	0	250	M/M	2-Phase
Ti-25Al-5Nb-1Hf	#58	2000	80.0	0	260	S-M/S	2-Phase
Ti-25Al-5Nb-1V	#59	2000	80.0	0	256	M/S	2-Phase
Ti-25Al-5Nb-1Ni-1W	#65	2000	79.9	0	209	M/M	
Ti-25Al-5Nb-0.5Ni-1W	#55	2000	87.0	0	273	M/M	Coarse Acicular
Interaction Effects							
Ti-25Al-5Nb-0.7C	Ti-1	2000	75.0	S	320	-	Carbides
Ti-25.9Al-9Nb	#31	2000	84.9	0	294	S/S	
Ti-26Al-9.1Nb-0.4Hf-0.8Si	#32	2000	83.4	0	293	S/S	SiL-cides
Ti-27.1Al-18.7Zr-4.6B	Ti-30	2000	64.4	0	356	S/S	Complex
Ti-25Al-5Nb-5Zr-2.5Sn-2.5Si	#46	2000	78.8	0	305	M/M	
Ti-26Al-9.1Nb-0.4Hf-0.8Si	#32	2000	80.8	0	232	M/S	
Ti-26Al-11Nb-0.5Cu-0.25Si	Ti-50	2000	72.4	0	230	M/M	2-Phase

0 = None; S = Slight; M = Moderate; E = Extensive

TABLE 3 (Cont'd)

Composition (a/o)	Alloy Number	Forging Temperature*	Z Reduction	Forging Macroeffects (Cracking)	As Forged Hardness HV-10	Slip/Cracking	Microstructure
Ti-24Al-11Nb-0.5Mn-0.25Si	T1-51	2000	72.5	0	232	M-E/S	2-Phase
Ti-24Al-11Nb-0.5Fe-0.25Si	T1-52	2000	75.7	S	247	M/S	2-Phase
Ti-25Al-8Nb-1Mn-0.4C	T1-59	2000	68.3	0	269	S/VS	2-Phase
Ti-25Al-8Nb-1Fe	T1-60	2000	71.8	0	253	M/VS	Complex
Ti-25Al-8Nb-0.2B	T1-61	2000	71.6	0	249	M/S	2-Phase
Ti-25Al-11Nb-0.25Si	#57	2000	79.4	0	226	M/S	2-Phase
Ti-24.2Al-11Nb-0.15B	#60	2000	80.0	0	238	M/S	2-Phase
Ti-24.2Al-11Nb-0.18B	#61	2000	80.0	0	237	M-E/M	2-Phase
Alpha Plus Beta Systems							
Ti-24Al-11Nb	#42	2000	81.5	0	267	S/S	2-Phase
Ti-25.2Al-10.1Nb-0.1Mn	T1-44	2000	66.7	0	221	S/S	
Ti-25Al-10Nb-1Mn	T1-48	2000	63.5	0	263	M/S	
Ti-25Al-11Nb	#47	2000	79.4	0	232	S/S	2-Phase
Mixed Hexagonal and Cubic Systems							
Zr-75Ti-25Al-2Zr-1In	T1-17	2000	61.4	-	218	O/O	Multiphase
Mo-50Ti-50Al-2Zr-3In	T1-18	2000	65.9	-	309	E/S	Multiphase
Er-41	T1-21	2000	66.7	0	329	---	
Zr-75Ti-25Al-2Zr-1Al	T1-22	2000	66.7	0	367	---	
Al-50Ti-50Al-2Zr-3Al	T1-23(#21)	1700	66.7	0	329	S/S	
Zr-75Ti-25Al-2Zr-1Al	T1-24(#22)	1700	76.3	M	263	M/M	
Al-50Ti-50Al-2Zr-3In	T1-26	2000	67.6	0	322	S/M	
Mo-50Ti-50Al-2Zr-3Sn	T1-27	2000	67.5	0	324	S/S	
Zr-75Ti-25Al-2Zr-1Al-1Sc	T1-29(#23)	2000	81.8	0	29-	M/M	
Zr-75Ti-25Al-2Zr-1Al-1Y	#24	2000	87.8	0	302	S/M	Oxidized
Zr-75Ti-25Al-2Zr-1Al-1La	#25	2000	77.4	S	297	M/M	Oxidized
Zr-75Ti-25Al-2Zr-1Al-1Sn	#26	2050	83.3	0	370	S/S	
Zr-75Ti-25Al-2Zr-1In	T1-19	2000	56.8	0	294	E/S	Complex
Zr-75Ti-25Al-2Zr-1Al-1Sn	T1-43	2000	65.8	0	309	S/M	Complex
Zr-75Ti-25Al-2Zr-1Al	#22	2000	80.6	0	345	S/S	
Er-41-2Zr-1Al	#49	2000	81.0	0	272	M/M	Complex
Zr-75Ti-25Al-2Zr-1Al-1B	T1-49	2000	70.8	0	317	M/S	

0 = None M = Moderate
S = Slight E = Extensive

operation; even in alloys forged above the beta transus, a much finer beta grain size was evident compared with the as-cast structure. In most cases, however, no major improvement in slip/cracking characteristics were observed in as-forged material; the results tending to lie between as-cast and the homogenized evaluation cited above (Table 4). This result is not surprising in view of the structure/property relationships found in this class of alloys--a point that we shall elaborate on below.

B. Bend Test Results

Sections were prepared from the forged sections and three point bend tests performed over a range of temperatures in order to provide a more direct assessment of the mechanical property capability of the alloys. Before proceeding to the results obtained, some general aspects of these tests will be described. In the early tests performed, the total bend ductility was reported which includes both the elastic and plastic components; rather than change in the middle of the program, this procedure has been retained. As we shall see the total bend deflection corresponds reasonably well to the plastic strain obtained in a tensile test. However, in alloys with a high yield stress, the elastic deflection can be a large component of the total value cited. The maximum strain that can be achieved in the bend rig is 4 to 6% depending on specimen geometry at this point the specimen intersects the lower plate of the fixture thus preventing further displacement. This condition is represented by the designation "plastic" in the following tables. The correlation of the yield stress measured in these bend tests and values obtained in subsequent tensile tests was not as good as the ductility values, although trends were faithfully reproduced. This is no doubt related to the complex strain

TABLE 4

Forged Plus Heat Treatment Results for α_2 Alloy Compositions

Composition (a/o)	Alloy No.	Forged + 1650°F 8 Hr., A.C. HV-10	Slip/ Cracking	Forged + 2200°F 1 Hr. A.C. HV-10	Slip/ Cracking
Ti ₃ Al	-	226	E/M	-	-
Single Element Additions					
Ti-25Al-1Fe	28	247	M/M	334	M/M
Ti-25Al-8Nb	Ti-53	-	-	473	S/VS
Ti-30Al-7Zr	50	-	-	409	M/S
Ti-30Al-14Zr	51	-	-	589	S/VS
Two or more Element additions					
Ti-25Al-5Nb-1Cu	33	258	M/M	290	S/S
Ti-25Al-5Nb-1Ni	34	271	M/S-M	302	M/M
Ti-25Al-5Nb-1Hf	43	215	E-M/S	335	M/S
Ti-26.4Al-4.8Nb-0.8Fe	29	278	M/M	319	M/M
Ti-25Al-8Nb-1W	Ti-54	-	-	498	O/O
Ti-25Al-8Nb-1Mo	Ti-55	-	-	485	S/O
Ti-25Al-8Nb-1Ta	Ti-56	-	-	414	VS/O
Ti-25Al-8Nb-1Hf	Ti-57	-	-	456	S/VS
Ti-25Al-8Nb-1V	Ti-58	-	-	464	S/VS
Ti-25Al-8Nb-1Fe	53	-	-	288	S/S
Ti-25Al-8Nb-0.3Fe	54	-	-	305	S/VS
Ti-2.1Al-8Nb-1d	56	-	-	451	S/VS
Ti-25Al-8Nb-1Ta	57	-	-	402	S/O-VS
Ti-25Al-8Nb-1Hf	52	-	-	398	S/VS
Ti-25Al-8Nb-1V	59	-	-	342	S/M/S
Ti-25Al-5Nb-0.5Ni-1W	65	-	-	259	S/VS
Ti-25Al-5Nb-1Ni-1W	46	290	S/M	399	M/M
Interaction Effects					
Ti-25Al-5Nb-5Zr-2.5Sn-.25Si	46	307	S/M	329	M/M
Ti-26Al-9.1Nb-0.4Hf-0.8Si	32	256	S/S	331	M/S
Ti-24Al-11Nb-.5Cu-.25Si	Ti-50	-	-	464	O/O
Ti-24Al-11Nb-.5Ni-.25Si	Ti-51	-	-	402	S/S
Ti-24Al-11Nb-.5Fe-.25Si	Ti-52	-	-	487	S/S
Ti-25Al-8Nb-1Hf-.4C	Ti-59	-	-	302	S/VS
Ti-25Al-8Nb-1B	Ti-60	-	-	306	S/O
Ti-25Al-8Nb-.2B1	Ti-61	-	-	477	S/O
Ti-24.2Al-11Nb-0.15b	60	-	-	483	S-M/VS
Ti-24.2Al-11Nb-0.1B1	61	-	-	357	S-M/O-VS
Ti-24Al-11Nb-0.25Si	62	-	-	433	O/O
Alpha Two Plus Beta Systems					
Ti-24Al-11Nb	42	218	S/S	318	S/S
Ti-25Al-15Nb	47	-	-	404	O/O
Mixed Hexagonal and Cubic Systems					
75:25/Ti ₃ Al:Zr ₃ Al	22	293	M/S	423	M/S
75:25/Ti ₃ Al:Zr ₃ Al+11a	25	257	S/M	-	-
75:25/Ti ₃ Al:Zr ₃ Al+5Sn	26	342	S/S	362	S/M
87.5:12.5/Ti ₃ Al:Zr ₃ Al	49	-	-	393	M/S

O = None
S = Slight
M = Moderate
E = Extensive

gradients present in a bend bar compared with the homogeneous strain in a tensile test. Typically, values of yield strength measured in the bend tests were about fifty percent higher than tensile yield strength.

In the initial stages of this program it had been intended to use the Ti_3Al base compound as the reference point in order to assess relative changes in such factors as the ductile: brittle transition temperature. However, the first Ti_3Al ingot fabricated cracked during forging and thus sound material was not available for testing. Thus, instead, the alloy used in the characterization program (Section III), Ti-25Al-5Nb (Ti-16Al-10Nb weight %), was used to provide the baseline. As a substantial tensile data base was accumulated on this alloy, it formed a useful comparison point.

A data compilation for all alloys tested is given in Table 5. Nearly all of the initial testing was performed on material in the as-forged condition, as little or nothing was known about the influence of heat treatment. As our state of understanding has improved, material subjected to various thermal cycles has been tested and these results are also included in Table 5.

Turning to the results obtained, it can be seen that the Ti-25Al-5Nb alloy exhibits a reduction in ductility as the test temperature decreases, the values falling below 1% at temperatures <800°F. The alloy shows "plastic" behavior at 1200°F. Thus many tests were conducted in the temperature range 800-1200°F for comparison purposes. Most single element additions produced little or no change in bend properties in this temperature region. However, increasing the niobium content to 8% resulted in the achievement of plastic behavior at 800°F, about a 400 degree improvement with

TABLE 5

Three Point Bend Test Results for α_2 Alloy Compositions

Composition (g/o)	Alloy Number	Heat Treatment	Test Temperature (°F)	Strain Rate (in/in./min.)	0.2% Offset Yield Strength(ksi)	Maximum Fiber Stress at Fracture (ksi)	Maximum Fiber Strain at Fracture (%)
Ti-16Al-10Nb (w/o) ** (Program Alloy)	-	Beta Forged +2200°F/1Ac+ 1650°F/8/Ac	RT 600 800 1000 1100 1200	0.0011 0.0012 0.0010 0.0010 0.0011 0.0011	- 57.0 92.0 85.5 82.0 65.5	60.8 58.6 109.1 119.2 117.9 112.7	0.662 0.896 1.37 2.61 2.59 Plastic
Ti-3Al	-	As-Forged	800	-	109.2	113.9	0.935
Single Element Additions							
Ti-25Al-1 Sc	Ti-8	As-Forged	1000 1100 1200	0.0012 0.0011 0.0012	- - 74.4	60.9 62.1 74.9	0.529 0.613 1.08
Ti-25Al-5Cu	Ti-11	As-Forged	1000 1100 1200	- 0.0010 0.0010	78.5 81.0 -	80.0 99.2 64.3	1.08 1.38 1.45
Ti-25Al-1Cu	Ti-10	2100/1/Ac	800	0.0010	-	95.5	0.746
Ti-25Al-1Mn	Ti-12	2100/1/Ac	800 1000	0.0007 0.0010	68.0 100.0	78.2 130.7	1.21 2.32
Ti-25Al-1Mn	Ti-33	As-Forged	1000	0.0010	-	88.7	0.743
Ti-25Al-1Ag	Ti-31	As-Forged	800	0.0010	-	63.9	0.537
Ti-25Al-1Sb	Ti-35	As-Forged	1000	0.0010	-	80.8	0.688
Ti-25Al-1Fe	#28	As-Forged As-Forged 2200/1/Ac	RT 800 RT	** ** **	- 75.0 -	67.4 102.5 93.4	0.700 1.25 0.600

TABLE 5 (Cont'd)

Composition (a/o)	Alloy Number	Heat Treatment	Test Temperature (°F)	Strain Rate (in/in/min.)	0.2% Offset Yield Strength(Ksi)	Maximum Fiber Stress at Fracture (Ksi)	Maximum Fiber Strain at Fracture (%)
Ti-25Al-2Nb-20a	Ti-4	As-Forged	1000	0.0012	61.0	61.9	1.05
Ti-25Al-5Nb-5Ta	Ti-3	As-Forged	1000 1832	-	-	90.3 48.6	0.912 Plastic
Ti-25Al-5Nb-10Cu	Ti-7(433)	As-Forged	1000 1100 1200	0.0002 0.0012 0.0011	71.0 62.0 61.0	73.3 30.3 92.9	1.79 1.46 Plastic
Ti-23.75Al-3.75Nb-Ti-25 1.25Sn	Ti-25	As-Forged	1000	0.0011	-	70.3	0.570
Ti-22.5Al-7.5Nb- 2.5Sn	Ti-28	As-Forged	17 400 400 500 600 600 900 1000 1200	0.0007 0.0010 0.0021 0.0011 0.0011 0.0008 0.0011 0.0011 0.0010	- - - 117.0 120.5 104.0 95.0 83.5 68.8	92.3 117.9 101.1 129.6 130.2 113.7 108.1 107.3 88.1	0.653 1.01 1.10 1.81 1.85 1.63 2.24 3.56 3.71
Ti-30Al-5Nb-1W	Ti-39	As-Forged	1000 1100 1100	0.0011 0.0011 0.0016	179.0 174.5 158.5	196.2 189.8 183.9	1.93 Plastic Plastic
Ti-16Al-10Nb-17a (w/o)	#29	As-Forged	1000 1100 1200	0.0009 0.0010 0.0005	120.5 106.5 66.0	121.8 142.6 82.7	1.39 Plastic Plastic
Ti-15Al-5Sn-50a	Ti-16	As-Forged	800	0.0012	-	118.2	1.01
Ti-25Al-5Nb-1Nb- 1Nb	Ti-40	As-Forged	RT 400 800 RT 400 800	- - 108.0 - - 87.4	115.2 122.8 142.0 101.2 106.4 130.7	0.825 0.927 3.12 0.675 0.783 3.07

TABLE 5 (Cont'd)

Composition (a/o)	Alloy Number	Heat Treatment	Test Temperature °F	Strain Rate (Outer Fiber) in/in/min.	0.2% Offset Yield Strength(Ksi)	Maximum Fiber Stress at Fracture (Ksi)	Maximum Fiber Strain at Fracture (%)
Ti-25Al-5Nb	Ti-41	As-Forged	800	..	-	99.5	0.881
		As-Forged	RT	..	131.7	134.1	1.09
	Ti-53	As-Forged	800	..	88.1	133.9	Plastic
		As-Forged	RT	..	-	134.6	0.877
Ti-25-5Nb-.5Mn-.5Mg	Ti-55	As-Forged	500	..	-	228.3	1.69
		As-Forged	RT	..	-	122.9	0.78
	Ti-50	As-Forged	500	..	161.8	130.0	1.00
		As-Forged	RT	..	145.5	175.7	1.38
Ti-30Al-7Zr	Ti-50	As-Forged	500	..	-	197.9	2.40
		As-Forged	RT	..	80.5	90.1	0.648
	Ti-51	As-Forged	800	..	-	114.2	3.02
		As-Forged	RT	..	309.6	245.9	1.44
Ti-30Al-14Zr	Ti-51	As-Forged	800	..	-	345.9	2.42
		As-Forged	RT	..	-	111.0	0.642
	Ti-52	As-Forged	800	..	-	150.7	1.17
		As-Forged	RT	..	-	279.2	1.45
Ti-25Al-5Nb-1Mn	Ti-53	As-Forged	500	..	-	284.3	1.80
		As-Forged	RT	..	-	110.9	0.768
	Ti-54	As-Forged	600	0.0017	91.0	103.8	1.39
		As-Forged	800	0.0010	91.0	117.8	1.88
Ti-25Al-5Nb-1Mn-1Ti	Ti-55	As-Forged	900	0.0012	80.5	127.4	3.98
		As-Forged	1000	0.0012	63.0	107.2	Plastic
	Ti-56	As-Forged	1000	0.0012	77.0	130.3	Plastic
		As-Forged	1200	0.0012	54.0	77.2	Plastic

Two or more element additions

T1-25A1-5Nb-LW1 T1-5 (#34) As-Forged

TABLE 5 (Cont'd)

Composition (a/o)	Alloy Number	Heat Treatment	Test Temperature (°F)	Strain Rate (Outer Fiber) in/in/min.	0.2% Offset Yield Strength (ksi)	Maximum Fiber Stress at Fracture (ksi)	Maximum Fiber Strain at Fracture (%)
Ti-25Al-5Nb-1Hf	Ti-37	As-Forged	400	0.0010	-	124.2	0.952
		As-Forged	600	0.0010	117.0	120.4	1.11
		As-Forged	800	0.0011	109.0	148.0	3.18
		2100/1/AC	600	0.0009	-	130.8	0.993
Ti-25Al-5Nb-1W	Ti-38	2100/1/AC	800	0.0007	126.0	154.1	1.70
		As-Forged	400	0.0007	162.0	162.4	1.22
		As-Forged	600	0.0014	151.0	157.1	1.77
		As-Forged	900	0.0018	145.0	178.2	3.87
Ti-25Al-5Nb-1Cu	#33	As-Forged	1000	0.0011	137.0	174.4	3.65
		2100/1/AC	1100	0.0016	121.5	146.9	Plastic
		As-Forged	800	0.0013	183.0	177.5	2.45
		As-Forged	RT	-	-	80.4	0.71
Ti-25Al-5Nb-1Hf	#34	As-Forged	800	-	58.8	104.9	3.77
		1650/8/AC	RT	-	-	67.7	0.579
		2200/1/AC	RT	-	-	92.5	0.642
		2200/1/0Q+1500/8/AC	RT	-	-	76.4	0.493
Ti-25Al-5Nb-1Hf	#43	As-Forged	RT	-	-	40.0	0.516
		As-Forged	800	-	62.0	99.2	2.06
		2200/1/AC	RT	-	-	61.8	0.379
		2200/1/0Q+1500/8/AC	PT	-	-	112.9	0.682
Ti-25Al-5Nb-1Hf	#43	As-Forged	RT	-	-	81.6	0.668
		As-Forged	800	-	80.4	135.1	3.26
		1650/8/AC	RT	-	-	77.7	0.629
		2200/1/AC	RT	-	-	158.1	0.933
Ti-26.4Al-4.8Nb-0.8W	#29	As-Forged	RT	-	-	70.8	0.605
		As-Forged	800	-	89.2	121.1	1.99
		2200/1/AC	RT	-	136.7	136.7	1.19
		2200/1/AC	RT	-	-	134.3	8.838
Ti-25Al-5Nb-1W	#45	As-Forged	RT	-	-	147.7	1.34
		1650/8/AC	RT	-	125.6	150.5	3.62
		2200/1/AC+1650/8/AC	800	-	120.1	151.8	1.06
		2200/1/AC	1200	-	-	136.3	Plastic

TABLE 5 (Cont'd)

Composition (a/o)	Alloy Number	Heat Treatment	Test Temperature (°F)	Strain Rate (Outer Fiber) in/in/min.	0.2% Offset Yield Strength (Ksi)	Maximum Fiber Stress at Fracture (Ksi)	Maximum Fiber Strain at Fracture (%)
Ti-25Al-8Nb-1W	T1-54	As-Forged	RT	—	153.5	157.4	1.15
		As-Forged	800	—	116.3	107.3	Plastic
		2200/1/AC	RT	—	349.8	356.5	2.52
Ti-25Al-8Nb-1W	T1-54	2200/1/AC	500	—	256.5	286.6	2.58
		As-Forged	RT	—	145.5	149.2	1.19
		As-Forged	800	—	107.1	161.9	Plastic
Ti-25Al-8Nb-1W	T1-55	2200/1/AC	RT	—	—	255.9	1.72
		2200/1/AC	500	—	309.2	348.1	2.77
Ti-25Al-8Nb-1W	T1-56	As-Forged	RT	—	133.3	149.5	1.76
		As-Forged	800	—	83.5	123.2	Plastic
		2200/1/AC	RT	—	234.9	275.3	2.60
Ti-25Al-8Nb-1W	T1-57	2200/1/AC	500	—	213.7	258.1	2.91
		As-Forged	RT	—	134.4	144.5	1.41
		As-Forged	800	—	91.1	137.1	Plastic
Ti-25Al-8Nb-1W	T1-58	2200/1/AC	RT	—	297.9	327.4	2.5
		2200/1/AC	500	—	215.0	238.6	1.87
		As-Forged	RT	—	126.9	148.3	1.89
Ti-25Al-8Nb-1W	#53	As-Forged	800	—	84.4	128.9	Plastic
		2200/1/AC	RT	—	272.1	255.9	1.83
		2200/1/AC	500	—	—	329.3	3.36
Ti-25Al-8Nb-1W	#53	As-Forged	RT	—	—	91.6	0.76
		As-Forged	500	—	98.9	122.2	1.54
		2200/1/AC	RT	—	156.1	202.6	1.07
Ti-25Al-8Nb-0.8W	#54	2200/1/AC	500	—	—	204.2	2.78
		As-Forged	RT	—	112.3	104.8	0.78
		As-Forged	500	—	137.1	125.1	1.36
Ti-25Al-8Nb-0.8W	#54	2200/1/AC	RT	—	135.3	152.4	1.43
		2200/1/AC	500	—	—	205.1	3.70

TABLE 5 (Cont'd)

Composition (o/o)	Alloy Number	Heat Treatment	Test Temperature (°F)	Strain Rate (Outer Fiber) in/in/min.	0.2% Offset Yield Strength(Ksi)	Maximum Fiber Stress at Fracture (Ksi)	Maximum Fiber Strain at Fracture (%)
Ti-25Al-8Nb-1W	#56	As-Forged	RT	•	141.8	141.8	1.10
			500		138.9	148.6	1.49
			800		119.3	179.4	Plastic
			800		262.9	276.0	1.97
Ti-25Al-8Nb-1W	#57	As-Forged	RT			288.1	3.36
			500				
			800				
			800				
Ti-25Al-8Nb-1W	#58	As-Forged	RT			107.0	0.86
			500		96.2	116.8	1.33
			800		88.2	135.8	Plastic
			800		209.8	264.9	3.01
Ti-25Al-8Nb-1W	#59	As-Forged	RT		155.9	217.1	Plastic
			500				
			800				
			800				
Ti-25Al-8Nb-1W	#59	As-Forged	RT			94.1	0.72
			500		90.2	122.1	2.05
			800		86.0	140.6	Plastic
			800		226.2	167.3	1.06
Ti-25Al-8Nb-1W	#59	As-Forged	RT			273.6	2.73
			500				
			800				
			800				
Ti-25.2Al-11Nb-0.18b	#60	As-Forged	RT			105.7	0.94
			500		87.8	119.0	2.07
			800		85.0	133.7	Plastic
			800		140.9	170.3	1.33
Ti-25.2Al-11Nb-0.18b	#60	As-Forged	RT			213.7	3.89
			500		100.0	135.8	2.80
			800		87.5	135.2	3.48
			800		75.5	130.9	Plastic
Ti-25.2Al-11Nb-0.18b	#61	As-Forged	RT		171.4	253.4	Plastic
			500		140.5	204.9	Plastic
			800				
			800				
Ti-24.2Al-11Nb-0.18b	#61	As-Forged	RT		101.7	140.4	2.92
			500		82.1	133.1	4.69
			800		69.7	114.0	2.78
			800		166.0	247.0	Plastic
Ti-24.2Al-11Nb-0.18b	#61	As-Forged	RT		142.5	210.4	Plastic
			500				
			800				
			800				

TABLE 5 (Cont'd)

Composition (a/o)	Alloy Number	Heat Treatment	Test Temperature (°F)	Strain Rate (Outer Fiber) in/in/min.	0.2% Offset Yield Strength(Ksi)	Maximum Fiber Stress at Fracture (Ksi)	Maximum Fiber Strain at Fracture (%)
Interaction Effects							
Ti-25Al-5Nb- 0.7C	Ti-1	1650/1/Ac	RT	0.0006	-	91.1	0.425
			400	0.0009	-	119.8	0.717
			600	0.0009	-	121.7	0.880
			800	0.0018	-	132.9	1.23
			900	0.0004	-	125.7	0.948
			1000	-	-	123.1	0.917
Ti-23.1Al-18.7Zr- 4.6B	Ti-30	As-Forged	1100	0.0004	103.0	118.8	Plastic
			600	0.0010	147.0	172.6	1.55
			800	0.0012	152.0	170.7	1.73
Ti-24Al-11Nb-2.5- B	Ti-32	As-Forged 2200/1/No	RT		98.1	118.5	1.69
			RT		109.2	129.9	1.76
			RT		258.6	271.1	2.16
			800		201.8	204.1	Plastic
Ti-25Al-7Nb-5Zr- 2.58a.2581	Ti-6	As-Forged 2200/1/Ac	800		111.8	130.1	1.52
			RT		-	116.7	0.863
			800		105.7	144.5	2.31

TABLE 5 (Cont'd)

Composition (g/o)	Alloy Number	Heat Treatment	Test Temperature (°F)	Strain Rate (Outer Fiber) in/in/min.	0.2% Offset Yield Strength(Ksi)	Maximum Fiber Stress at Fracture (Ksi)	Maximum Fiber Strain at Fracture (%)
Ti-24Al-11Nb- 5Cu-.25Si	Ti-50	As-Forged	RT	"1	118.1	140.9	1.78
		800	800		80.1	126.2	Plastic
		2200/1/Ac	RT		-	204.2	1.37
Ti-24Al-11Nb- 0.5Mn-.25Si	Ti-51	As-Forged	500		205.2	273.6	Plastic
		800	800		117.3	125.9	1.32
		2200/1/Ac	RT		80.2	135.6	Plastic
Ti-24Al-11Nb- .5Fe-.25Si	Ti-52	As-Forged	RT		-	199.1	1.40
		800	800		-	246.6	1.90
		2200/1/Ac	500		114.3	147.6	2.25
Ti-25Al-8Nb- 1Hf-.4C	Ti-59	As-Forged	RT		79.1	142.2	Plastic
		800	800		-	213.4	1.44
		2200/1/Ac	500		-	248.3	1.82
Ti-25Al-8Nb-1B	Ti-60	As-Forged	RT		-	150.9	1.09
		800	800		99.1	134.6	Plastic
		2200/1/Ac	RT		165.9	193.9	1.97
Ti-25Al-8Nb-.2Mn	Ti-61	As-Forged	500		122.0	179.8	Plastic
		800	800		-	113.4	1.00
		2200/1/Ac	RT		87.5	126.9	Plastic
Ti-25Al-8Nb-.2Mn	Ti-61	As-Forged	RT		162.5	193.7	1.36
		800	800		-	210.1	2.43
		2200/1/Ac	500		79.5	130.9	1.16
Ti-25Al-8Nb-.2Mn	Ti-61	As-Forged	RT		-	126.6	Plastic
		800	800		-	266.9	1.88
		2200/1/Ac	500		-	278.0	1.91

TABLE 5 (Cont'd)

Composition (e/o)	Alloy Number	Heat Treatment	Test Temperature (°F)	Strain Rate (Outer Fiber) in/in/min.	0.2% Offset Yield Strength(ksi)	Maximum Fiber Stress at Fracture (ksi)	Maximum Fiber Strain at Fracture (%)
Alpha two plus Beta Systems							
Ti-24Al-11Nb	#42	As-Forged	RT		105.8	128.8	2.08
			800		86.0	157.3	Plastic
			1000		66.0	104.9	Plastic
			1200		68.7	108.2	Plastic
			1400		46.9	72.3	Plastic
Ti-25.2Al-10.1Nb- .3W	Ti-44	As-Forged	RT		97.8	108.6	1.27
			800		134.0	179.2	2.77
			800		103.0	157.8	Plastic
			800		102.3	130.6	2.17
Ti-25Al-10Nb- 1W	Ti-48	As-Forged	RT		86.1	127.4	3.60
			800		65.3	103.6	Plastic
			800		131.9	150.4	1.89
			800		-	96.6	1.03
			800		-	96.3	1.11
Ti-25Al-13Nb	#47	As-Forged	RT		83.8	100.9	1.55
			800		68.4	125.8	Plastic
			800		193.1	232.8	2.68
			800		149.7	239.9	6.30
			1200		101.5	141.8	Plastic
Ti-25Al-10Nb- 1W	Ti-48	As-Forged	RT		108.9	165.1	Plastic
			800		114.3	168.9	3.96
			800		96.7	143.3	Plastic
			800		249.0	292.1	2.74
Ti-25Al-10Nb- 1W	Ti-48	As-Forged	RT		288.5	283.4	3.44
			800				

TABLE 5 (Cont'd)

Composition (o/o)	Alloy Number	Heat Treatment	Test Temperature (°F)	Strain Rate (Outer Fiber) Yield in/in/min.	0.2% Offset Yield Strength(Ksi)	Maximum Fiber Stress at Fracture (Ksi)	Maximum Fiber Strain at Fracture (%)
Mixed Hexagonal and Cubic Systems							
50:50/Ti ₃ Al:Zr ₃ In	T1-18	As-Forged	RT	0.0012	158.5	217.4	Plastic
			400	0.0012	155.0	210.4	Plastic
			600	0.0010	152.0	200.9	Plastic
			800	0.0011	162.0	205.5	Plastic
			1000	0.0009	153.5	211.3	Plastic
25:75/Ti ₃ Al:Zr ₃ In	T1-17	As-Forged	1100	0.0012	-	108.1	1.22
			1200	0.0012	90.0	102.9	1.72
75:25/Ti ₃ Al:Zr ₃ In	T1-19	As-Forged	400	0.0012	102.0	119.0	1.27
			600	0.0018	111.5	146.8	2.20
			800	0.0011	100.0	150.1	2.74
			900	0.0011	110.0	171.9	4.76
			800	0.0006	-	218.4	1.50
95:5/Ti ₃ Al:Zr ₃ Sn	T1-26	As-Forged	1000	0.0012	-	79.9	0.901
90:10/Ti ₃ Al:Zr ₃ Sn	T1-27	As-Forged	1000	0.0012	112.0	125.5	1.50
				0.0010	137.0	162.7	Plastic
Zr ₃ Al	T1-21	As-Forged	RT	0.0010	124.0	130.7	Plastic
			800	0.0010	-	238.1	1.95
25:75/Ti ₃ Al:Zr ₃ Al	T1-22	As-Forged	800	0.0011	-	-	-
50:50/Ti ₃ Al:Zr ₃ Al	T1-23	As-Forged	1000	0.0019	-	157.9	1.69

TABLE 5 (Cont'd)

Composition (g/o)	Alloy Number	Heat Treatment	Test Temperature (°F)	Strain Rate (Outer Fiber) in/in/min.	0.2% Offset Yield Strength(Ksi)	Maximum Fiber Stress at Fracture (Ksi)	Maximum Fiber Strain at Fracture (%)
75:25/Ti ₃ Al:Zr ₃ Al	Ti-24	As-Forged	RT	0.0019	136.0	144.8	1.43
			400	0.0019	135.0	166.0	1.93
			600	0.0018	126.0	194.4	3.38
			800	0.0018	118.0	209.9	Plastic
75:25/Ti ₃ Al:Zr ₃ Al+5In	Ti-43	As-Forged	RT	0.0012	-	123.0	0.964
			400	0.0011	131.0	135.9	1.38
			600	0.0013	126.5	159.1	1.78
			800	0.0012	126.0	168.4	2.67
75:25/Ti ₃ Al:Zr ₃ Al	#22 (Ti-21)	As-Forged	RT	-	-	105.5	0.789
			800	-	101.3	165.8	Plastic
			1650/8/AC	-	-	96.5	0.768
			2200/1/AC	-	-	189.5	1.26
			1652/500/AC	-	-	159.2	1.36
			RT	-	82.1	102.5	0.794
75:25/Ti ₃ Al:Zr ₃ Al+ 11In	#25	As-Forged	RT	-	-	171.6	Plastic
			400	-	-	81.2	0.762
			600	-	90.0	130.8	0.707
			800	-	-	126.4	2.31
75:25/Ti ₃ Al:Zr ₃ Al+ 5In	#26	As-Forged	RT	-	-	104.9	0.744
			800	-	149.9	175.2	2.37
			1650/8/AC	-	-	96.1	0.618
			2200/1/AC	-	-	79.9	0.510
			RT	-	-	82.7	0.539
82.5:12.5/Ti ₃ Al: Zr ₃ Al	#49	As-Forged	RT	-	-	81.9	0.598
			RT	-	-	174.5	1.15
			800	-	196.0	256.5	2.94

TABLE 5 (Cont'd)

Composition (g/o)	Alloy Number	Heat Treatment	Test Temperature (°F)	Strain Rate (Outer Fiber) in/in/min.	0.2% Offset Yield Strength(Ksi)	Maximum Fiber Stress at Fracture (Ksi)	Maximum Fiber Strain at Fracture (%)
75:25/Ti ₃ Al: Zr ₃ Al ₁₅	T1-49	As-Forged 2200/1/Ac	RT	..	129.1	0.902	
			800	↓	223.1	Plastic	
			RT	..	174.5	1.17	
			500	↓	248.3	2.58	

*These numbers represent total strain

**Outer fiber strain rate 0.0007 to 0.0020 inch/inch/minute

respect to the baseline alloy. In the two (or more) element additions group, nickel results in a slight improvement in properties with respect to the baseline, but most other modifications tend to produce a wider and flatter ductility transition zone. For example, the addition of one atomic percent tungsten (Ti-38) results in an equivalent ductility value at 400°F to the baseline alloy at 800°F although "plastic" values are observed at nearly the same temperature. By increasing the base niobium contents to 8% in this class of alloys, considerable improvements are evident. For example, alloys Ti-54 through 58, containing a fourth transition element, show bend ductilities at room temperature equal to those at 800°F for the baseline alloy. Scaling up these alloys to the two-pound ingot level led to some reduction in properties in the as-forged condition, but these could be restored by heat treatment (again these differences can be traced to Section Size/Heat Treatment/Structure Effects discussed in more detail below).

Results from the Interactions Group, which contains examples of the higher niobium content alloys discussed in more detail below, conform in general to comparable alloys without additions of silicon, carbon, etc. As the aim of these additions was to modify creep rupture behavior, the retention of bend properties can be taken as an encouraging preliminary result.

Alloys from the third subdivision, Alpha Two Plus Beta Alloys, show the best bend ductility. For example, the Ti-24Al-11Nb alloys show bend values at room temperature equivalent to the baseline alloy at 1000°F. It would appear that the onset of good low temperature plasticity occurs between 5 and 11% Nb and these attractive characteristics are maintained up to 15% Nb. Further, the addition of small amounts of bismuth,

antimony or silicon do not change the ductility values at room temperature. Indeed the alloy containing antimony (#60) was the first example of an alloy with >4% bend ductility at ambient temperature. We shall deal with the effect of heat treatment on structure and tensile properties in the next section; it is sufficient at this stage to note that results in Table 5 indicate a strong effect. A summary of the improved ductility characteristics produced by increasing niobium content is given in graphical form in Figure 12.

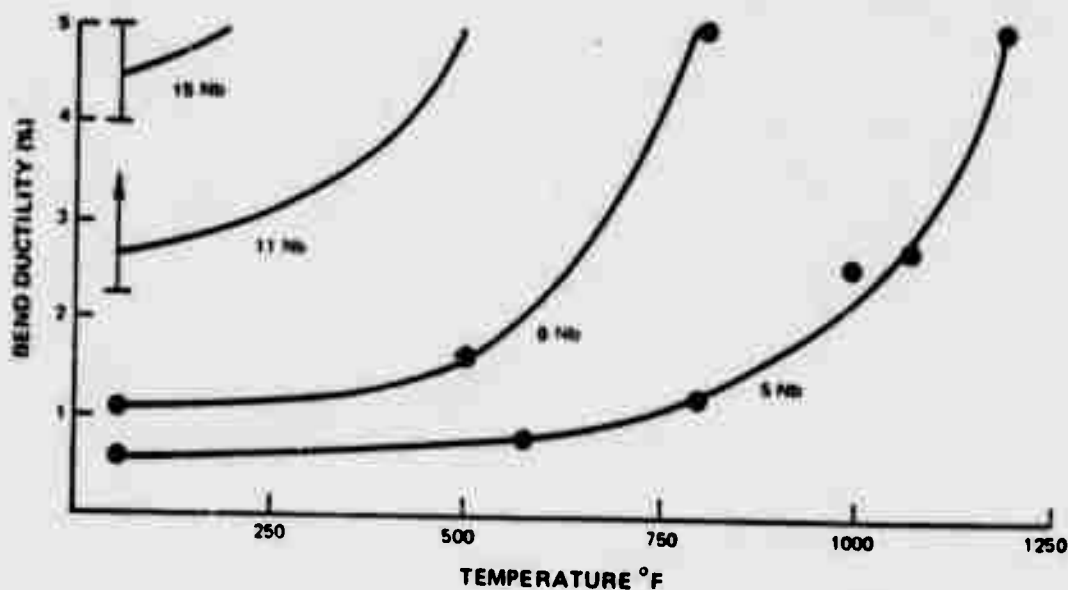


Figure 12. Bend Ductility as a Function of Temperature in Ti-Al-Nb Alloys

The last group of alloys, mixed cubic plus hexagonal type, were evaluated before the alpha two plus beta systems discussed above. Initial results were encouraging in that the model system, $\text{Ti}_3\text{Al-Zr}_3\text{In}$, showed plastic behavior over the entire range of temperatures tested. Further, the results obtained on the $\text{Ti}_3\text{Al:Zr}_3\text{Al}$ base alloy (#22, $(\text{Ti}_{0.75}\text{Zr}_{0.25})_3\text{Al}$) showed good bend properties compared with the baseline alloy.

Evidence of plastic behavior at room temperature in the heat treated condition was obtained. However, it was noted that the quite high zirconium content of the alloys tended to compromise the oxidation characteristics of the base alloy, for evidence of rapid oxidation at temperatures as low as 800°F was obtained. Reducing the zirconium content (e.g., alloy #49) improved the oxidation characteristics but bend ductility was reduced. Another discouraging feature was that all attempts to modify the properties of the $(\text{Ti}_{0.75}\text{Zr}_{0.25})_3\text{Al}$ base alloy by additions of a fourth element were unsuccessful. Indium, tin or lanthanum containing alloys showed lower ductility and the several heat treatments applied to these alloys did not produce any improvement. Thus, we have tended to de-emphasize these alloys in more recent studies.

C. Heat Treatment and Structure

As the program has proceeded, it has become increasingly clear that the structural modifications that can occur in various alloys have a critical effect on material properties. It should be noted at the outset that many of the kinetic and structural details of transformation in these alloys are imperfectly known. Much needed analysis by TEM and other techniques is in progress at the present time at Carnegie-Mellon University and the University of Florida. However, the general characteristics of transformation are known and especially in the Ti-Al-Nb system show many similarities with most dilute alloy systems.

A schematic phase section along the composition line $\text{Ti}_3\text{Al}-(\text{TiNb})_3\text{Al}$ is shown in Figure 12, which also includes the approximate position of the martensitic transformation that occurs on quenching from the beta phase field. The characteristics of the martensite formed in Ti-Al-Nb alloys

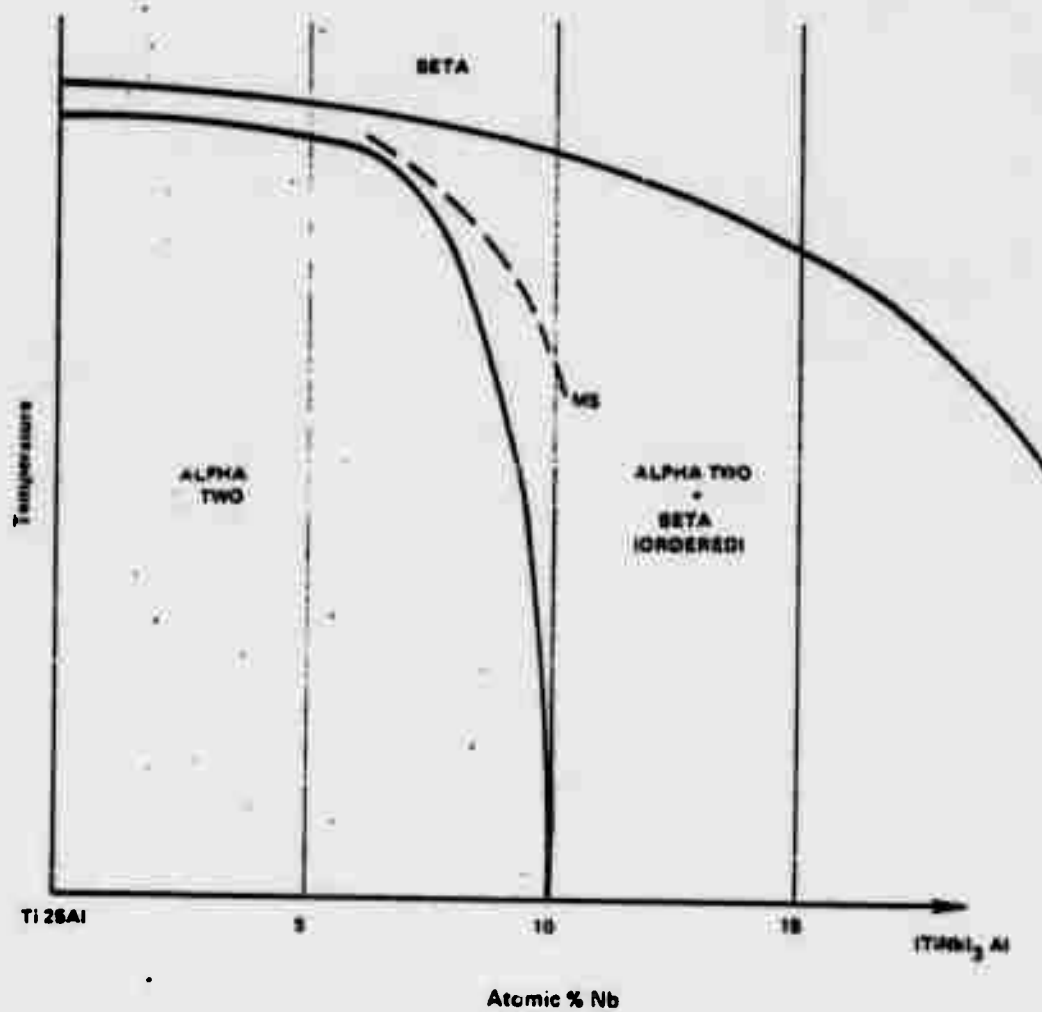


Figure 13. Schematic Phase Section Along the Composition Line $(\text{TiNb})_3\text{Al}$

(although with slightly different compositions) were studied by Williams and Blackburn.⁽⁷⁾ It was shown that the transformation in the base Ti_3Al and dilute alloys was similar to that observed in pure titanium; large rather ragged plates of the alpha two phase forming on quenching. Although the ordering reaction could not be suppressed the domain size can be very small in quenched structures. At higher niobium contents ($\sim 10\%$) very fine martensitic structures are formed and at yet greater concentrations the beta phase is retained on quenching. Tempering of the quenched structures can lead to rather complex structures; there is a tendency in both the single and two-phase regions for a recrystallization type reaction to occur at the grain boundaries. An example is shown in Figure 14(a). Such transformations, if taken to completion, can convert a fine acicular structure to a coarse almost equiaxed condition, see Figure 14(b). As the niobium content increases the tendency to this recrystallization tends to diminish. The tempering reactions in the beta phase have not been studied in great detail to date, but it appears that the anticipated precipitation of the alpha two phase occurs in the form of fine lathes.

As we shall see, very rapid quenching of these alloys from the beta phase field is not a practical heat treatment method as it results in strong and rather brittle structures; further these structures may be unstable on tempering. The tendency to form cracks on quenching is another reason for avoiding such treatments.

Structures formed by less severe cooling rates are therefore of more interest from a practical standpoint. Here again the parallel with conventional titanium alloys is quite striking, including the dependence on initial structure. If a conventional alpha-beta alloy is worked in the two-phase



500X

- (a) Initiation of reaction at grain boundaries in Ti-25Al-2.5Fe water quenched from 2050°F and tempered for one hour at 1400°F.



100X

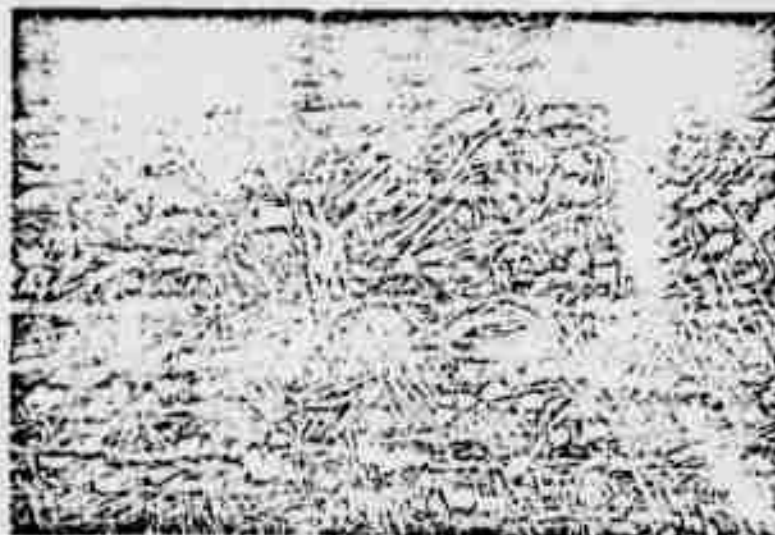
- (b) Completion of the reaction to form an equiaxed structure in Ti-25Al-5Nb water quenched from 2200°F and tempered for 87 hours at 1500°F.

Figure 14. "Recrystallization" Reaction Produced by Tempering Some Martensitic Structures in Alpha Two Alloys

region, an equiaxed mixture of the two phases is formed and the beta phase may transform on subsequent cooling. Similar structures can be formed in alpha two alloys, examples are shown in Figure 15(a) and (b). Heat treatment or forging above the beta transus will result in acicular structures. In alpha two type alloys, these may range from a virtually unresolvable structure after quenching, Figure 16(a), to a coarse colony (groups or packets of plates with similar orientation) structure, Figure 16(b). Intermediate cooling rates produce a Widmanstatten arrangement of much smaller alpha two plates; an example is shown in Figure 16(c).

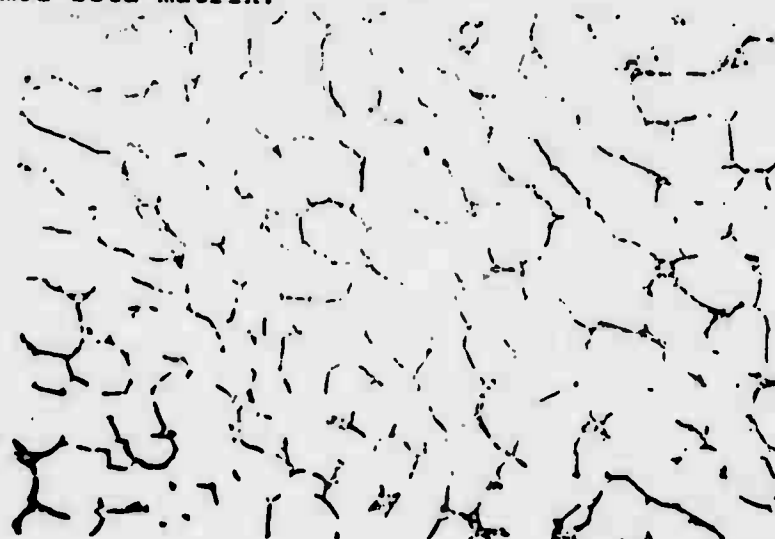
Compositional modification of a Ti-Al-Nb base alloy can change the phase equilibria, however, the evidence seems to indicate that these changes are reasonably straightforward. Transition elements tend to act as beta stabilizers, and it appears that the higher the group number, the greater is this tendency. Thus the addition of 1% of nickel can stabilize the beta phase in a Ti-25Al-5Nb alloy; this element may also influence the ordering tendency in the beta phase, but additional information is needed to prove this. It is possible that additional phases may be found as more is learned; for example, iron additions could lead to the formation of Ti_2Fe identified in Ti-Al-Fe alloys.

The Ti-Al-Zr system and related alloys have not been as extensively evaluated in the present study. The anticipated lowering of the beta transus by increasing zirconium content was confirmed. Two-phase mixtures of the DO_{19} and $L1_2$ phases were found in the Ti-Al-Zr-In alloys and produced rather photogenic structures, an example is shown in Figure 17, and it appears that a rather small amount of $L1_2$ structure can form in the $(Ti_{0.75}Zr_{0.25})_3Al$ alloy. In modifications of the latter alloy the phase structure becomes very complex and is not fully understood.



200X

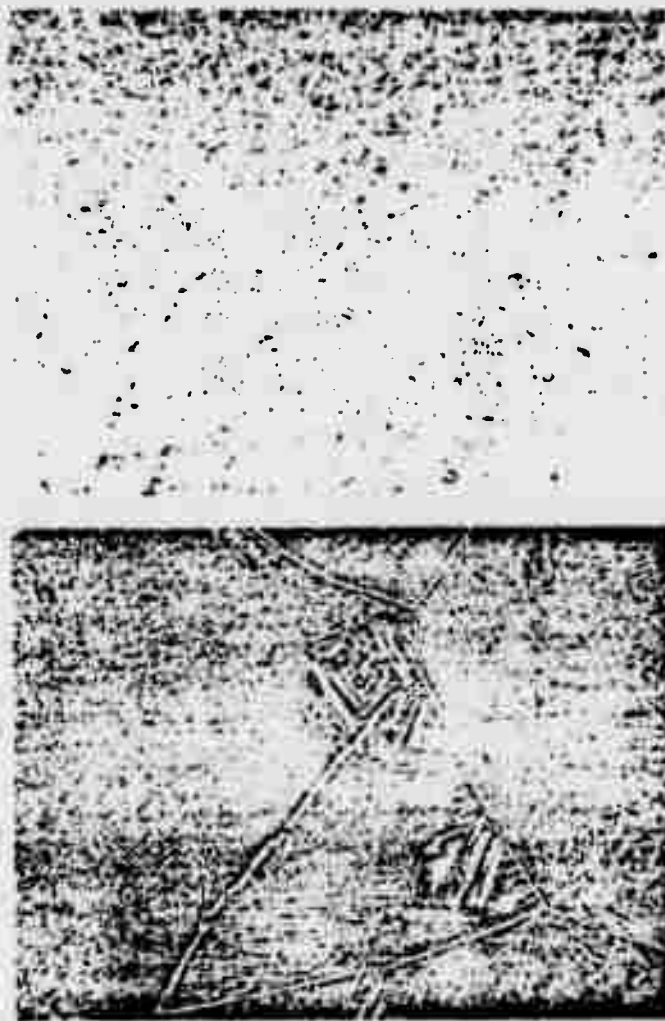
- (a) Ti-24Al-11Nb-0.5Ni-0.25Si forged near the beta transus showing equiaxed primary alpha two in a coarse transformed beta matrix.



500X

- (b) Ti-25Al-5Nb-1Ni worked low in the alpha-beta phase field showing predominantly equiaxed alpha two and grain boundary transformed beta.

Figure 15. The Influence of Alpha-Beta Working on Alpha Two Alloy Structure



- | | |
|------|--|
| 100X | (a) Ti-25Al-8Nb-1Hf
water quenched showing
unresolved marten-
sitic structure. |
| 50X | (b) Ti-25Al-5Nb-1Ni-1W
slowly cooled showing
an acicular colony
structure. |
| 200X | (c) Ti-25Al-10Nb
intermediate cooling
rate showing an acicular
Widmanstätten structure. |

Figure 16. The Influence of Cooling Rate from the Beta Phase Field on Structure of Alpha Two Alloys



Figure 17. Transmission Electron Micrograph Illustrating the Heavily Faulted $\text{DO}_{19}:\text{L}_{12}$ Phase Mixture Observed in Alloy $\text{Ti-12.5Al-37.5Zr-12.5In}$, $(\text{Ti}_3\text{Al})_{0.5}(\text{Zr}_3\text{In})_{0.5}$

7. Mechanical Properties

A. Hardness

As can be seen from the above sections, a large number of hardness determinations have been performed during the course of these studies. In cases in which tensile properties have been measured subsequently, it has been found that the hardness (VDN) can be correlated with the room temperature yield strength (σ_y) through the following relationship.

$$\sigma_y = \frac{VDN}{3.2}$$

Use of this equation has proved a quick and inexpensive method for assessing the mechanical property capability of the alpha two type alloys after heat treatment.

B. Tensile Testing

A much smaller number of alloys were selected for tensile testing and it must be noted that many tests remain to be completed. Table 6 lists the results obtained up to April, 1977. Again, a useful point of comparison are the tensile data obtained for the Ti-25Al-5Nb alloy presented in Section III. In nearly all cases, specimen blanks were heat treated prior to machining; the heat treatments selected were derived in part from the bend results cited above and also by an iterative process. It must also be noted at this point that oxygen content of this class of alloys may prove to have a dominant effect on ductility. As noted in II.4., these materials were prepared with a very low oxygen content in the 0.04 to 0.05% range.

TABLE 6

Tensile Results for α_2 Alloy Compositions

Com- position (a/o)	Alloy No.	Heat Treat- ment	Test Temper- ature (°F)	0.2% Offset Yield Strength (ksi)	Ultimate Tensile Strength (ksi)	% Elong- ation (Plastic)	% Reduction in Area
Ti ₃ Al	22	1800/1/AC	RT	-	80.4	-	-
			RT	80.6	80.6	0.42	-
			800	68.8	94.3	1.4	2.4
Ti-25Al-5Nb-1Cu	33	2200/1/AC	RT	83.5	97.8	1.4	2.3
			500	73.2	122.6	2.4	-
			1200	68.8	85.1	5.4	9.3
Ti-25Al-5Nb-.5Ni-1W	55	2200/1/AC	RT	106.8	112.6	0.4	-
			500	89.0	109.3	1.2	1.7
			900	81.1	120.6	1.3	7.6
			1200	69.7	91.4	5.6	12.0
Ti-25Al-5Nb-1Ni-1W	45	2200/1/AC	RT	131.1	144.0	0.75	-
			RT	123.8	140.9	0.91	-
			500	108.0	152.3	4.8	-
			1200	67.4	91.1	3.6	3.1
			1200	62.1	59.2	4.6	-
Ti-26.4Al-4.8Nb-0.8Fe	29	2200/1/AC	RT	-	87.0	0.30	-
			500	75.2	83.8	0.63	1.7
Ti-25Al-3Nb-1Fe	53	2200/1/AC	RT	89.5	89.9	0.4	1.6
			500	71.8	85.0	1.1	2.5
			900	70.1	102.5	3.8	9.2
			1200	62.9	77.7	5.5	6.4
Ti-25Al-3Nb-.8Fe	54	2200/1/AC	RT	100.0	109.0	0.6	0
			500	81.1	121.7	4.4	6.5
			900	65.9	111.2	5.3	11.2
			1200	77.9	107.0	9.2	9.3
Ti-26Al-9.1Nb-.4Hf-.8Si	32	2200/1/AC	RT	140.6	141.0	0.43	-
			500	127.2	151.2	1.9	2.4
			1200	106.2	127.7	2.1	3.1
Ti-24Al-11Nb	42	As-Forged	RT	66.2	75.0	0.90	3.3
			RT	60.2	74.4	1.45	3.2
			1200	35.9	57.2	12.6	12.8
		2200/1/AC	RT	157.7	165.7	1.0	3.9
			RT	175.4	188.0	0.73	-
		2200/1/TC	RT	110.3	140.1	4.9	7.1
		1975/1/AC	RT	67.5	86.2	1.68	3.3
Ti-24Al-11Nb-.25Si	52	2200/1/TC	RT	66.4	86.5	3.1	4.9
			1200	42.2	66.8	14.9	31.0
		2000/1/2/AC	RT	78.2	105.8	3.1	3.1
		2000/1/AC	RT	92.5	119.6	3.2	5.0
Ti-25Al-15Nb	47	2200/1/TC	RT	102.4	128.6	3.9	4.9
			500	86.1	123.8	9.3	7.3
			1200	79.1	103.3	4.0	12.2

TABLE 6 (Cont'd)

Con- position (a/c)	Alloy No.	Heat Treat- ment	Test Tempe- rature (°F)	0.2% Offset Yield Strength (ksi)	Ultimate Tensile Strength (ksi)	% Elong- ation (Plastic)	% Reduction in Area
T1-25A1-5Nb	38	2200/1/AC	RT	60.4	67.2	0.3	2.8
T1-25A1-6Nb-1A	50	2050/1/SC ¹ & 2/RT AC	RT	115.7	138.1	0.95	→
T1-25A1-6Nb-1Ta	57	2000/1/AC	RT	127.0	130.2	0.3	→
T1-25A1-6Nb-1Mo	58	2050/1/SC 3 Min/AC	RT	130.4	-	(40.2)	→
T1-25A1-6Nb-1V	59	2000/1/AC	RT	150.3	-	(70.2)	→
T1-2-.2Al-11Nb-.1Sb	60	2000/1/AC	RT	118.9	149.9	2.90	→
T1-2-.2Al-11Nb-.1B1	61	2000/1/AC	RT	154.0	-	(70.2)	→

S.C. - Slow Cool

S.Q. - Salt Quench

* - Broke in Grip

* - Broke in Extensometer Ridge

The alloys based on Ti-25Al-5Nb with ternary and quaternary additions show limited ductility at room temperature, although the copper modification (#35) does show over 1% elongation and 2% reduction in area. Alloys containing nickel and tungsten appear to have improved ductility at intermediate temperatures compared to the baseline alloy. Likewise, the modifications of the 8Nb base alloy show improved intermediate temperature characteristics. However, it can be seen that major improvements are available at higher niobium contents.

In the Ti-24Al-11Nb alloy, the ductility and strength can be related to the structure as is done in Figure 18. A rapid cooling rate results in a partially transformed structure with a high yield strength and finite but not large ductility. Intermediate cooling rates result in a fine Widmanstätten structure with good ductility and a strength level >100 ksi. Slow cooling rates give a colony type structure with associated low strength and ductility. Similar strength results were obtained for the same alloy modified with silicon but the ductility values showed less variation.

C. Creep Rupture

Testing to date has been performed at 1200°F/55 ksi for the majority of alloys. As a point of reference, the alloy Ti-25Al-5Nb (Ti-16Al-10Nb weight %) exhibited a life of 90 hours under these conditions which on a density corrected basis is equal to INCO 713C. Data for alloys tested to date in this program are given in Table 7, and it can be seen that large variations in creep capability are observed. In Ti-25Al-5Nb base alloys, both copper and nickel additions reduce creep rupture life; comparison of the lives of alloy #55 and #45 show that the lower the nickel content, the better the lives. On the other hand, iron additions may have much



2°F/sec

65 Ksi

1.8%



7°F/sec

110 Ksi

4.9%



25°F/sec

170 Ksi

1.4%

Cooling rate

σ_y

Elongation

Figure 18. Structure Heat Treatment Effects on Ti-24Al-11Nb

TABLE 7
Creep Rupture Results for α_2 Alloy Compositions

Composition (a/o)	Alloy No.	Heat Treat- ment (°F/HRS)	Test Temper- ature (°F)	Stress (ksi)	1% Creep (Hrs)	Time To Rupture (Hrs)	Elong- ation (%)	Reduction In Area (%)
75:25/Ti3Al-Zr3Al	22	1800/1/AC	1200	55	-	0.1	-	-
Ti-25Al-5Nb-1Cu	33	2200/1/AC	1200	55	2.37	7.5	7.6	9.3
Ti-24Al-9.2Nb-.49Nb-.55Si-1.0%	55	2200/1/AC	1200	55	12.87	52.0	6.6	6.6
Ti-25Al-5Nb-1Ni-1%	45	As-Forged 2200/1/AC	1200	55	0.64	2.8	7.0	6.0
				55	-	3.0	4.0	-
Ti-26.4Al-4.8Nb-.8Fe	29	2200/1/AC	1200	55	101.1	345.0	4.8	-
Ti-25Al-8Nb-1Fe	53	As-Forged 2200/1/AC	1500	15	1.83	25.0	21.6	71.0
				55	4.74	60.8	7.2	9.6
Ti-25Al-8Nb-.8Fe	54	As-Forged 2200/1/AC	1500	15	1.36	25.4	20.6	60.4
				55	3.26	79.7	11.4	17.2
Ti-26Al-9.1Nb-.4Hf-.8Si	32	2200/1/AC	1200	55	178.7	344.2	1.5	2.8
Ti-24Al-11Nb	42	As-Forged 2200/1/AC	1200	55	-	B.O.L.	32.1	33.3
				55	1.52	14.1	7.8	4.6
Ti-24Al-11Nb-.25Si	52	2200/1/FC 2000/1/2/AC	1200	55	0.0	5.5	14.4	23.2
		2000/1/AC	1200	55	3.37	61.4	9.4	12.5
				55	3.08	68.1	9.2	4.2
Ti-25Al-15Nb	47	2200/1/FC	1200	55	23.4	130.9	3.6	6.4

less influence on life; in alloy #29, however, the aluminum content is slightly higher and this in itself may contribute to the excellent life of >340 hours. As the niobium content of the alloys is increased to 8% and in the presence of iron (#53 and #54), the creep rupture capability is close to the goal. Again in a similar base alloy with slightly higher aluminum content and small additions of hafnium and silicon, a threefold increase in life is obtained.

Further increases in niobium level into the range in which ambient temperature tensile ductility is achieved produces a marked change. The Ti-24Al-11Nb alloy shows very poor life in the as-forged condition, which it should be remembered exhibits low strength. Even in the heat treated condition, however, the life capability is still about an order of magnitude less than the goal level. The addition of silicon (#52) improves the situation considerably bringing the life values back to about two-thirds of the required level. Surprisingly, the rupture life improves again in the Ti-25Al-15Nb alloy, indicating that low temperature ductility can be combined with adequate stress rupture properties.

In most of the alloys tested stress rupture ductility was adequate; if we take the nickel base alloy INCO 713C as the guideline about 5% elongation would indicate a useful goal. A slight trend to lower ductility can be detected for alloys with aluminum contents >25%. The other point of interest is the outstanding ductilities of the iron-containing alloys tested at 1500°F, although the rupture lives are poor. Earlier work at P&WA had indicated the beneficial effect of iron on ductility although the effect seems confined to the higher temperature range.

The one test performed on a Ti-Al-Zr type alloy resulted in

a very low life which could serve to reinforce the conclusion that this base system is not a good base for further alloy development.

Testing on the Ti-Al-Hf-C alloy (Tl-1) was conducted in the early stages of the study and the results demonstrated for the first time the superiority of beta processed structure. The test result at 1200°F showed a life improvement of five over goal properties, but this advantage was not maintained at higher temperatures.

8. Summary and Conclusions

From an initial "broad brush" attack on the problem of ductility in alpha two type alloys, the search for attractive alloys is narrowing to the Ti-Al-Nb system. Even within the Ti-Al-Nb system, some property compromises are evident, for the achievement of ductility is accompanied by reductions in stress rupture capability. The situation can be represented schematically on a ternary diagram as shown in Figure 19, which includes both rupture lives and also indicates alloys in which ductility has been observed at room temperature. It can be seen that improved ductility and creep rupture properties can be achieved in alloys with high niobium contents (e.g., Ti-25Al-15Nb) which is an undesirable direction because the density increases. Another direction is to increase the aluminum content, a more desirable modification from a density viewpoint, but indications are that tensile ductility tends to be reduced by such modifications. A more complete study of the influence of Nb:Al ratio in these alloys is clearly warranted and will be undertaken in the third year of this program.

An alternative method of improving stress rupture properties,

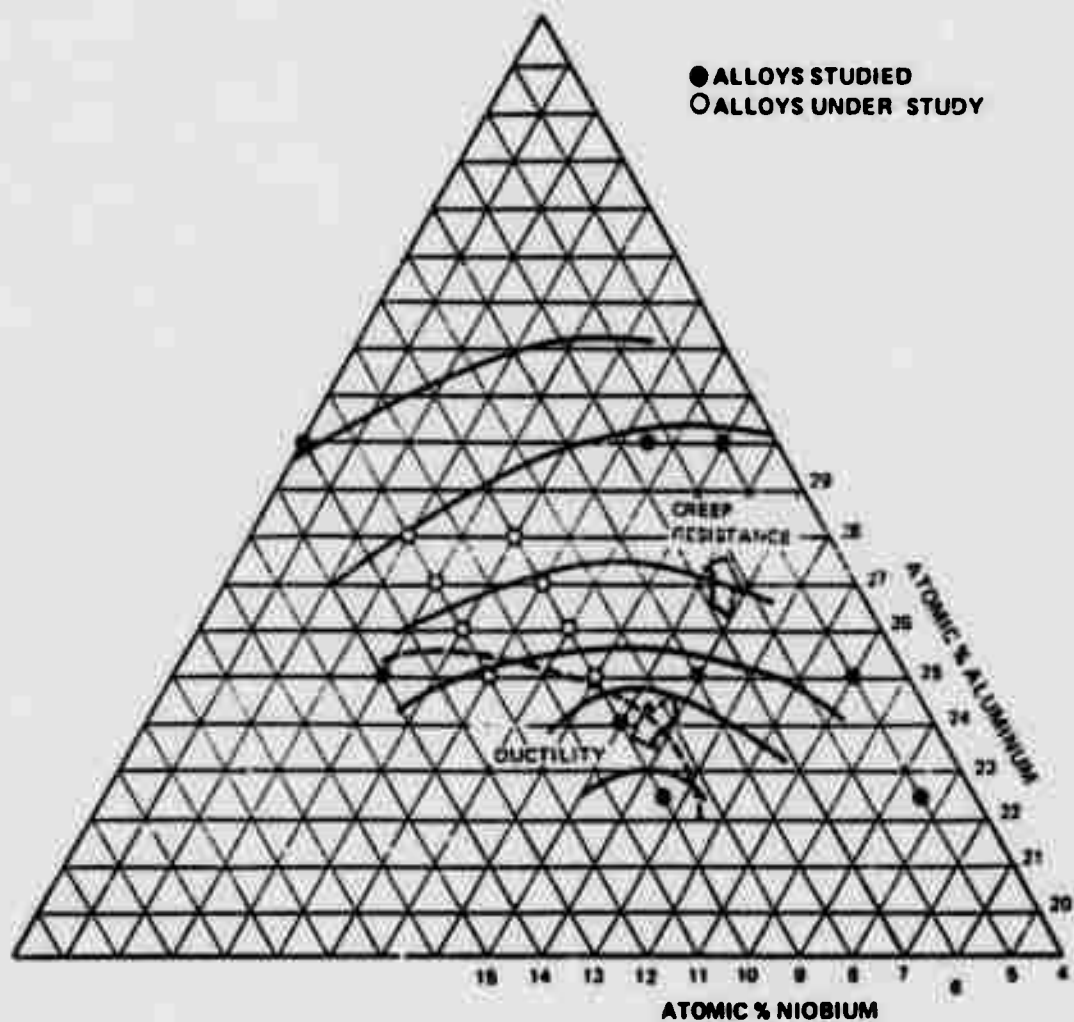


Figure 19. Schematic Presentation of Creep Resistance and RT Tensile Ductility in the Ti-Al-Nb System

without compromising ductility, is the addition of elements capable of introducing dynamic strain aging at high temperatures. One experimental alloy containing silicon has been tested and the results indicate that an improvement in creep rupture life has been achieved. It is probable that other elements or combinations may be necessary to produce improvements at higher temperatures ($\sim 1400^{\circ}\text{F}$) but, at present, this is speculation. This approach is derived directly from conventional high temperature titanium alloy practice; it will be interesting to see how far the parallels between these and the alpha two systems extend. For example, would zirconium be an effective addition to a silicon alloy modification?

Another direction of alloy development that is being actively pursued is the replacement of some of the niobium in Ti-Al-Nb alloys by other transition elements. Depending on which element is selected, reductions in density could be accomplished by such modifications. There are indications that the strength levels can be markedly changed by the addition of the early transition elements, as the results from the Ti-25Al-8Nb series indicate. The latter transition elements, such as copper, iron and nickel, may produce some changes in ductility, but appear to reduce both elevated temperature tensile strength and stress rupture capability. The only problem with evaluating these potential effects are the large number of variables or compositional modifications that can be produced. Completion of the test program currently in progress may indicate some of the more promising directions.

One difference between the Ti-Al-Nb base alpha two alloys and conventional titanium alloys is in the influence of structure on properties. Beta processing of conventional alloys tends to produce both lower strength and ductility

while the reverse seems true in alpha two alloys. There are certain parallels in achieving creep rupture resistance between both alloys, but even in this case the details seem to differ somewhat. Thus a fine Widmanstätten structure appears to produce the best creep rupture properties in alpha two alloys, whereas coarser colony acicular structures are superior in conventional alloys. One of the most challenging aspects of the successful development of alpha two alloys is defining the optimum heat treatment. The efforts to do so have been discussed above and some progress can be claimed, however, thermal stability and other factors still need elucidation. The achievement of the desired structures in material of various section sizes is not a trivial problem and will be discussed in more detail in Section III.

The other alloys that have been studied, although offering some advantage in at least ductility over the base compound, do not seem to be as attractive as the Ti-Al-Nb base alloys discussed above. Although some of the model systems based on the Ti-Al-Zr system show attractive ductility characteristics, the alloys are impractical. Further attempts to perturb the $DO_{19} > L1_2$ reaction towards the Ti_3Al composition have not been successful and this approach has been abandoned for at least the present. No other candidate ternary system has emerged from the studies.

Thus we conclude that the Ti-Al-Nb system appears to offer the best systems for achieving the goal properties in Ti_3Al base systems. Ductility at room temperature can be produced coupled with useful tensile strength levels. Heat treatment/structural control are a critical element of controlling properties. The results obtained to date are promising and can be used to point the way to additional alloy development.

III. ALLOY SCALE-UP AND CHARACTERIZATION

1. Introduction

The objectives of this segment of the program were to produce sufficient quantities of high quality wrought product to conduct a detailed property evaluation. The mechanical property evaluations were performed using test techniques and conditions pertinent to the requirements of high temperature engine components.

In the first year of the program, one alloy was selected for evaluation. Although little background information was available at that point in time, it was decided to choose an alloy from the Ti-Al-Nb system; specifically, the alloy Ti-16Al-10Nb* (Ti-25Al-8Nb). Further a powder metallurgical approach to alloy fabrication was selected based on the success of this method for TiAl alloys at the Air Force and the Government Products Division of Pratt & Whitney Aircraft. The powder was consolidated by HIP and subsequently forged. After a screening program to determine the process cycle which gave the best combination of properties, this procedure was applied to sections of the forgings. A comprehensive mechanical and physical property evaluation was performed on this material.

Alloy selection for the second year effort was based on the results of the Alloy Development program described in Section II. Three alloys were chosen all based on the Ti-Al-Nb system

* In this section the alloy compositions will be given in weight percent; the composition in atomic percent will be given in brackets the first time an alloy is cited.

as follows:

Ti-13.5Al-21.5Nb	(Ti-24Al-11Nb)
Ti-13.5Al-21.5Nb-0.1Si	(Ti-24Al-11Nb-0.25Si)
Ti-15Al-16Nb-3.8Hf	(Ti-25Al-8Nb-1Hf)

Ingots of these alloys were prepared by conventional consumable arc melting, conditioned and forged. A more limited mechanical property test program is in progress on material from these forgings. Emphasis is placed on the determination of tensile and creep rupture properties over a range of temperatures and a fatigue evaluation at 800°F.

2. Experimental Techniques and Results

First Year Program - The alloy selected for study in the first year's program was Ti-16Al-10Nb (Ti-25Al-5Nb atomic %). The planned characterization program is represented in Figures 20 and 21. Task I effort centered on the screening of process conditions to define the parameters for Task II characterization.

A. Material Procurement and Consolidation

Eighty-five (85) pounds of nominal Ti-16Al-10Nb rotating electrode powder produced by Nuclear Metals Corporation was supplied by the Air Force. Starting ingot for this powder was produced by Teledyne Titanium. The analysis of ingot and powder materials is shown in Tables 8 and 9.

Powder consolidation was performed by hot isostatic pressing using the following procedure. Four powder containers welded from 0.065" thick Ti-5Al-2.5Sn sheet stock, with the configuration shown in Figure 22, were fabricated. Net cylinder length prior to consolidation was approximately 9" with a

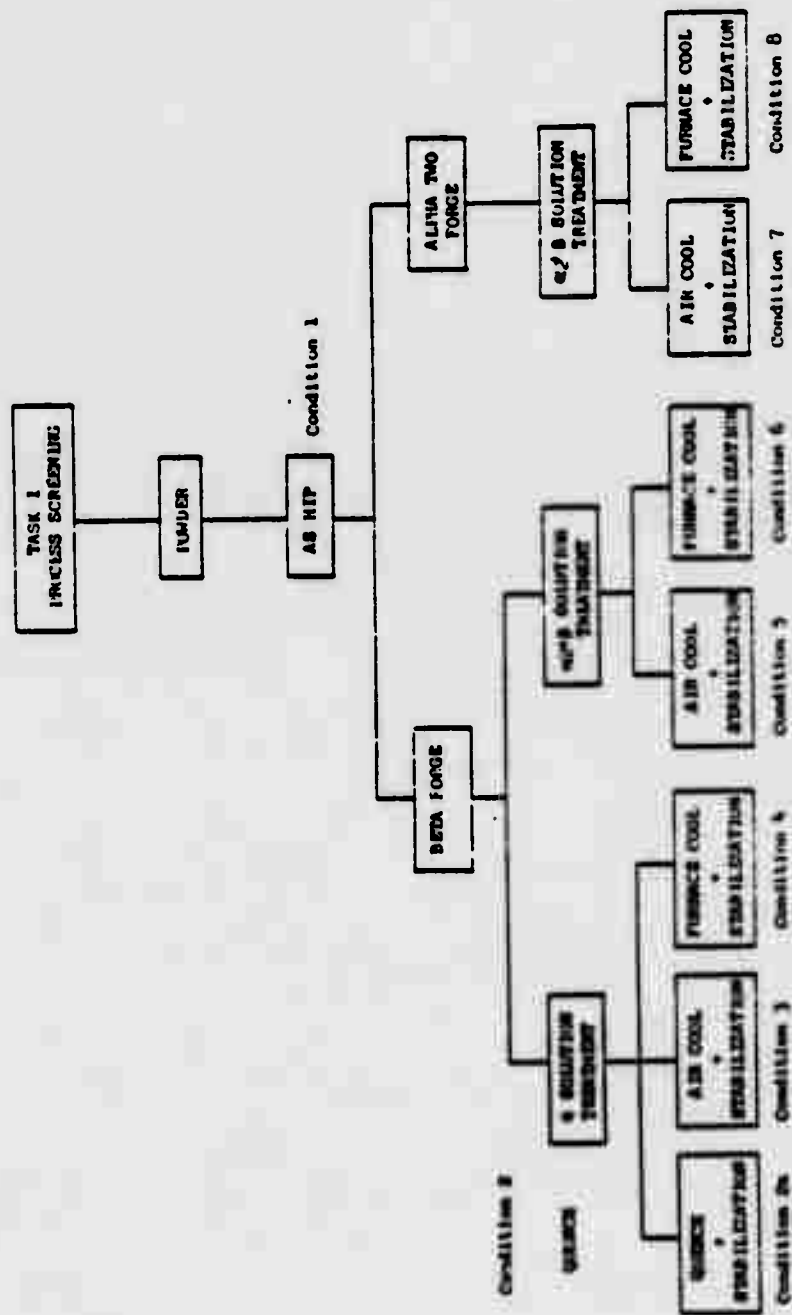


Figure 20. Process Selection

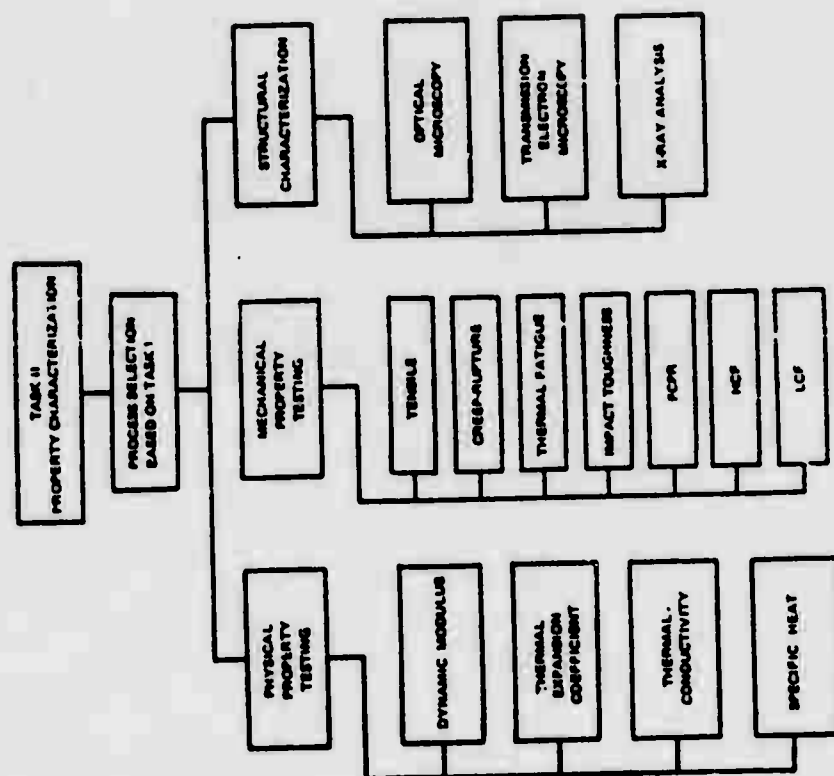


Figure 21. Property Characterization

TABLE 8

Chemical Composition of Titanium Aluminide Alloy

Heat 398 - Ti-15.8Al-10Cb

<u>Element</u>	<u>Spec. Max.</u>	<u>Cast Bar</u>	<u>Powder (Nuclear Metals)</u>	<u>Powder (P&WA)</u>
Ti		Bal.	Bal.	Bal.
Al	16.3	16.25	16.46	15.9
Cb		9.94	10.25	10.3
H	.01	.0089	.0041	.0019
N	.01	.0086	.0012	.01
O	.10	.12	.0839	.08
Zn	.01	<.01	<.01	<.01
C	.02	.010	.0070	.006
Cu	.02	.025	.01	<.01
Fe	.05	.065	.06	.04
S	.05	.025		<.002
W	.05	<.05	<.01	<.01
Ni	.01	.035	<.01	.01
Mg	.01	<.001	<.01	<.01
Mn	.01	<.001	<.01	.002
Mo	.02	<.001	<.01	<.1
Sn	.02	<.001	.04	.01
Si			.015	<.1

TABLE 9
Nuclear Metals Reported
REP Titanium Aluminide Powder Size Distribution

HEAT 398 - Ti-15.8Al-10Cb

Percent Retained on Screen:

<u>Mesh Size</u>	<u>Percent</u>
35	0
45	0.1
60	5.4
80	49.5
120	23.1
170	13.3
230	5.8
325	2.2
Pan	0.5

Average particle size: 185 microns
Apparent density : 2.67 gm/cm³
Top density : 2.83 gm/cm³

THIS REPORT HAS BEEN DELIMITED
AND CLEARED FOR PUBLIC RELEASE
UNDER DOD DIRECTIVE 5200.20 AND
NO RESTRICTIONS ARE IMPOSED ON
ITS USE AND DISCLOSURE.

DISTRIBUTION STATEMENT A

APPROVED FOR PUBLIC RELEASE;
DISTRIBUTION UNLIMITED.

2 OF 3

ADB

029256



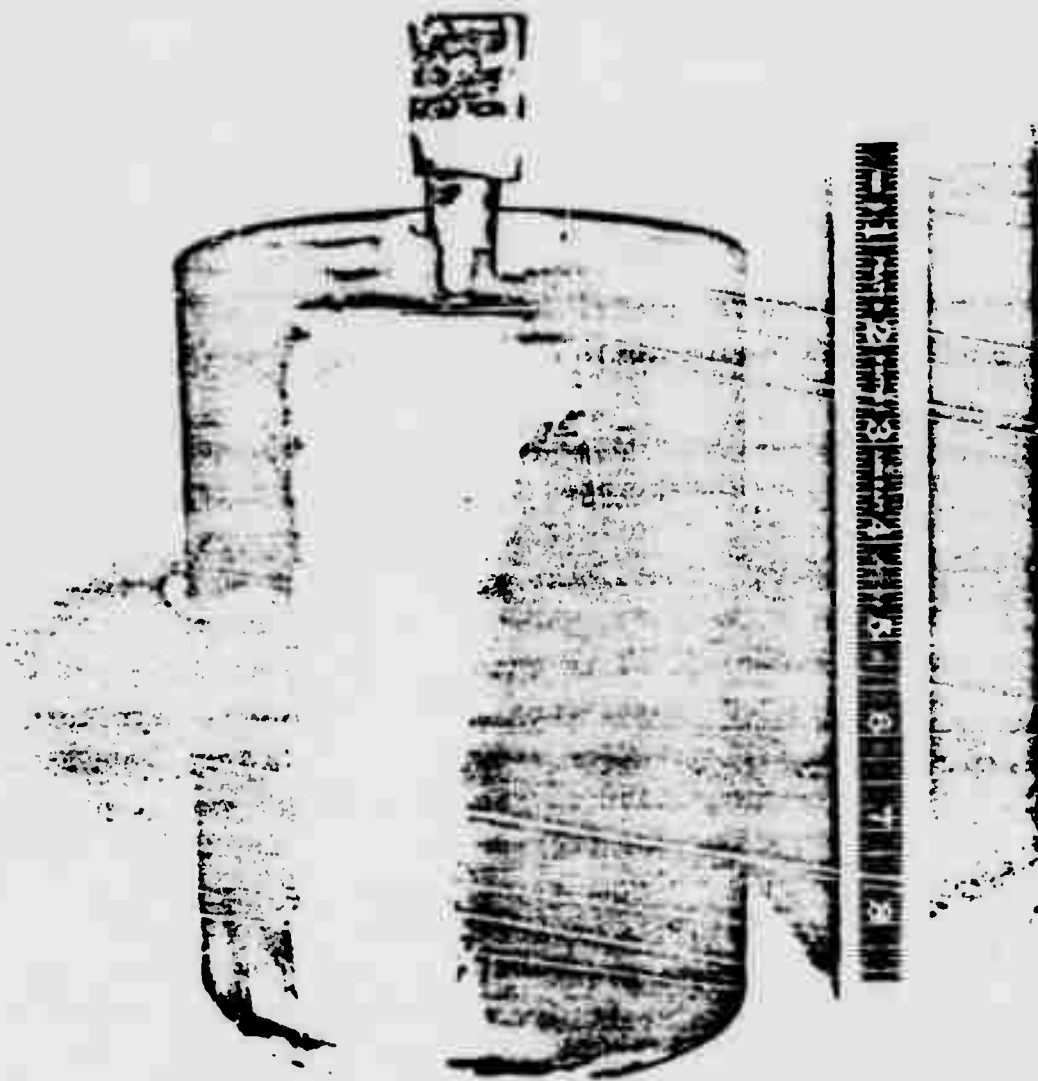


Figure 22. Photo Showing Titanium Hot Isostatic Press (HIP) Container After Can Filling and Sealing - Note "Dished" End Cover

diameter of 5.75". All welds were produced by standard inert gas tungsten electrode techniques. Each container was checked with a helium leak detector to verify its integrity prior to filling. Powder was outgassed in a vacuum chamber at room temperature for 16 hours to a pressure of 2×10^{-5} mm Hg, followed by hot tumbling in vacuum for 4.5 hours at a temperature of 400°F to a pressure of 2×10^{-5} mm Hg prior to filling. Approximately 17.5 pounds of powder was loaded into each evacuated container and the fill tubes were crimped and TIG weld sealed while maintaining full vacuum conditions.

Hot isostatic pressing was conducted at Industrial Materials Technology Incorporated (IMT), Woburn, Massachusetts, under conditions of 2250°F (1232°C)/15,000 psi argon pressure for three hours. Containers were supported by a bed of 0.25" diameter Al_2O_3 balls during isostatic pressing. A consolidated powder billet is shown in Figure 23. Thermally induced porosity (TIP) tests were conducted on micro sections cut from the fill tube for each container. This test consists of micro-examination of the consolidated powder after high temperature-ambient pressure exposure and is designed to determine the general effectiveness of argon outgassing. If argon outgassing is unsatisfactory or if minor leaks occur during cold argon pressurization prior to hot isostatic pressing, argon "bubbles" occur at powder particle interfaces during the thermal exposure. TIP samples for each of the four consolidated containers were exposed to 2250°F for four hours. Microexamination showed no thermally induced porosity in any consolidation. Typical photomicrographs after this test are shown in Figure 24.

Since all consolidation were sound and free from porosity, one container was selected at random and sectioned into three pieces for forging process evaluation. A one-inch thick

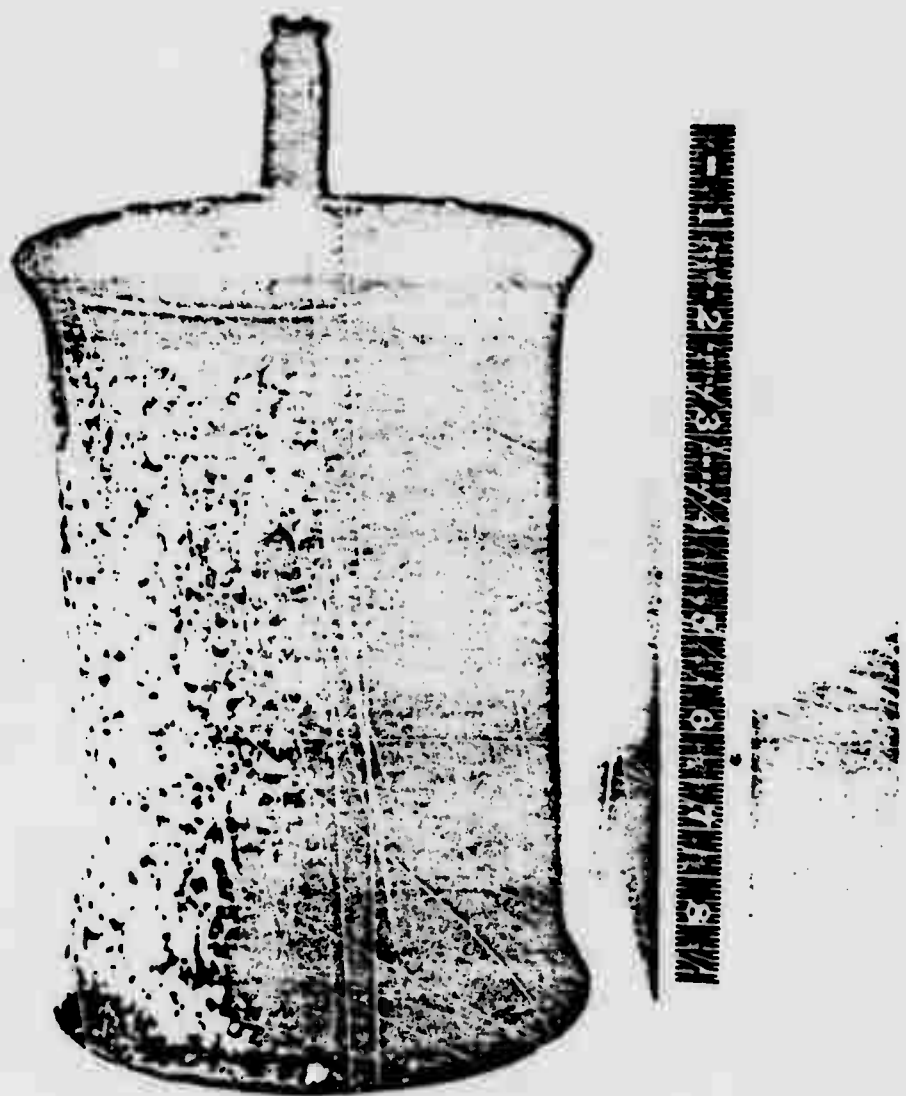
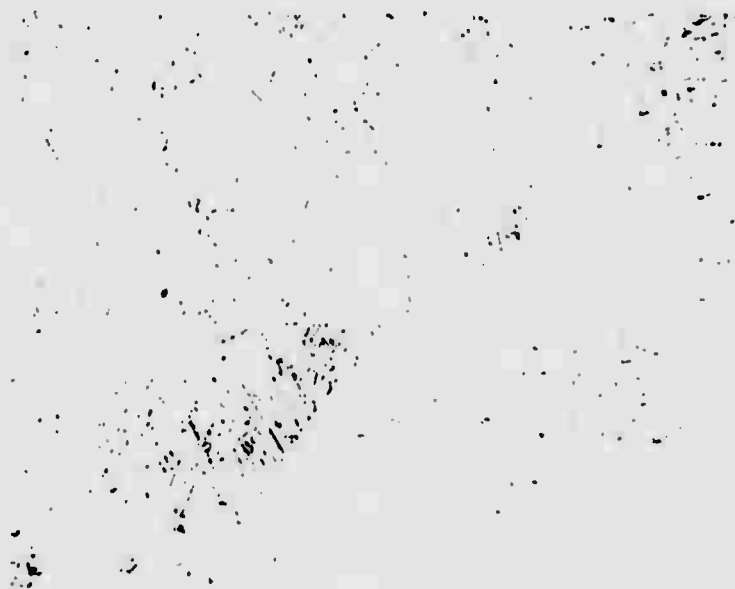
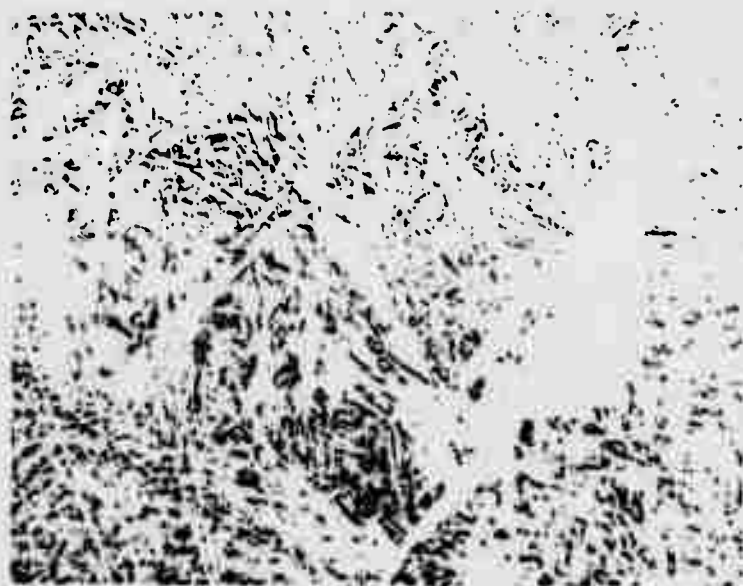


Figure 23. Photo Showing HIP Container After Hot Isostatic Press at 2250°F/3 Hours/15 ksi



50X



100X

Figure 24. Microstructure of Material Exposed to 2250°F/4 Hours Thermally Induced Porosity Test

circular section was retained for "as-HIP" evaluation and two sections, approximately 2½" thick, were used to produce simple upset forgings.

B. Forging

The beta transus of the consolidated powder billet was determined by micro-examination of thermocoupled samples which were thermally exposed over a range of temperatures and water quenched. The beta transus temperature was determined to be in the range of 2150°F to 2175°F (1176°C to 1190°C). Figure 25 shows the microstructure of samples used for this determination.

Based on this information, a beta forging temperature of 2200F (1215°C) and alpha two plus beta forging temperature of 2050°F (1120°C) were selected. One upset hot die forging was produced for each of these conditions and the resultant forgings are shown in Figure 26. The forgings were completed on sub-scale GatorizingTM equipment in a chamber evacuated to 5×10^{-5} mm Hg and at a controlled strain rate of 0.05 inch/inch/minute. Billet sections were spray coated with boron nitride lubricant prior to pump down. The thermocoupled dies and work piece were equilibrated at the selected forging temperature with induction heating coils for one hour prior to deformation.

C. Screening Program

The completed forgings were sectioned and heat treated according to the schedule shown in Table 10. (Description of the specimen configuration and preparation procedures are given below.) Three tensile and two creep rupture specimens were machined for each processing condition. Standard tensile tests were performed at room temperature, 1200°F (649°C) and 1400°F

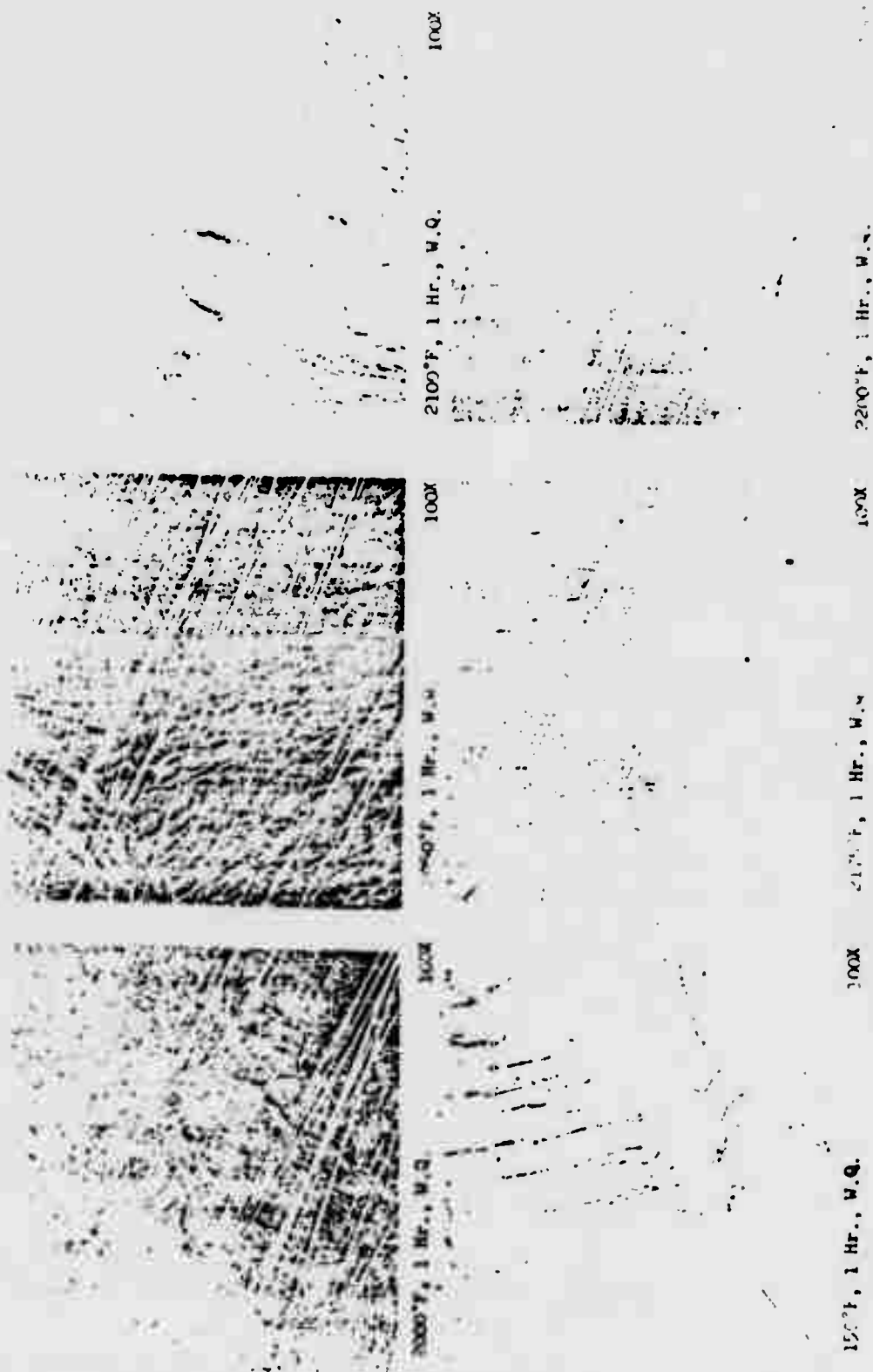


Figure 25. Effect of Solution Treatment Temperature on Microstructure of Ti-16Al-10Nb After HIP at 2250°F/3 hours/15 ksi - Etchant: Kroll's Etch



(a) β forged



(b) $\alpha_2 + \beta$ forged

Figure 26. Isothermal Forgings Produced for Screening Evaluation

TABLE 10
Phase I, Task I Process Screening Mechanical Properties of Ti-16Al-10Nb

Forming Condition	Heat Treatment	Test Condition	Tensile				Life hrs	Stress Intensity	
			0.2% YS	YS	UTS	EA		FEI	RA
1 As MIP		Room Temperature	25,000	25,000	25,000	2.5			
		1200°F	27,000	27,000	27,000	3.8			
		1200°F (5 hrs) oil					rupture on 6.0 Loading	9.3	
		1200°F (5 hrs) air							
2 Beta (2250°F)	2200°F (1 hr) Oil Quench	Room Temperature	41,000	41,000	41,000	2.6			
2a Beta (2250°F)	2200°F (1 hr) Oil Quench - 1050°F (5 Hrs) Air Cool	Room Temperature	43,000	43,000	43,000	2.6			
		1200°F					rupture on 6.0 Loading	9.3	
		1200°F (5 hrs)							
3a Beta (2250°F)	2200°F (1 hr) Air Cool - 1650°F (5 Hrs.) Air Cool	Room Temperature	46,000	46,000	46,000	2.6			
		1200°F					rupture on 6.0 Loading	9.3	
		1200°F (5 hrs)							
5 Beta (2250°F)	2200°F (1 hr) Furnace Cool - 1650°F (5 Hrs.) Air Cool	Room Temperature	47,000	47,000	47,000	2.6			
		1200°F					rupture on 6.0 Loading	9.3	
		1200°F (5 hrs)							
6 Beta (2250°F)	2200°F (1 hr) Air Cool - 1550°F (5 Hrs.) Air Cool	Room Temperature	48,000	48,000	48,000	2.6			
		1200°F					rupture on 6.0 Loading	9.3	
		1200°F (5 hrs)							
6 Beta (2250°F)	2200°F (1 hr) Furnace Cool - 1550°F (5 Hrs.) Air Cool	Room Temperature	49,000	49,000	49,000	2.6			
		1200°F					rupture on 6.0 Loading	9.3	
		1200°F (5 hrs)							

TABLE 10 (Cont'd)

Forging Condition	Heat Treatment	Test Condition	Tensile				Life (hrs)	Stress Rupture ksi
			0.2% R _s (ksi)	UTS (ksi)	4EL (ksi)	4RA (ksi)		
7 Alpha ₂ - Beta 2050°F (48 hrs.) Air Cool - 1650°F (5 hrs.) Air Cool		Room Temperature	Incomplete					
		1200°F	38,400	54,500	2.1	3.2		
		1400°F	32,900	41,800	2.4	6.5		
		1200°F/55 ksi 1400°F/40 ksi	Test Deferred					
5	2075°F (48 hrs.) Furnace Cool - 1650°F (8 hrs.) Air Cool	Room Temperature		27,900				
		1200°F	Incomplete					
		1400°F	27,000	33,400	2.1	4.9		
		1200°F/55 ksi 1400°F/40 ksi	Test Deferred					

• Possible prior crack in specimen

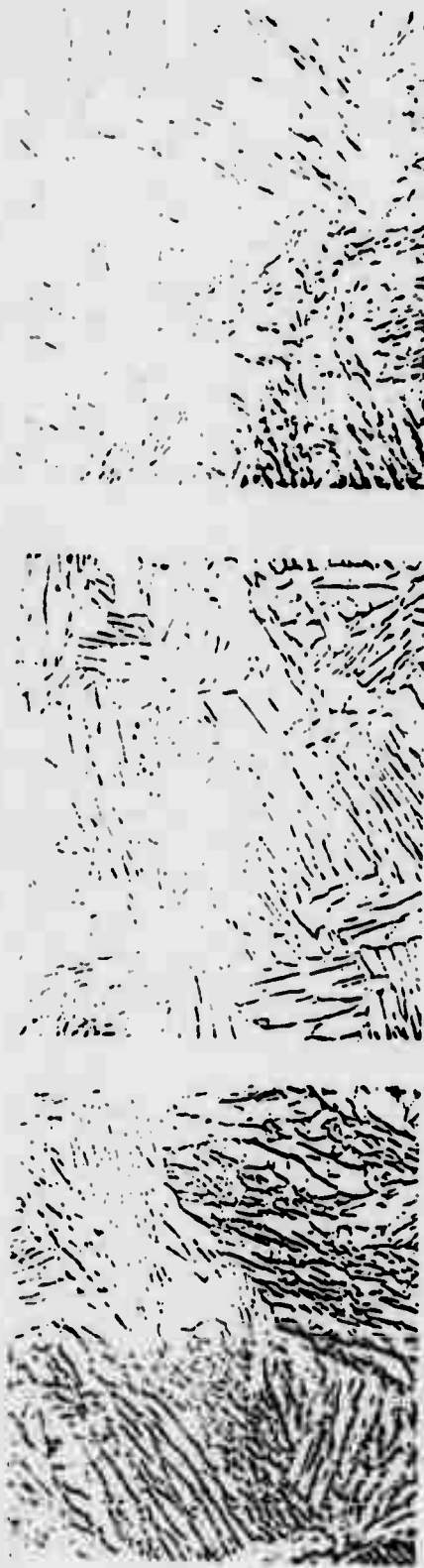
Temperature conversions
 2075°F = 1135°C
 2250°F = 1232°C
 2200°F = 1204°C
 1650°F = 899°C
 1200°F = 649°C
 1400°F = 760°C

(760°C) at a strain rate of 0.005 inch/inch/minute. Rupture tests were performed in conventional lever operated load frames at 1200°F/55 ksi and 1400°F/40 ksi. In each elevated temperature test, temperature was equilibrated for one hour prior to loading.

The microstructures of material given the various treatment cycles are given in Figures 27(a)-(f). In the as-oil quenched condition, an extremely fine martensite is produced which is extremely unstable upon subsequent aging at temperatures as low as 1200°F, Figures 28 and 29. As a result of this instability, the beta solution treated quenched and stabilized condition 2a (Figure 27), exhibits large apparent alpha two grains near prior beta grain boundaries and occasional large grain patches dispersed through the structure.

The mechanical property data for the screened structural conditions are given in Table 10 and it can be seen that only two treatments result in adequate tensile and stress rupture properties, conditions 2 and 3.

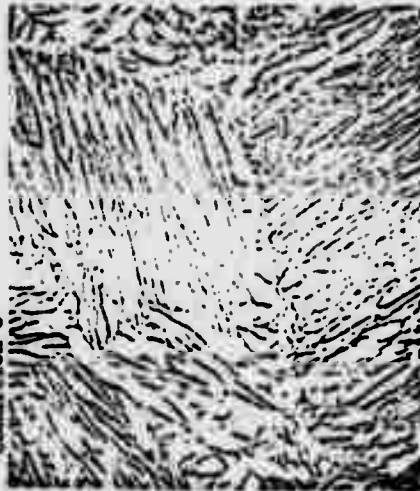
The tensile strength and stress rupture properties of the oil quenched and tempered condition are similar or slightly superior to those of the air-cooled condition 3, however, the tensile ductility of quenched material is significantly lower than that of air-cooled material. Because of the generally low tensile strengths at 1200 and 1400°F, all other conditions exhibited poor stress rupture properties at these temperatures (Table 10). In fact, the ultimate tensile strengths were near to, or slightly lower than, the selected screening stresses for stress rupture testing. Tensile and stress rupture tests were conducted concurrently as a result of schedule limitations so no readjustment of rupture test stresses was possible for the screening effort.



a. As Beta Forged
Not Tested 100X

b. 2075°F/1/F.C. + 1650°F/8/A.C. 100X
Condition 8

c. 2075°F/1/A.C. + 1650°F/8/A.C. 100X
Condition 7

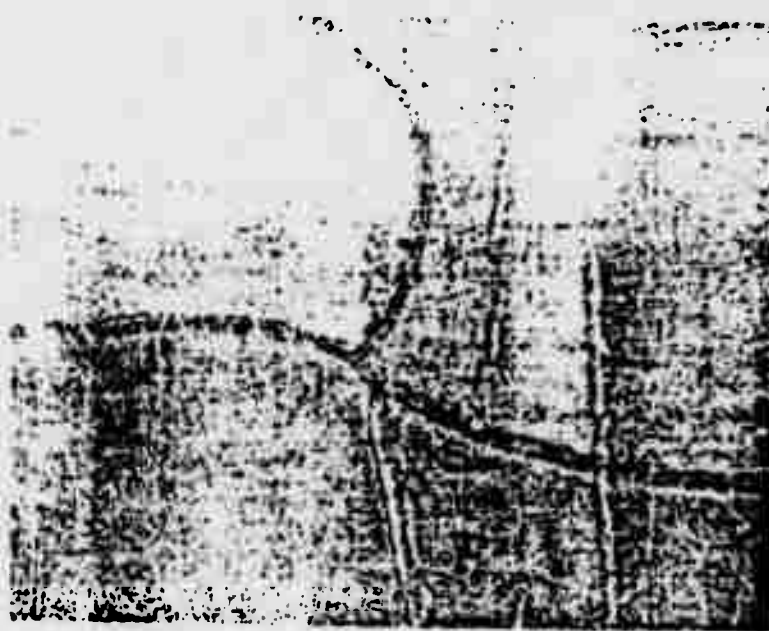


d. 2200°F/1/F.C. + 1650°F/8/A.C. 100X
Condition 4

e. 2200°F/1/A.C. + 1650°F/8/A.C. 100X
Condition 3

f. 2200°F/1/F.C. + 1650°F/8/A.C. 100X
Condition 2a

Figure 27. Effect of Solution Treatment Temperature and Cooling Rate on Microstructure of Ti-16Al-10Nb After HIP and Beta Forging - Etchant: Kroll's Etch



50X



100X

Figure 28. Microstructure of Ti-16Al-10Nb Alloy, Beta Forged + 2200°F/1 Hour/OO + 1200°F/87 Hours/AC Showing Instability of Quenched Martensitic Phase



Figure 29. Microstructure of Ti-16Al-10Nb Alloy, Beta Forged + 2200°F/1 Hour/OO + 1500°F/67 Hours/AC Showing Instability of Quenched Martensitic Phase

D. Test Program

Based on the results of the screening program, conditions were selected for the forging and heat treatment of the HIP'ed billets. Prior to forging the ends of three HIP'ed billets (the fourth billet was used in the process screening portion of the program), they were sectioned and the billet ends were machined flat and parallel. Protective tantalum sheets were spot welded to the end of each ingot to prevent billet/die diffusion bonding. Isothermal forging was conducted at Ladish Company, Cudahy, Wisconsin, under the supervision of Pratt & Whitney Aircraft personnel. Forging was completed in their Production Gatorizing equipment on TZM molybdenum alloy tooling. Ingot sections and die surfaces were spray coated with boron nitride lubricant prior to pump down. Forging was conducted in vacuum at a pressure of 10^{-3} mm Hg

and at a controlled strain rate of 0.1 inch/inch/minute.

The beta transus temperature was previously determined to be in the 2150°F to 2175°F (1176°C to 1190°C) temperature range. Based upon this information, an alpha two plus beta forging temperature of 2050°F to 2075°F (1120°C to 1135°C) was selected for processing in order to obtain a fine prior beta grain size in the resulting forging.

All billets were preheated in an attached vacuum furnace prior to being mechanically transferred, via air locks, to the Gatorizing chamber. The thermocouples dies and work piece were equilibrated at the forging temperature with induction heating coils for one-half hour prior to deformation. Subsequent to each forging run, the die surfaces were spray coated with boron nitride lubricant. Forgings were air cooled off the dies in all cases by means of air locks.

Table 11 summarizes the forging results for the three trials and Figure 30 shows a typical forged pancake. The processing sequence yielded a heavily worked equiaxed microstructure as shown in Figure 31.

Based on the processing screening effort, a beta phase field solution heat treatment (2200°F) was selected for the alloy characterization effort. In an effort to maintain the smallest possible prior beta grain size, an experiment was conducted to determine the grain size resulting from heating to 2200°F as a function of time between 15 minutes and 2 hours. Examination of polished micro-sections for all conditions showed a beta grain size of approximately 0.7 mm, indicating very rapid grain growth at a temperature only slightly above the beta transus.

TABLE 11
Isothermal Forging Results

Billet Number	135	136	137
Temperature, °F	2050±25	2075±25	2075±25
Strain Rate, in/in/min	0.1	0.1	0.1
Initial Height, in	5.06	5.0	4.38
Final Height, in	1.06	1.19	1.13
Percent Reduction	79	76	74
Estimated Final Flow Stress, ksi	4.2	4.4	5.0

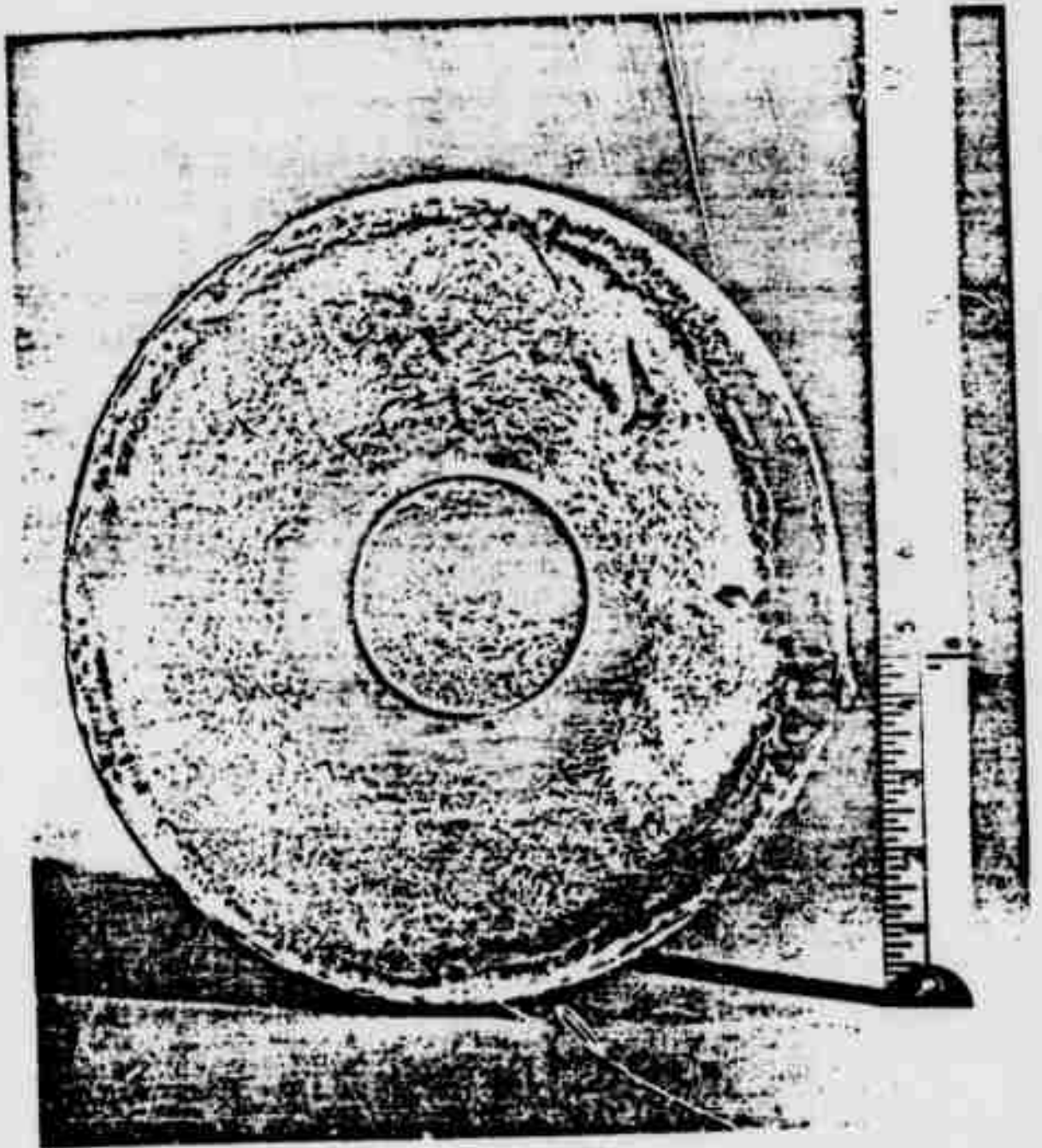


Figure 30. Pancake Forging Configuration Produced for Ti-16Al-10Nb Alloy Characterization



100X

Figure 31. As-Forged Microstructure of Ti-16Al-10Nb Pancake Forging

Based on these results a solution treatment of 2200°F for one hour was selected to achieve uniformity in the full forging sections. The rapid beta grain growth characteristic during heat treatment obliterates the alpha-beta forging grain size.

The completed forgings were given a 2200°F/1 hour/fan air cool solution treatment followed by a 1650°F/8 hours/air cool stabilization treatment. It was found that a fan air cool was necessary to produce an acicular microstructure throughout the approximately one-inch thick forging; an as-heat treated microstructure is shown in Figure 32. Subsequent to heat treatment, the forgings were sectioned for machining. Table 12 lists the specimens utilized in the characterization program. In most cases test specimens were prepared for the physical and mechanical property evaluation using conventional machining techniques for brittle materials, electrochemical machining (ECM), electro-discharge machining (EDM) and electrochemical grinding (ECG) were possible. Threaded specimens were eliminated also based on the restricted low temperature ductility of the material. Mechanical test specimens prepared by conventional machining techniques (notch rupture, thermal fatigue, FCHR, HCF, notched LCF and, in some cases, impact (toughness)) were given a vacuum stress relief at 1650°F for four hours. This stress relief treatment produced no observable effect on microstructure. After machining each specimen was examined by zyglo inspection techniques to reveal any surface cracks or imperfections. All subsequent mechanical tests were performed in air.

1) Tensile Testing

The specimen used for tensile property evaluations is shown



100X

Figure 32. Microstructure of Ti-16Al-10Nb Pancakes Heat
Treated at 2200°F/1 Hour/Rapid Air Cool +
1600°F/8 Hours/Air Cool

in Figure 3. Tensile data for Ti-16Al-10Nb in the range of room temperature to 800°F (427°C) to 1500°F (815°C) are shown in Table 12 and Figure 33. Considerable scatter in these data is apparent for test conditions where ductility is limited. Plastic deformation sufficient to define a yield strength is not consistently observed in this alloy until temperatures of 1000°F and above. The static modulus of elasticity determined from strain gaged tensile specimens was 19.5×10^6 psi at room temperature. Two 800°F tensile tests were conducted for beta anneal (2200°F (1204°C)/1 hour/air cool) heat treatments without the addition of the 1650°F/8 hour stabilization originally selected as baseline for the characterization task. An increase in ultimate tensile strength was observed with the elimination of the stabilization step; however, there was no increase in ductility (Table 13).

2) Charpy Impact

Conventional Charpy impact tests were performed over the range from room temperature to 1600°F (871°C). The data are shown in Table 14 and Figure 34. Impact fracture energy increases significantly between 800°F (427°C) and 1200°F (649°C). This is the same apparent transition range observed for tensile ductility. This result is considered promising since it might have been expected that the general strain rate sensitivity of the material would cause the impact transition to occur at a significantly higher temperature than the tensile ductility transition. Impact toughness in the projected operating temperature range of 1200-1500°F is generally equivalent to advanced nickel-base alloy materials.

TABLE 12
Summary of Phase I, Task II -
Characterization Property Testing

<u>Test Type</u>	<u>Test Specimen</u>	<u>Test Temperature (°F)</u>	<u>Number of Specimens</u>	<u>Machining Technique</u>
Modulus	Button Head	70	4	ECG
Thermal Exp. Conf.	Bar	70 - 1500	1	Conventional
Specific Heat	Bar	70 - 1500	1	Conventional
Thermal Cond.	Bar	70 - 1500	1	Conventional and EDM
Tensile	Button Head with Extensometer Ridges		20	ECG
Creep Rupture	Button Head with Extensometer Ridges	1000 - 1500°F	20	ECG
Notch Rupture	MDL 2362	1000 - 1500°F	10	Conventional
Thermal Fatigue	NGTE Disk MDL 4694	Cyclic 1500° - 70°F	16	Conventional
Impact Toughness	MDL 2317	RT, 800, 1200	6	Conventional
FCPK	MDL 6197	800, 1200	2	Conventional and EDM
HCF				
Smooth	Westinghouse MDL 2331	800, 1400	12	Conventional
Notched	Westinghouse MDL 2332	800, 1400	12	Conventional
LCF				
Smooth	AML 42-2-68	800, 1200	12	ECG
Notched	(MERL 4) K ₁₂	800, 1200	12	Conventional

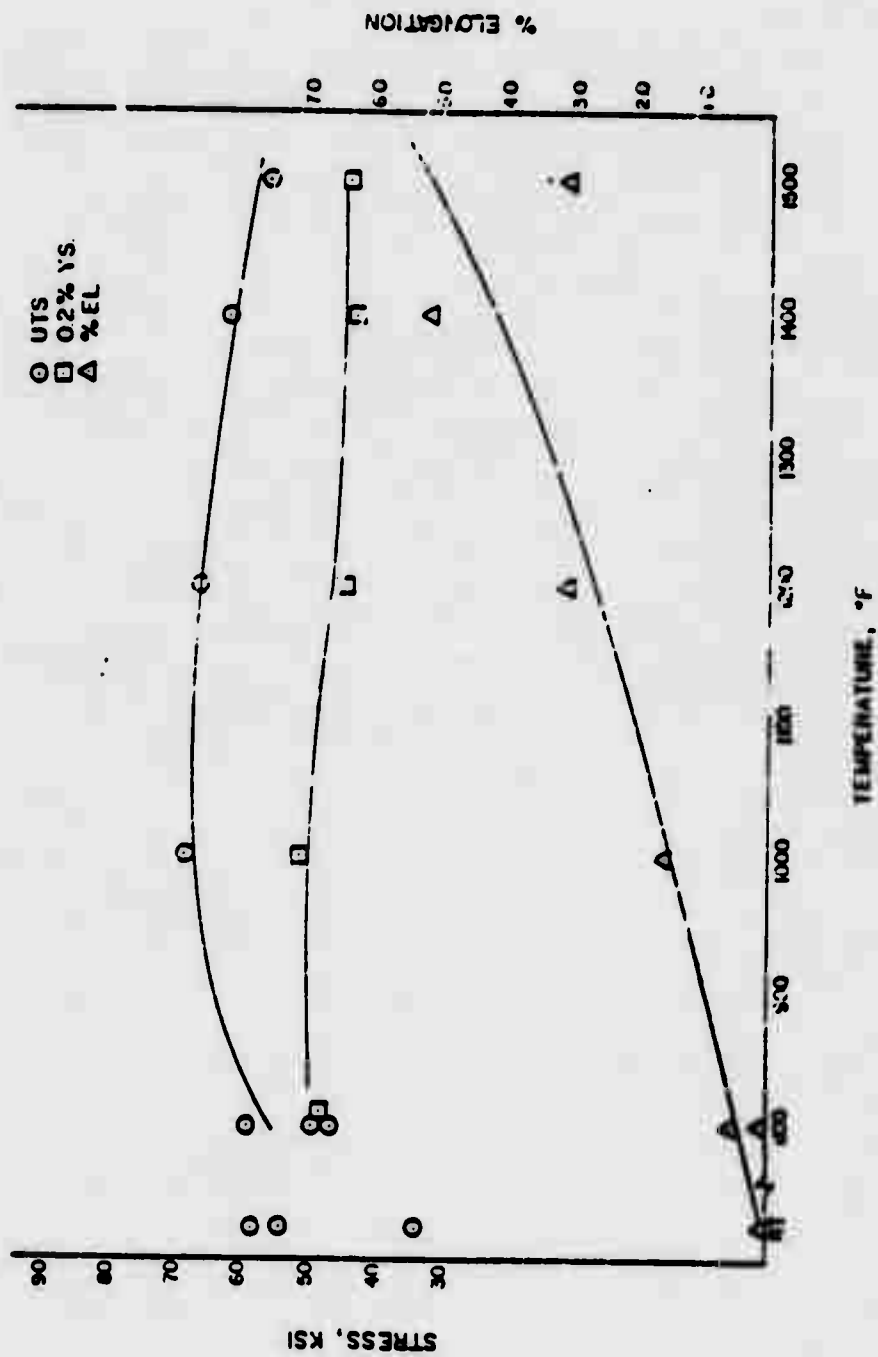


Figure 33. Yield Strength, Ultimate Strength, Elongation for Ti-16Al-10Nb

TABLE 13
Tensile Properties for Ti-16Al-10Nb

Heat Treatment	Test Temperature °F	0.2% Yield Strength ksi	Ultimate Strength ksi	Elongation %	Reduction in Area %
2250°F, 1 Hr. A.C. + 1650°F, 8 Hr. A.C.	RT	-	58.2	-	-
	RT	-	53.9	0.05	-
	RT	-	34.0	-	-
	800	-	47.1	-	-
	900	-	49.6	0.15	-
	800	48.4	58.9	0.58	2.4
	1000	51.6	58.4	1.6	3.8
	1200	44.5	66.5	3.1	4.2
	1400	43.0	62.0	5.2	9.0
	1500	43.8	55.9	3.1	5.3
2200°F, 1 Hr. A.C.	800	-	83.6	-	-
2050°F, 1 Hr. A.C.	900	47.9	63.8	0.90	-

*Specimens stress relieved: 1650°F, 4 Hrs., Vacuum

TABLE 14
Charpy Impact Toughness of Ti-16Al-10Nb

<u>Test Temperature (°F)</u>	<u>Charpy Impact Toughness ft. lbs.</u>
RT	1.03
RT	1.03
RT*	0.69
400*	1.32
800	2.1
800	1.7
800*	1.7
1200	4.9
1500*	8.8

*Specimens stress relieved: 1650°F, 4 Hr. Vacuum

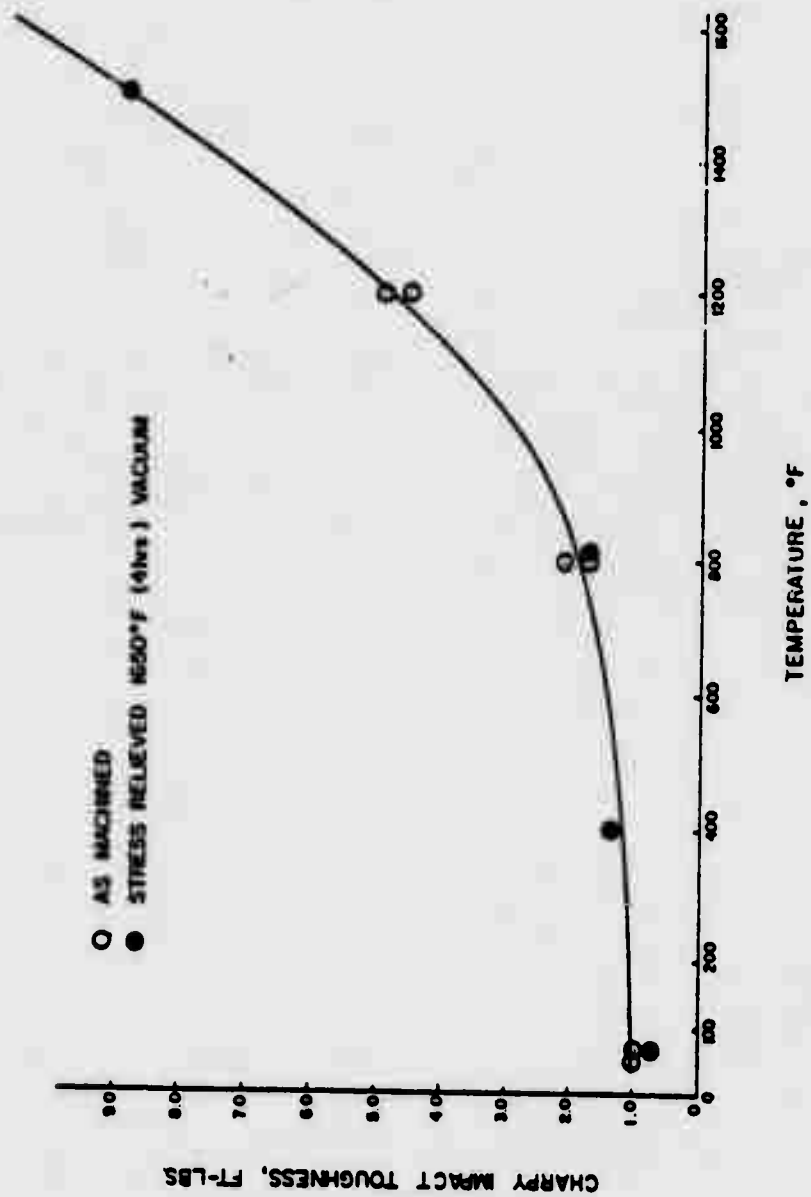


Figure 34. Charpy Impact Toughness vs. Temperature for Ti-16Al-10Nb

3) Creep Rupture

Specimens used for the creep rupture evaluation are shown in Figure 3. Smooth section creep rupture testing was conducted over the temperature range 1100-1800°F (593-982°C). Data are shown in Table 15 and Figure 35. Both 1% creep and stress rupture capability exceed original predictions by a significant margin. The data are consistent with a potential extension of the useful application temperature beyond the original estimate of 1500°F.

The notched K_t 3.8 stress rupture capability for Ti-16Al-10Nb is indicated in Table 16 and Figure 35. The alloy is generally not notch sensitive in the 1200 to 1500°F (648 to 815°C) temperature range at this notch acuity. There is a large noticeable tendency for notch stress rupture life to exceed smooth life by a larger margin as temperature increases. At lower temperatures (~1100°F), notch and smooth capability are about equal. Although an extended operating temperature range could be predicted from these results, the limit could be set by another criterion such as surface stability. Microstructural analysis of creep rupture test specimens showed interesting behavior related to long-time air exposure at elevated temperature. During exposure at 1200°F (649°C) and above, a thin oxygen enriched layer (alpha case) is formed on specimen surfaces which grows very slowly with time. At exposure times of 100 hours, this diffusion layer is less than 0.6 mils (1.5×10^{-3} cm) for test temperatures of 1200, 1300 or 1400°F (649, 704 or 760°C). As a result of the large creep strains occurring during stress rupture, small surface cracks are formed which extend to the depth of the alpha case (Figure 36). The cracks stop at this interface and only extend as the alpha case grows. At creep strains

TABLE 15
Creep Rupture Properties for Ti-16Al-10Nb

<u>Test Temperature °F</u>	<u>Stress ksi</u>	<u>Time to 1% Creep Hr.</u>	<u>Time to Rupture Hr.</u>	<u>Elongation %</u>	<u>Reduction in Area %</u>
1100	60.0	43.0	235.3	0.8	5.9
1200	50.0	24.5	379.6	7.4	7.3
1200	55.0	3.5	92.2	9.4	7.3
1300	35.0	126.0	803.5	9.8	10.5
1300	40.0	41.0	144	5.8	7.9
1300	45.0	8.3	84.2	9.1	7.5
1400	20.0	172	449 Disc.	3.4	3.6
1400	30.0	33.0	335.1	22.9	21.3
1400	40.0	-	32.3	10.7	9.2
1500	10.0	244	306.3 Disc.	1.3	N/A
1500	15.0	70.0	1654.8	26.7	51.4
1500	25.0	17.6	138.5	18.4	19.6
1500	30.0	5.0	54.9	15.3	16.9
1600	10.0	38.5	526.4 Disc.	8.9	6.3
1600	15.0	13.0	308.3	36.6	35.9
1600	20.0	9.0	81.0	23.3	20.1
1700	5.0	34.5	1030 (Running)		
1700	10.0	5.0	323.6	47.0	50.8
1800	7.0	3.0	208.3	57.9	57.5

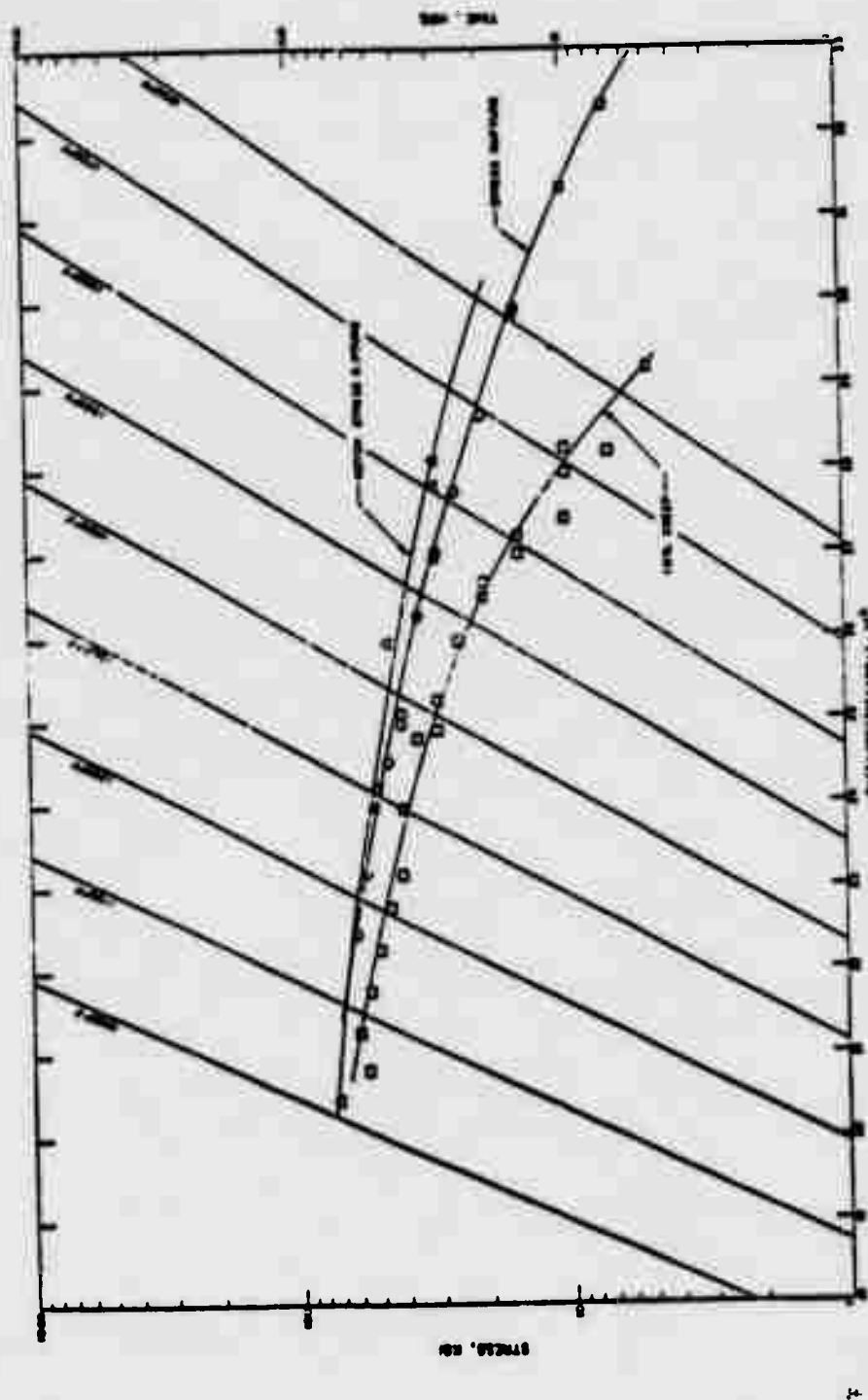


Figure 35. Larson-Miller Plot of Creep Rupture Data

TABLE 16
Notched Stress Rupture Properties for Ti-16Al-10Nb

<u>Test Temperature °F</u>	<u>Stress ksi</u>	<u>Kt</u>	<u>Time to Failure Hr.</u>	<u>Time to Failure for Smooth Specimen (Equivalent Condition) Hr.</u>
1100	60	3.9		163.7 Running
1200	50		246.2	379.6
1200	10		24.3 Uploaded	
1200	20		23.7 Uploaded	
1200	30		23.9 Uploaded	
1200	40		24.0 Uploaded	
1200	50		73.7 Uploaded	379.6
1200	60		22.5 Uploaded	
1200	70		2.0 Rupture	8.0 (From Larson Miller Curve)
1300	45		522.3	84.2
1400	30		1200 Running	335.1
1500	10		336.8 Uploaded	306.3 Disc.
1500	30		144.7	94.9
1500	15		1670 Running	1654.8
1500	5.		705.4 Uploaded	
1600	10		1250 Running	(1575 From Larson Miller Curve)

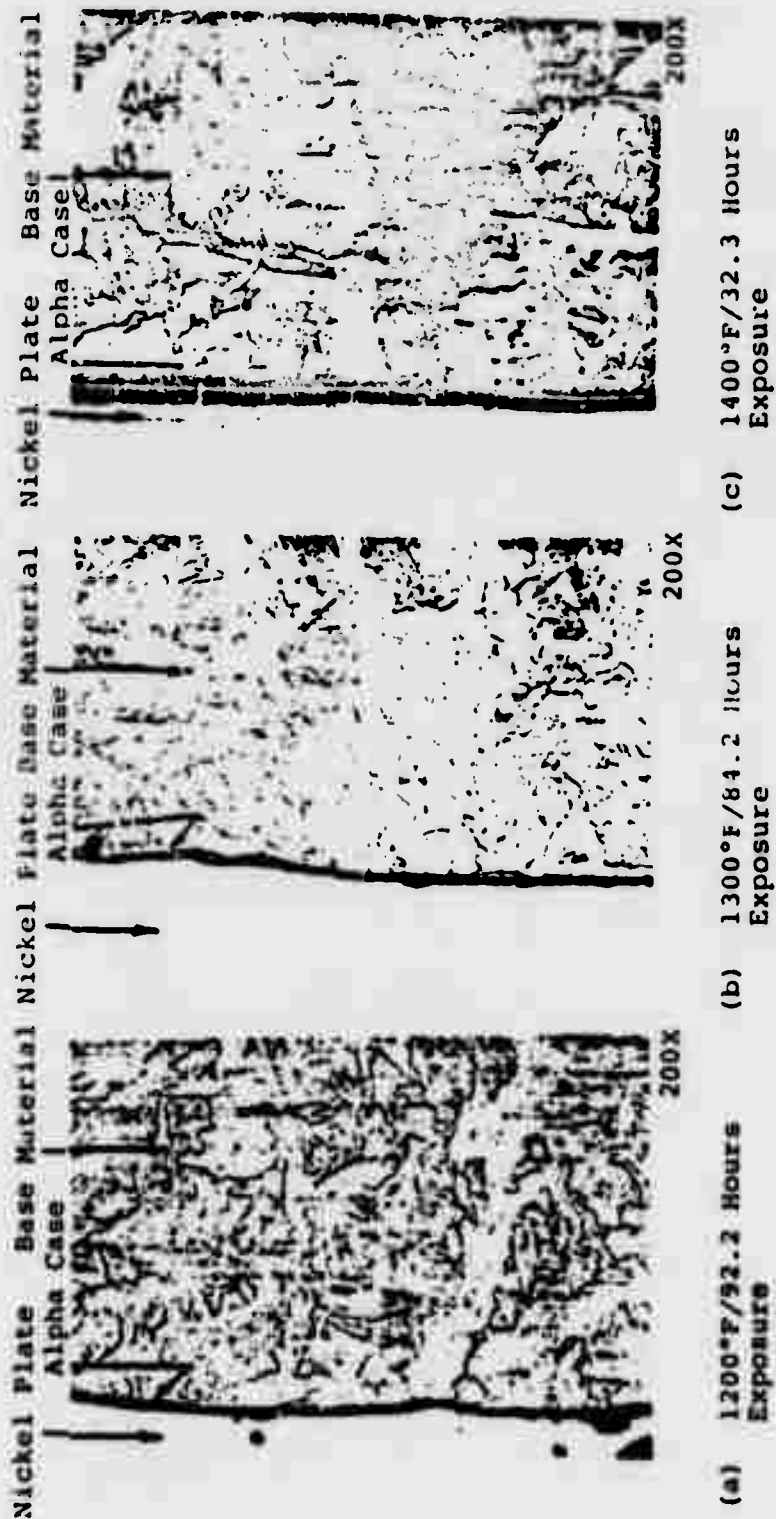


Figure 36. Longitudinal Cross Sections of Ti-16Al-10Nb Creep Specimens Showing Alpha Case on Specimen Surface.

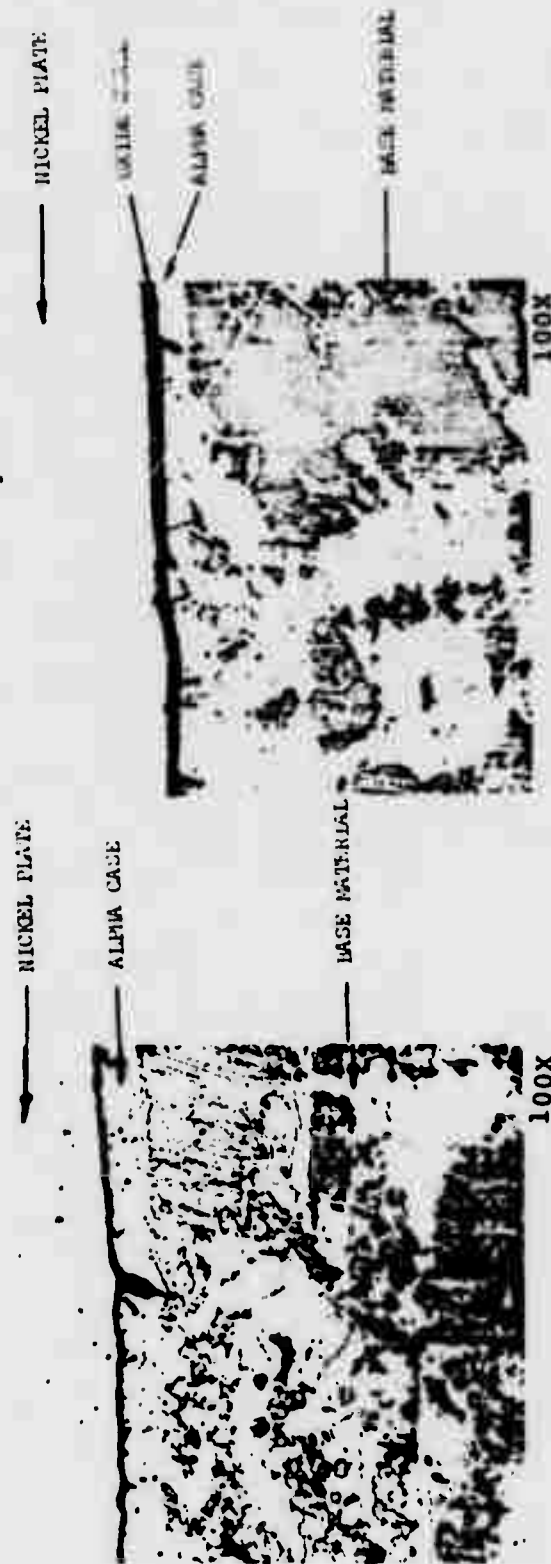
of less than 1%, these cracks apparently do not form at all. At higher temperatures and longer times the diffusion layers are somewhat deeper so that after 1500°F (816°C)/1655 hour exposure, the layer is approximately 2 mils (5×10^{-3} cm) thick. The surface cracking phenomena is again observed at very large creep strains, but the cracking is contained within the diffusion layer at high temperatures also (Figure 37).

4) High Cycle Fatigue (HCF)

High cycle fatigue tests at both 800°F (427°C) and 1200°F (649°C) were conducted for both smooth, K_t 1 and notched, K_t 3.8 specimens after 1650°F (899°C)/4 hours/vacuum stress relief. The low stress electrochemical grinding technique used for the majority of the other specimen configurations could not be used for the high cycle fatigue specimens since tooling was not available.

Conventionally machined notched HCF specimens were inspected by fluorescent penetrant which indicated that several specimens contained grinding cracks. In order to alleviate high residual grinding stresses, the specimens were stress relieved and specimens were again inspected by fluorescent penetrant; although no cracks were detected after this procedure, some specimens were found to contain very small tight craze cracks during post-HCF test microexamination. (Since these cracks were apparent in the grip area which has a very low applied stress during the fatigue test, they are assumed to have been present prior to testing.) Data from these potentially pre-cracked specimens were not used in estimating 10^7 cycle fatigue capability.

The data for all HCF testing is shown in Table 17 and plotted



(a) 1500°F/1654.8 Hours Exposure

(b) 1600°F/91 Hour Exposure

Figure 37. Longitudinal Cross Sections of T₁-16Al-10Nb Creep Specimens Showing Alpha Case on Specimen Surface

TABLE 17
Westinghouse High Cycle Fatigue Data for Ti-16Al-10Nb

$r = -1$

<u>Test Temperature °F</u>	<u>Kt</u>	<u>Frequency cpm</u>	<u>Stress ksi</u>	<u>Cycles to Failure</u>
800	1.0	1800	30.0	1.0×10^7 Disc. and Uploaded
800	1.0	1800	40.0	1.0×10^7 Disc. and Uploaded
800	1.0	1800	50.0	1.0×10^7 Disc. and Uploaded
800	1.0	1800	60.0	1.5×10^6
800	2.0	1800	3.0	1.0×10^7
800	1.0	1800	45.0	1.0×10^6 Potential Crack
800	1.0	1800	50.0	7.0×10^6
800	1.0	1800	50.0	9.5×10^5
800	1.0	1800	55.0	2.2×10^5
800	1.0	1800	60.0	1.3×10^5
1200	1.0	1800	40.0	1.3×10^6 Potential Crack
1200	1.0	1800	40.0	1.5×10^5 Potential Crack
1200	1.0	1800	45.0	6.5×10^6
1200	1.0	1800	50.0	6.0×10^6
1200	1.0	1800	55.0	2.2×10^5
1200	1.0	1800	60.0	3.0×10^5
800	3.8	1800	15.0	1.0×10^7 Disc.
800	3.8	1800	20.0	1.0×10^7 Disc.
800	3.8	1800	25.0	1.0×10^7 Disc.
800	3.8	1800	30	1.0×10^7
1200	3.8	1800	10.0	1.0×10^7 Disc.
1200	3.8	1800	15.0	1.0×10^7 Disc.
1200	3.8	1800	20.0	1.7×10^5

in Figure 38. The smooth (K_t 1) HCF stress capability for 10^7 cycle life for Ti-16Al-10Nb is estimated to be 45 to 50 ksi at 800°F and 40 to 45 ksi at 1200°F. Only runout ($>10^7$ cycle life) data are available for K_t 3.8 specimens at 800°F, reflecting apparently unjustified conservatism in planning the first tests; however, a runout stress of 25 to 30 ksi was clearly evident. Limited K_t 3.8 testing at 1200°F suggests a runout stress of 15 ksi.

5) Strain Controlled Low Cycle Fatigue (LCF)

Strain controlled low cycle fatigue tests were performed at 800°F (426°C) and 1200°F (650°C) on specimens shown in Figure 39. The test results are given in Table 18 and Figure 40. The 1200°F tests show very little scatter and are fully comparable with behavior expected for nickel-base alloys such as Waspaloy^R and INCO 718 in this temperature range. Data for the 800°F condition show considerably more variability which is probably related to the limited tensile plasticity of the material at this temperature.

In spite of the limited plasticity at 800°F, there was evidence of some work hardening during the tests as shown by the load range versus cycle plot for the longer life tests (Figure 41). At 1200°F the work hardening behavior of the material was quite marked (Figure 42). An improved alloy composition with a lower ductile brittle transition temperature should markedly improve LCF characteristics for applications where very high tensile loads can occur at relatively low temperatures. Examination of overload surfaces showed considerable evidence of cleavage intermixed with local areas of ductile tearing (Figure 43(a)). Fatigue striations, similar to those observed in conventional materials, were clearly observed in the cyclic fracture

○ - 800°F, Ni=1
 □ - 1200°F, Ni=1
 ◇ - 300°F, Ni=3.8
 △ - 1200°F, Ni=3.8

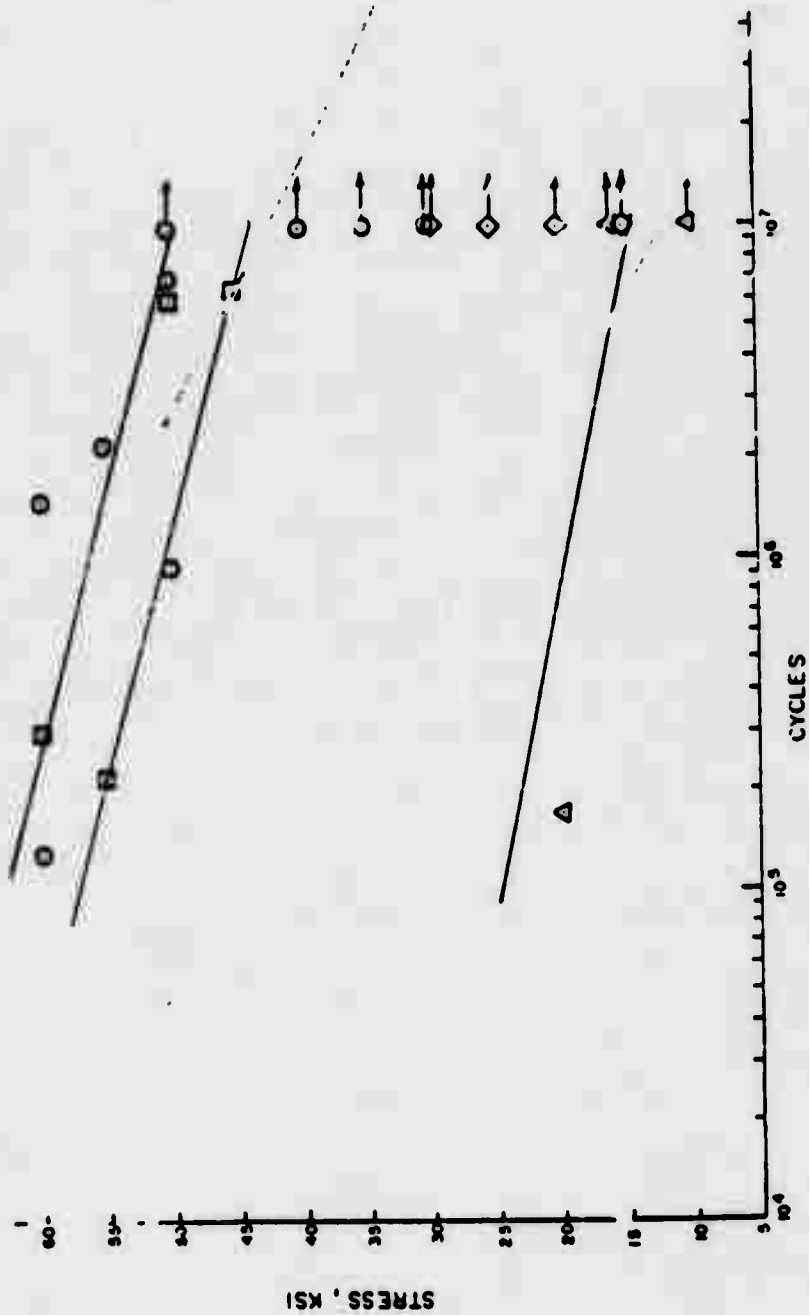


Figure 38. Westinghouse HCF Data for Ti-16Al-10Nb

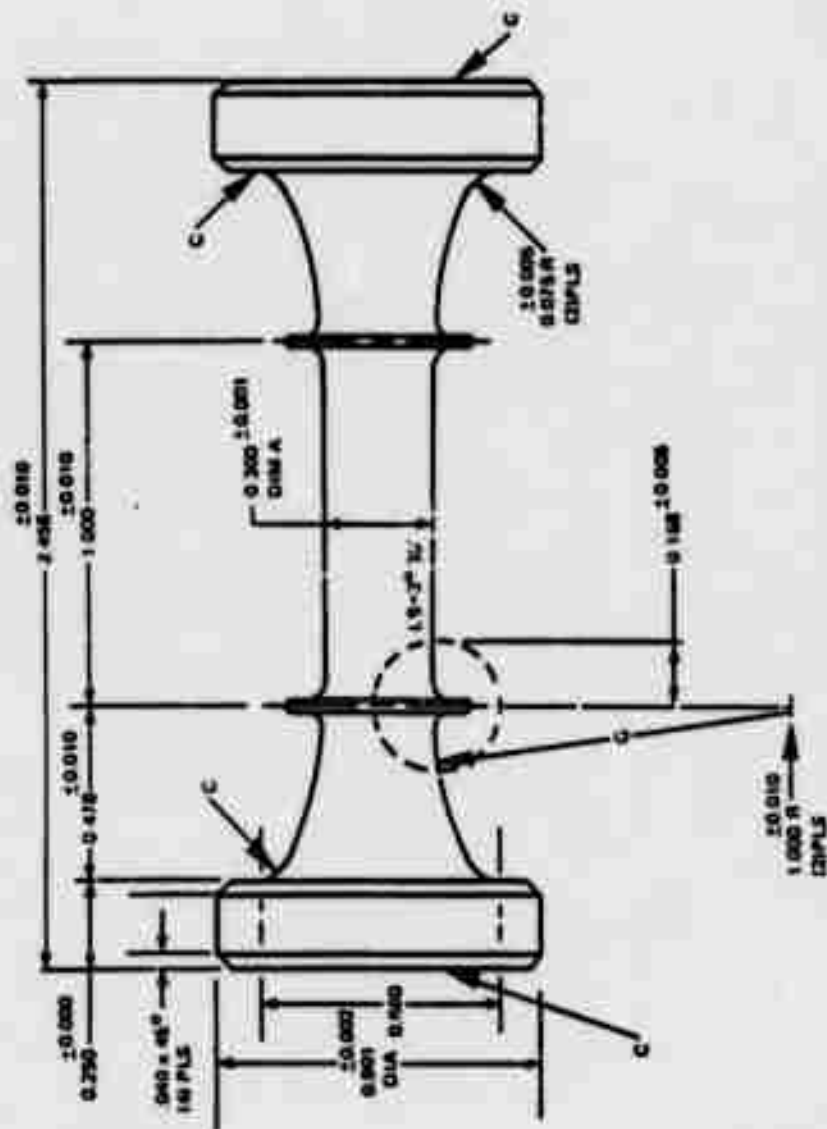


Figure 39. Strain Controlled Low Cycle Fatigue Specimens

TABLE 18
Smooth Low Cycle Fatigue Properties
of Ti-16Al-10Nb, Strain Controlled

<u>Test Temperature °F</u>	<u>Longitudinal Strain Range</u>	<u>Kt</u>	<u>Frequency, cps</u>	<u>Cycles to Failure</u>
800	0.0030	1.0	5	To be Run
800	0.0035	1.0	5	45
800	0.0035	1.0	5	1,270
800	0.0040	1.0	5	65
800	0.0040	1.0	5	8700
800	0.0050	1.0	5	1650
1200	0.0035	1.0	5	105,089 Disc.
1200	0.0060	1.0	5	1,655
1200	0.0075	1.0	5	691
1200	0.0100	1.0	5	103

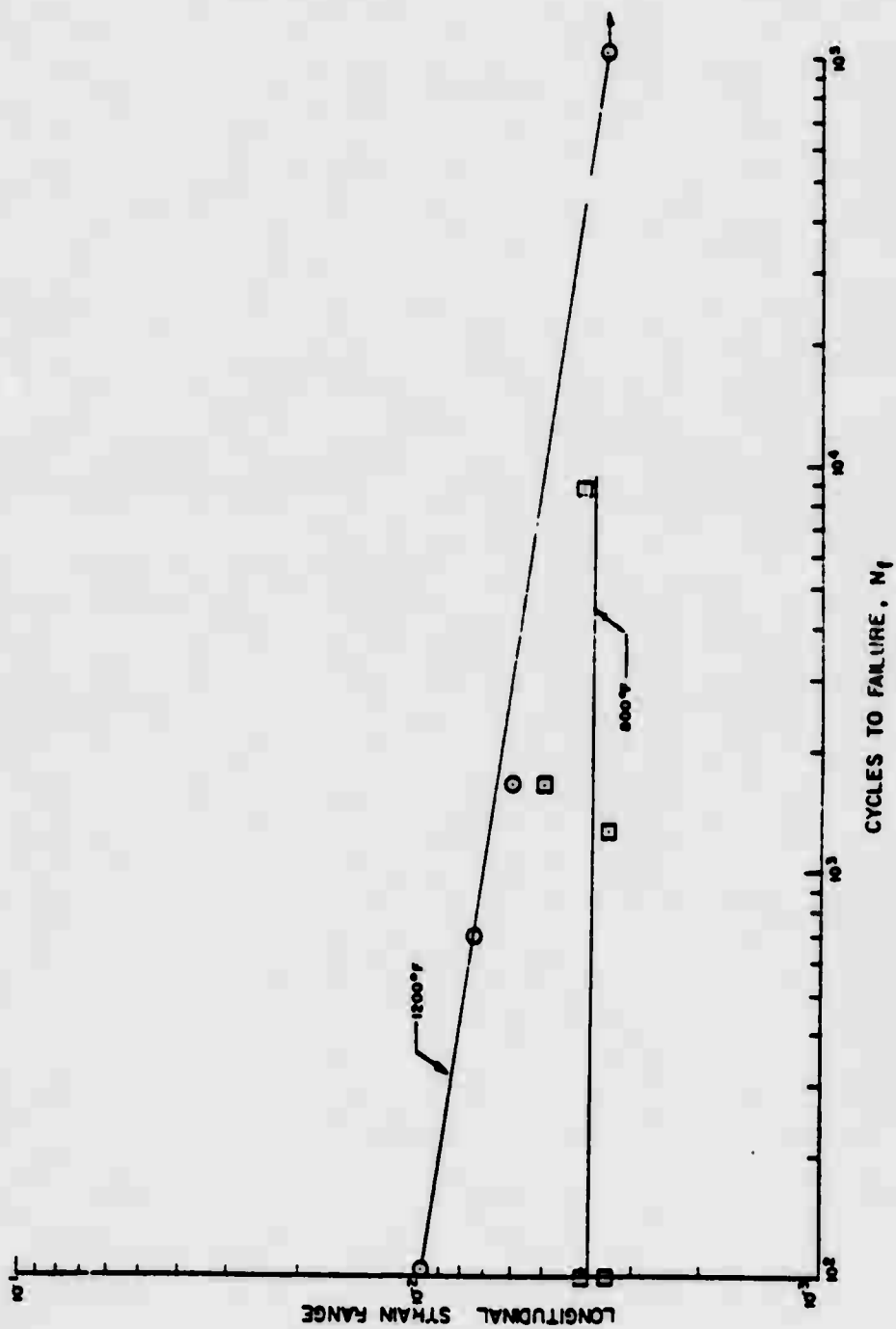


Figure 40. Longitudinal Strain Range vs. Cycles to Failure for Ti-16Al-10Nb (Strain Controlled)

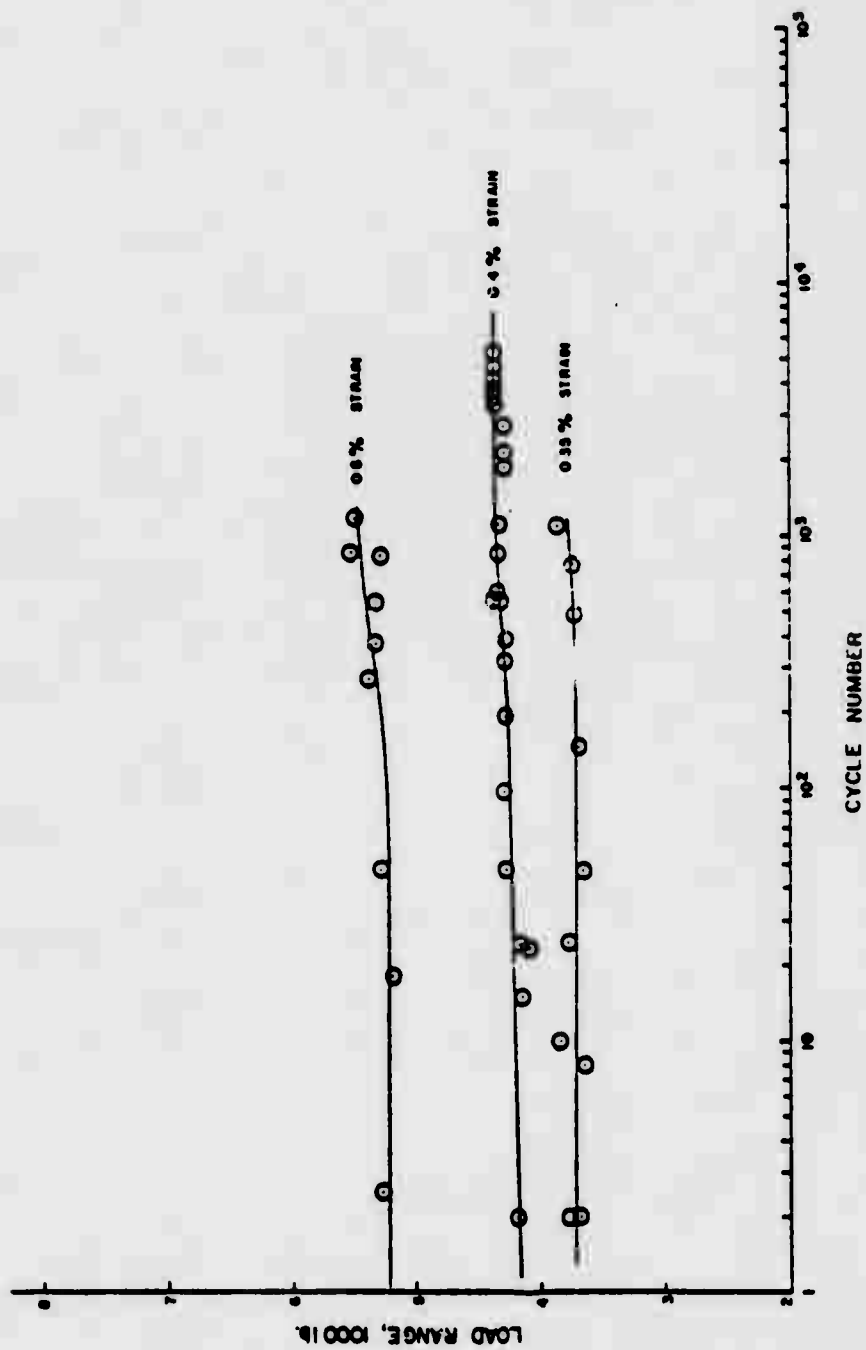


Figure 41. Load Range vs. Cycle Number for Ti-16Al-10Nb - Test Temperature: 800°F

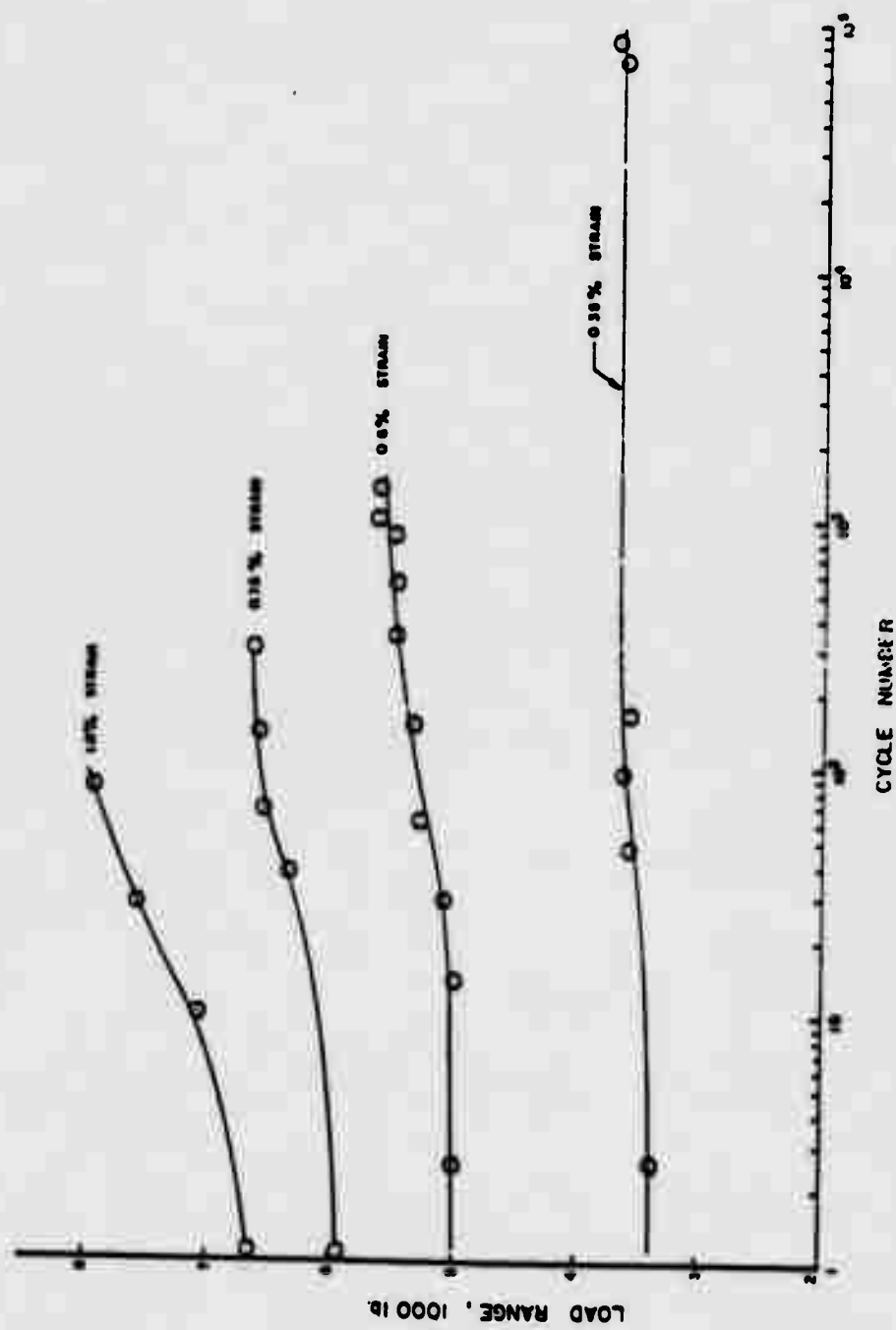


Figure 42. Load Range vs. Cycle Number for Ti-16Al-10Nb Strain Controlled LCF - Test Temperature: 1200°F

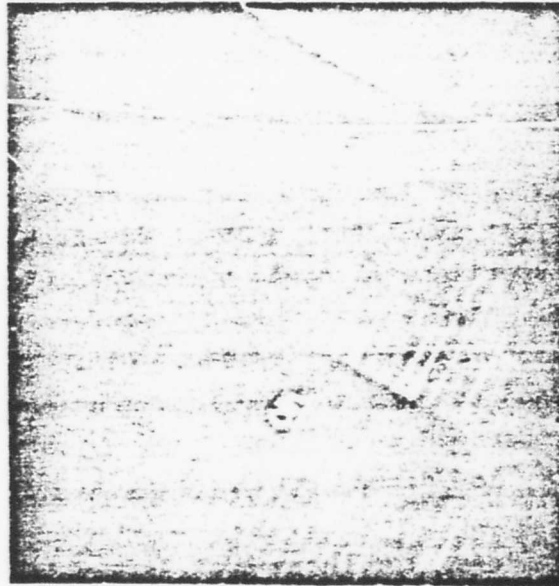
region as shown in Figure 43(b).

6) Notched (K_t 2.0) Low Cycle Fatigue

Notched (K_t 2.0) low cycle fatigue tests were performed at 800°F (427°C) and 1200°F (650°C) for stress relieved (1650°F/4 hours) specimens machined by conventional lathe turning techniques. The stress relief procedure was adopted based on fluorescent penetrant evidence of local cracking in the lathe turned notches of some specimens and the previous cracking observed in HCF specimens which were also not produced by low stress ECG techniques.

Data accumulated for these tests are shown in Table 19 and Figure 44. As with the notched HCF testing, considerable conservatism was used in planning the initial tests and as a result a series of long life tests were produced. An uploading procedure was adopted to determine the range of proper test stresses. To date, it has been determined that stresses in the range of 40-45 ksi are appropriate for the 800°F tests and that the 1200°F stress should be in the range of 37.5 to 42.5 ksi for less than 100,000 cycle life. These stresses are considerably higher than might be expected for the material based on its limited plasticity at low temperatures.

Micro-examination of the notch area of the 800 and 1200°F load controlled specimens shows an equiaxed recrystallized layer, approximately 2 mils (5×10^{-3} cm) thick at the specimen surface (Figure 45). This condition was not present on the K_t 1 specimens used for the strain controlled tests and apparently resulted from the rather severe conventional lathe turning operation used to produce the specimen notches. The recrystallized layer may have produced



6200X



200X

Figure 43. (a) Typical Low Cycle Fatigue Fracture of Ti-16Al-10Nb
(b) Fatigue Striations Observed on Ti-16Al-10Nb Low Cycle Fatigue Fracture

TABLE 19
Notched Low Cycle Fatigue Properties of Ti-16Al-10Nb

<u>Test Temperature</u>	<u>Stress ksi</u>	<u>Frequency cps</u>	<u>Kt</u>	<u>Cycles to Failure</u>
600	25.0	10	2.0	35,323 Disc.
800	27.5	10	2.0	106,510 Disc.
800	30.0	10	2.0	71,463 Disc. and Uploaded to:
800	35.0	10	2.0	109,760 Disc. and Uploaded to:
800	40.0	10	2.0	101,210 Disc. and Uploaded to:
800	45.0	10	2.0	10,290 Failed
1200	25.0	10	2.0	104,325 Disc.
1200	27.5	10	2.0	104,757 Disc.
1200	27.5	10	2.0	92,213 Disc.
1200	32.5	10	2.0	67,941 Disc. and Uploaded to:
1200	37.5	10	2.0	5,501 Failed
1200	37.5	10	2.0	100,000 Disc. and Uploaded To:
1200	42.5	10	2.0	In Test

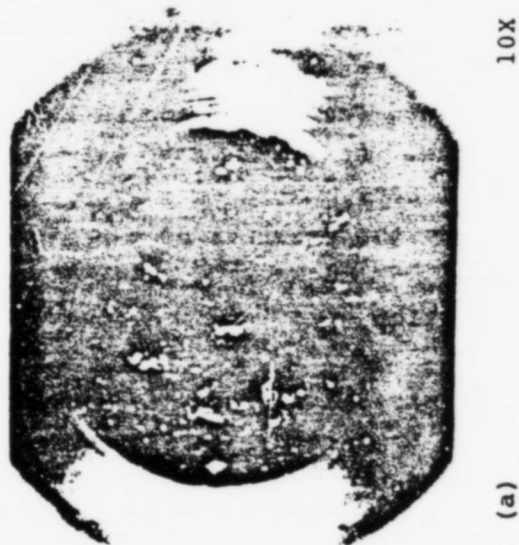


Figure 45. (a) Fracture Surface of Ti-16Al-10Nb Low Cycle Fatigue Specimen
 (b) Longitudinal Cross Section Showing Microstructure in Notch with Recrystallized Grains Adjacent to Specimen Surface.

the contrasting 800 and 1200°F behavior for smooth and notched conditions. In any case, it is not clear whether the recrystallized layer improved the 800°F notched life or reduced the 1200°F notched life.

7) Crack Growth Rate Testing

Crack growth testing was performed at both 800°F and 1200°F for precracked center notched panels, illustrated in Figure 46, which were machined from the original pancake forgings by conventional grinding techniques. Considerable surface cracking was observed on these panels prior to test similar to that found in the conventionally ground HCF specimens. Since limited material availability precluded replacing the specimens, it was decided to perform the tests noting that propagation of the surface cracks could affect the data. Some surface crack propagation and link up were observed during both 800°F and 1200°F tests, however, the data obtained (Figure 47) appear to plot in a generally consistent manner. Because of the machining crack phenomena, these data should be considered as only preliminary indications of crack growth rate. An indication of material toughness was obtained from crack length and load at onset of unstable fracture. At 800°F, a K_Q value of 15.7 ksi $\sqrt{\text{inch}}$ was obtained. At 1200°F, the K_Q was 21.3. These data also may be influenced by the presence of surface cracks.

8) Physical Properties

The thermal and electrical resistivity of Ti-16Al-10Nb in the range from room temperature to 1500°F are shown in Table 20 and specific heat is shown in Table 21. Table 22 gives data for the coefficient of linear thermal expansion. These data are slightly higher than the coefficients of

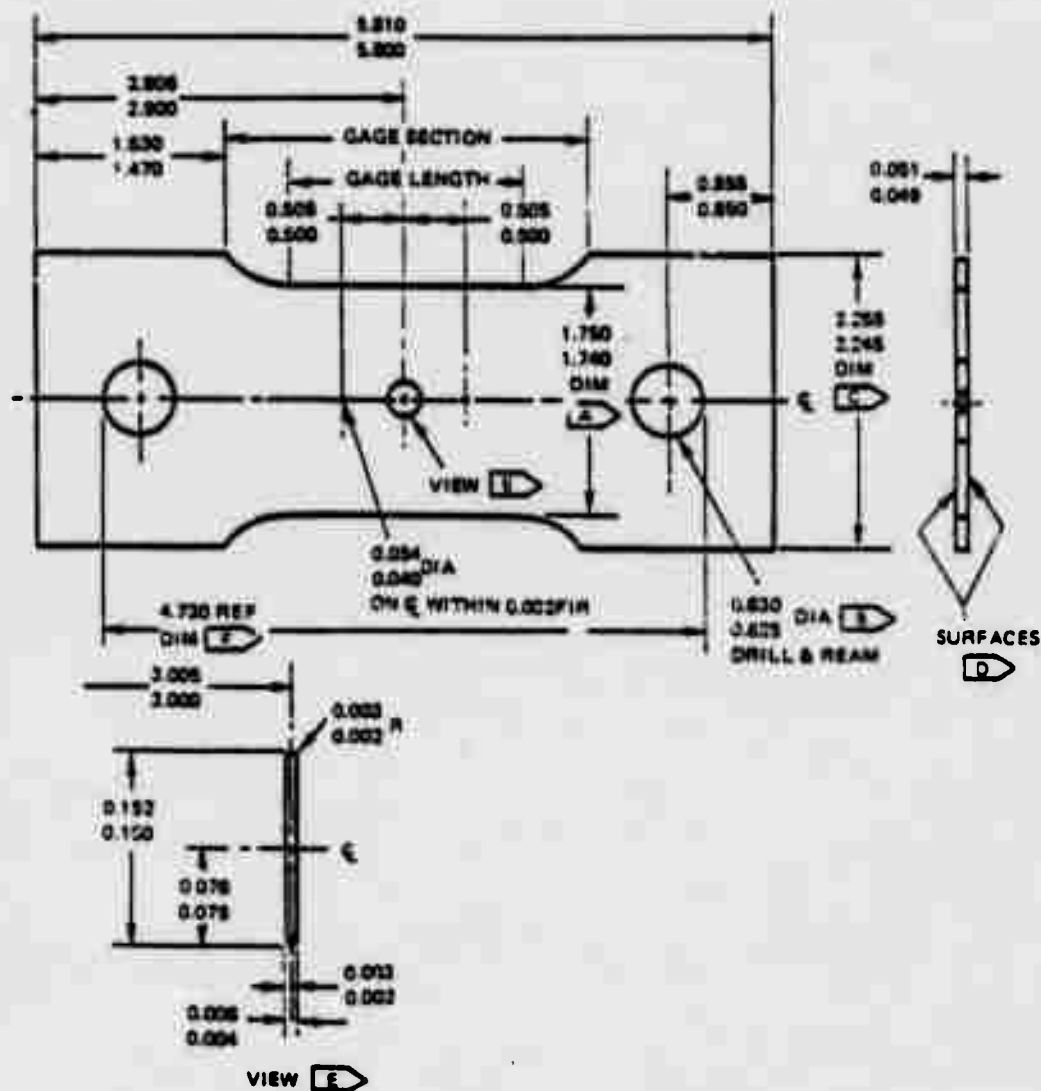


Figure 46. Center Notched Panel for Fatigue Crack Growth Measurement

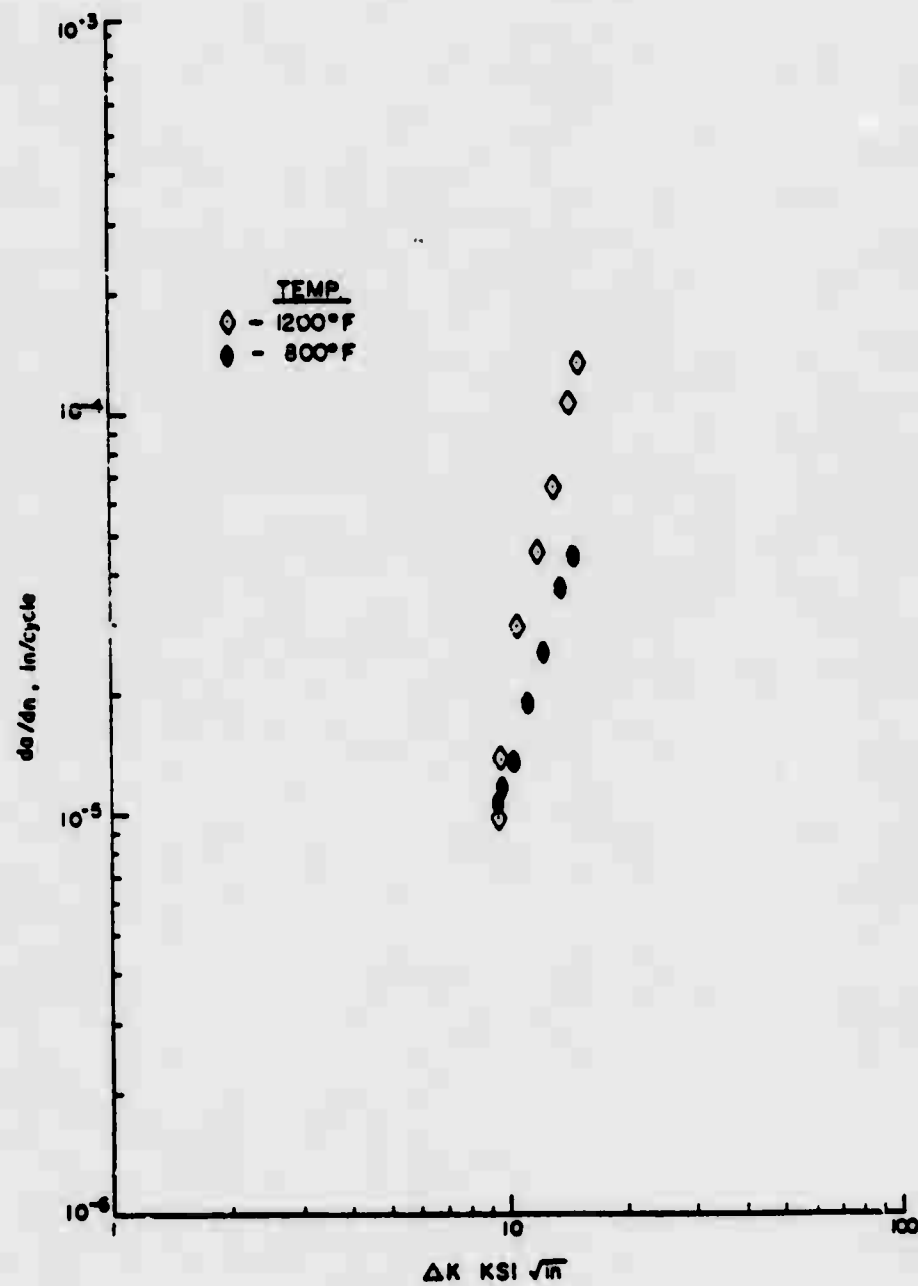


Figure 47. Crack Growth Rate for Ti-16Al-10Nb

TABLE 20
Thermal and Electrical Resistivity
of Ti-16Al-10Nb

Temperature		Electrical Resistivity $\times 10^{-6}$	Thermal Conductivity	
$^{\circ}\text{C}$	$^{\circ}\text{F}$		$\text{W m}^{-1} \text{ degK}^{-1}$	Btu in $\text{h}^{-1} \text{ ft}^{-1} \text{ degF}^{-1}$
25	77	173	7.0	48.5
200	392	185	9.0	62.5
400	752	188	11.5	79.5
600	1112	187	14.1	97.5
800	1472	187	16.6	115.0

TABLE 21
Specific Heat of Ti-16Al-10Nb

Temperature		Specific Heat	
$^{\circ}\text{C}$	$^{\circ}\text{F}$	$\text{J kg}^{-1} \text{ degK}^{-1}$	$\text{Btu lb}^{-1} \text{ degF}^{-1}$
25	77	560	0.134
200	392	610	0.146
400	752	660	0.158
600	1112	700	0.167
800	1472	740	0.177

TABLE 22
Coefficient of Linear Thermal Expansion
of Ti-16Al-10Nb

TEMPERATURE		THEMAL EXPANSION	TEMPERATURE RANGE		COEFFICIENT OF THERMAL EXPANSION	
C	F	($\Delta L/L_0$) $\times 10^{-4}$	C	F	$10^{-6} \text{ degC}^{-1}$	$10^{-6} \text{ degF}^{-1}$
20	68	-	-	-	-	-
100	212	7.6	20 - 100	68 - 212	9.5	5.3
200	392	17.3	20 - 200	68 - 392	9.6	5.3
300	572	28.0	20 - 300	68 - 572	10.0	5.6
400	752	38.8	20 - 400	68 - 752	10.2	5.7
500	932	49.9	20 - 500	68 - 932	10.4	5.8
600	1112	61.6	20 - 600	68 - 1112	10.6	5.9
700	1292	73.6	20 - 700	68 - 1292	10.8	6.0
800	1472	86.8	20 - 800	68 - 1472	11.1	6.2

expansion of conventional titanium alloys such as Ti-6Al-2Sn-4Zr-2Mo, but are considerably lower than nickel-base alloys such as INCO 713C and Waspaloy^R, Figure 48. The relatively low thermal expansion coefficient for Ti-16Al-10Nb should favorably impact the thermal fatigue resistance of the alloy.

9) Thermal Fatigue

A series of thermal fatigue tests were completed using standard NGTE disks with 0.020 and 0.040" edge radii. Considerable difficulty was encountered with machining cracks resulting from the conventional grinding operations used to produce these specimens as discussed in the previous section. An attempt was made to remove the machining cracks by a combination of electro-polishing and mechanical polishing prior to test, however, this was generally unsuccessful without modifying specimen edge geometry beyond acceptable limits. As a result, it was decided to perform the tests, even though small metallographically visible pre-cracks were present in all specimens, in order to determine the general tendency for cracks to propagate in thermal fatigue. The resulting test data are shown in Table 23.

The grinding cracks extended to the approximate 5 mil (1.3×10^{-2} cm) size, normally detected by fluorescent penetrant inspection as a pinpoint crack, within 50 to 100 cycles from 1500°F to room temperature for both 0.020 and 0.040" edge radius specimens. Growth to a 3/16" crack generally occurred after 200 to 450 cycles with the high stress 0.020" radius specimen and in greater than 700 cycles for the lower stress 0.040" edge radius specimen.

Second Year Program - The second series of alloys chosen* for more complete mechanical property characterization were

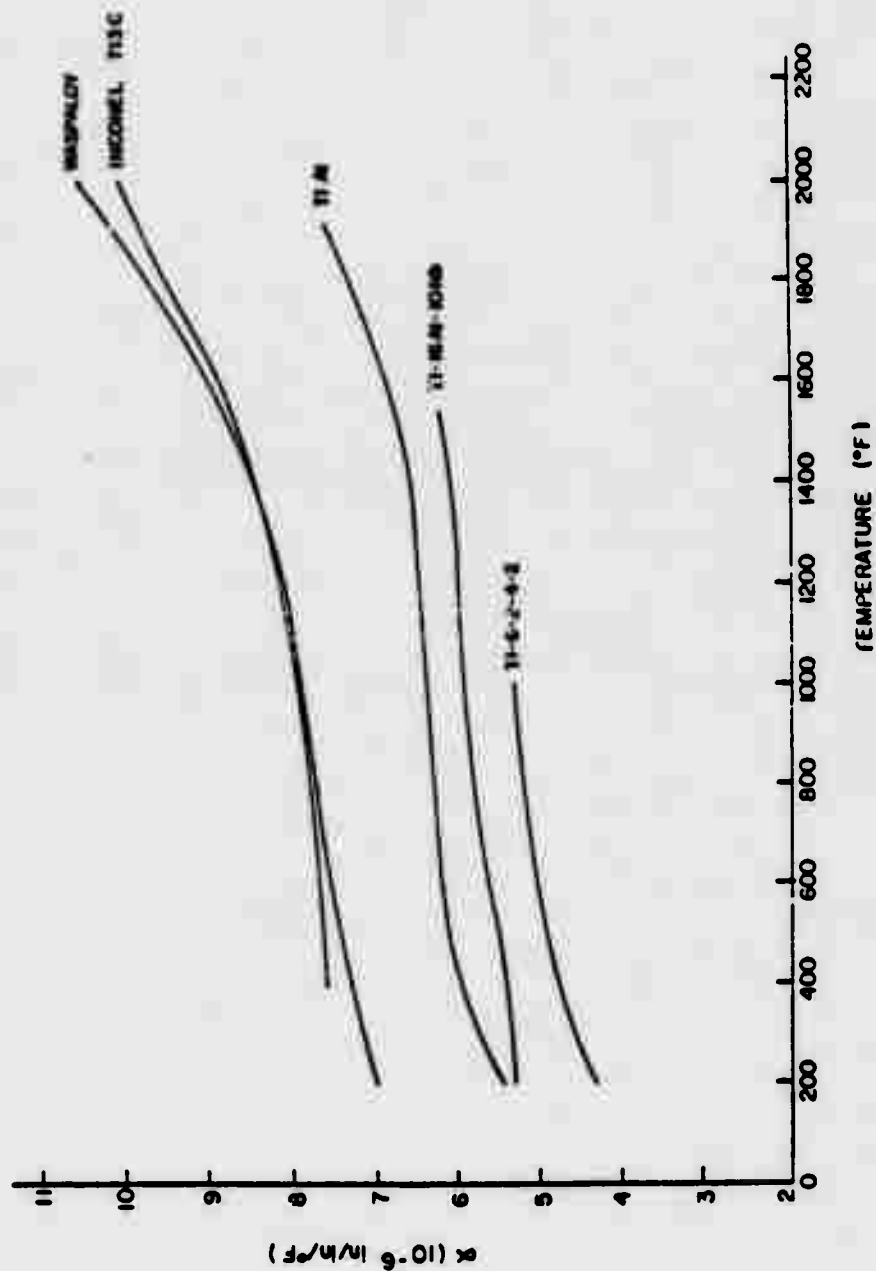


Figure 48. Comparison of the Thermal Expansion of Titanium Aluminides and Conventional Materials

TABLE 23
Thermal Fatigue Results for Ti-16Al-10Nb

Radius (in.)	$\frac{Temp_1}{^\circ F}$	$\frac{Temp_2}{^\circ F}$	$\frac{time_1}{min}$	$\frac{time_2}{min}$	Pin Point	Cycles To:				Discontinuation
						1/64	1/32	1/8	3/16	
0.020	RT	1500	2	2	50	-----	---	-----	200	3/16 @ 200
0.020	RT	1500	2	2	150	-----	---	250	350	3/16 @ 350
0.040	RT	1500	2	2	100	-----	---	-----	450	3/16 @ 450
0.020	RT	1500	2	2	50			100-150	200	3/16 @ 200
0.040	RT	1500	2	2	57	107	670	-----	---	3/16 @ 770
0.040	RT	1500	2	2	300	500-600	---	800		3/32 - 1/8 @ 150
0.040	RT	1500	2	2	50	150		510		3/16 @ 1275

selected from the results of the Alloy Development Program described in Section II. Ingots prepared from the chosen alloys, forged to pancakes and heat treated prior to specimen preparation. A more limited test program was performed on these specimens, emphasis being placed on tensile and creep rupture property characterization together with a limited fatigue evaluation. To date, three alloys have been melted and forged, with aim composition as given below:

Ti-13.5Al-21.5Nb

Ti-13.5Al-21.5Nb-0.1Si

Ti-14.5Al-16Nb-3.8Hf

Mechanical property testing is complete for the first alloy but is still in progress on the last two and results will be presented in later reports.

A. Characterization of Ti-13.5Al-21.5Nb Alloy

Based on the results of the subscale ingot program, an initial chemistry--Alloy #42, Ti-24Al-11Nb a/o, Ti-13.5Al-21.4Nb w/o--was selected for the scale-up evaluation. A 20-pound ingot was triple consumable melted by Titanium Metals Corporation of America (TMCA), Henderson, Nevada. In order to insure homogeneity, a Ti-Nb master alloy was used as starting stock for the 20-pound melt. The chemical analysis of the ingot is shown in Table 24.

Visual inspection of the cast product revealed the ingot to be sound and free of macroscopic cracking. The ingot top was also sound and no surface connected shrinkage porosity was observed. To improve product yield and integrity, hot isostatic pressing (HIP'ing) was conducted in the Pratt & Whitney Aircraft, East Hartford, Connecticut,

TABLE 24
Chemical Composition of Titanium Aluminide Alloy
TMCA Heat V5301, Ti-13.5Al-21.4Nb

<u>Element</u>	<u>TMCA*</u>	<u>P&WA</u>		<u>Air</u>
		<u>Top</u>	<u>Bottom</u>	
Ti	Balance	Balance	Balance	Balance
Al	13.3	14.7	13.7	13.5
Nb	18.6	20.8	19.9	21.4
Fe	0.16	0.09	0.10	--
O	0.19			--
N	0.024			--

* Average of top and bottom chemistry.

HIP unit under conditions of 2250°F (1232°C)/15,000 psi argon pressure for three hours. Subsequent to the HIP treatment, the ingot was x-rayed using an in-house facility to evaluate material integrity. Radiographic analysis revealed a completely sound ingot which was free of any observable internal porosity.

Prior to forging, the ends of the ingot were machined flat and parallel and the ingot OD was turned smooth. Protective tantalum sheets were spot welded to the end faces of the ingot. The ingot was isothermally processed at 2000°F (1090°C) and 0.05 inch/inch/minute to 1" thick plate configuration. The isothermally forged pancake was furnace cooled subsequent to deformation. Forging results are summarized in Table 25 and the pancake configuration is shown in Figure 49. The processing sequence yielded a fine, ASTM 9-10, equiaxed alpha and intergranular beta morphology, typical of a structure forged low in the alpha-beta field, illustrated in Figure 50(a), with an as-forged Vickers hardness of 257. The beta transus was determined to be 2175--2000°F (1190-1204°C). This transus temperature is higher than anticipated based on the 1975-2000°F (1079-1093°C) transus determined for Alloy #42 (Ti-13.5Al-21.4Nb w/o). However, the increase can probably be traced to the much higher oxygen content of the ingot material (0.19%) compared with the drop casting (0.03%). For future ingots, the oxygen level was controlled at <0.10%.

Several preliminary heat treatment trials were conducted on sections of the forging. As noted in the Alloy Development Section, the properties of the alloy are a function of the heat treatment and structure. It was found that the increased size of the ingot slices resulted in a different response (and structure) when cooled from

TABLE 25
Isothermal Forging Results

Material	Nominal Ti-24Al-11Nb a/o
Temperature	2000°F
Strain Rate, in/in/min.	0.05
Initial Height, in.	5.0
Final Height, in.	1.0
Percent Reduction	80%
Final Flow Stress, Ksi	4.75

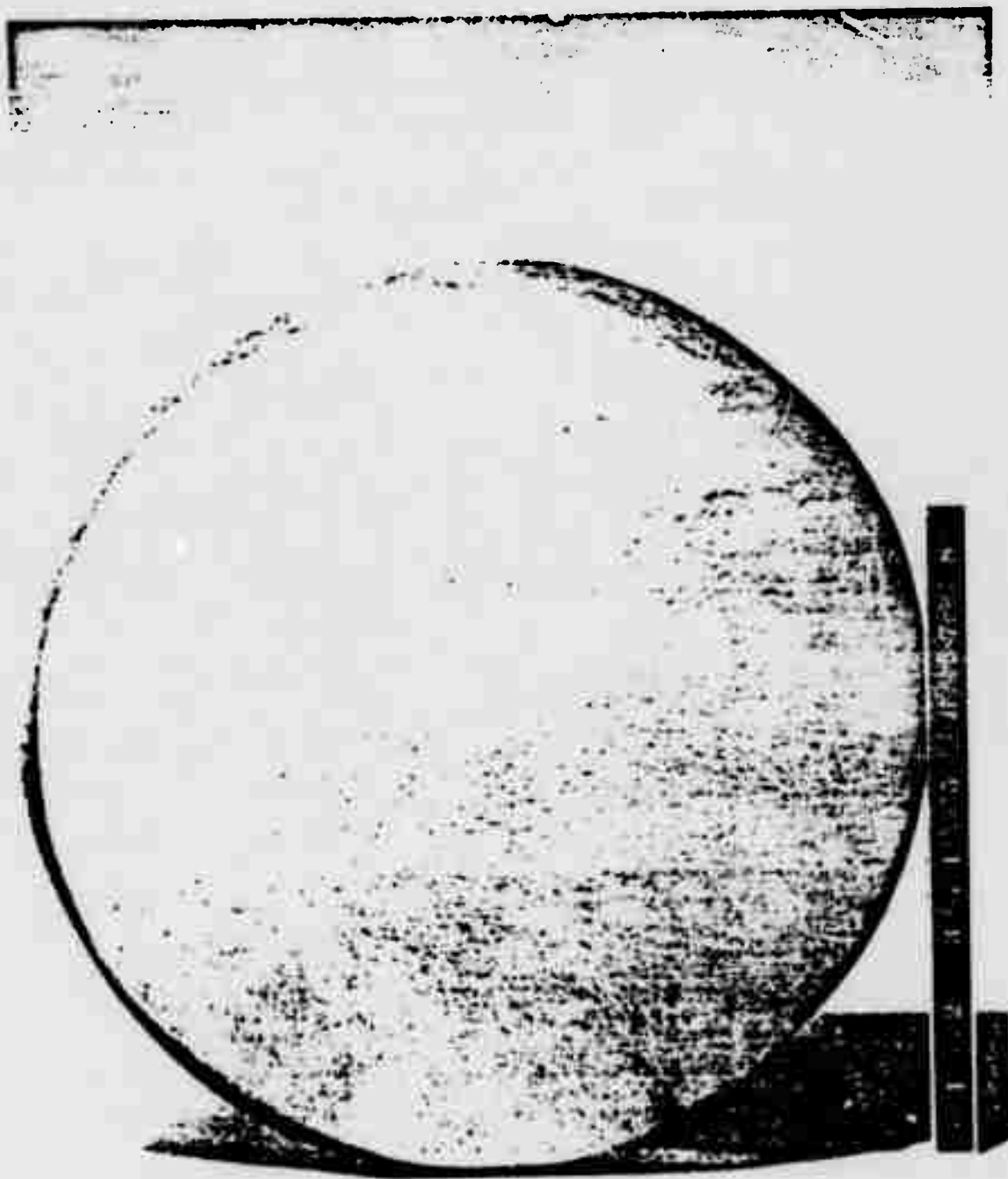


Figure 49. Pancake Forging Configuration Produced for the 20-Pound Ti-13.5Al-21.5Nb Alloy

the beta phase field compared with earlier experience on smaller sections. Screening studies showed that air cooling from a solution treatment temperature of 2200°F (1200°C) gave the required fine Widmanstätten structure, illustrated in Figure 50(b), and a hardness value of 365 VDN. The majority of tests were conducted on material in this condition, although this is one of a total of five heat treatment variations evaluated. Specimens used for the tests were the same as used in the first year program, shown in Figure 3. Tensile test results are presented in Table 26. The as-forged tensile values indicate a ductile-brittle transition temperature of about 500°F (260°C). As-forged strengths appear at least equivalent to the first year program alloy, Ti-16Al-10Nb, up to the 1200°F (650°C) test temperature. Subsequent to beta furnace cooling, strengths are somewhat increased and the ductile-brittle transition temperature appears to be lowered to RT.

The 0.2% yield strength, ultimate tensile strength and percent elongation versus temperature are illustrated in Figure 51 for the beta air cooled material. Examination of these results indicates additional improvements in strength and ductility values compared to the as-forged or furnace cooled material with RT yield strengths of approximately 110 ksi, ultimate tensile strengths of about 117 ksi and ambient temperature ductilities of approximately 0.65%. This is an improvement in the ductile-brittle transition temperature of about 800-900°F compared to the Ti-16Al-10Nb alloy. From Figure 51, it can be seen that the yield strength of the beta air cooled material drops off markedly between RT and about 500°F (260°C). At temperatures between 500°F (260°C) and 1000°F (540°C), yield strength is nearly constant, while above approximately 1000°F (540°C), yield strengths once again decrease. In contrast, ultimate

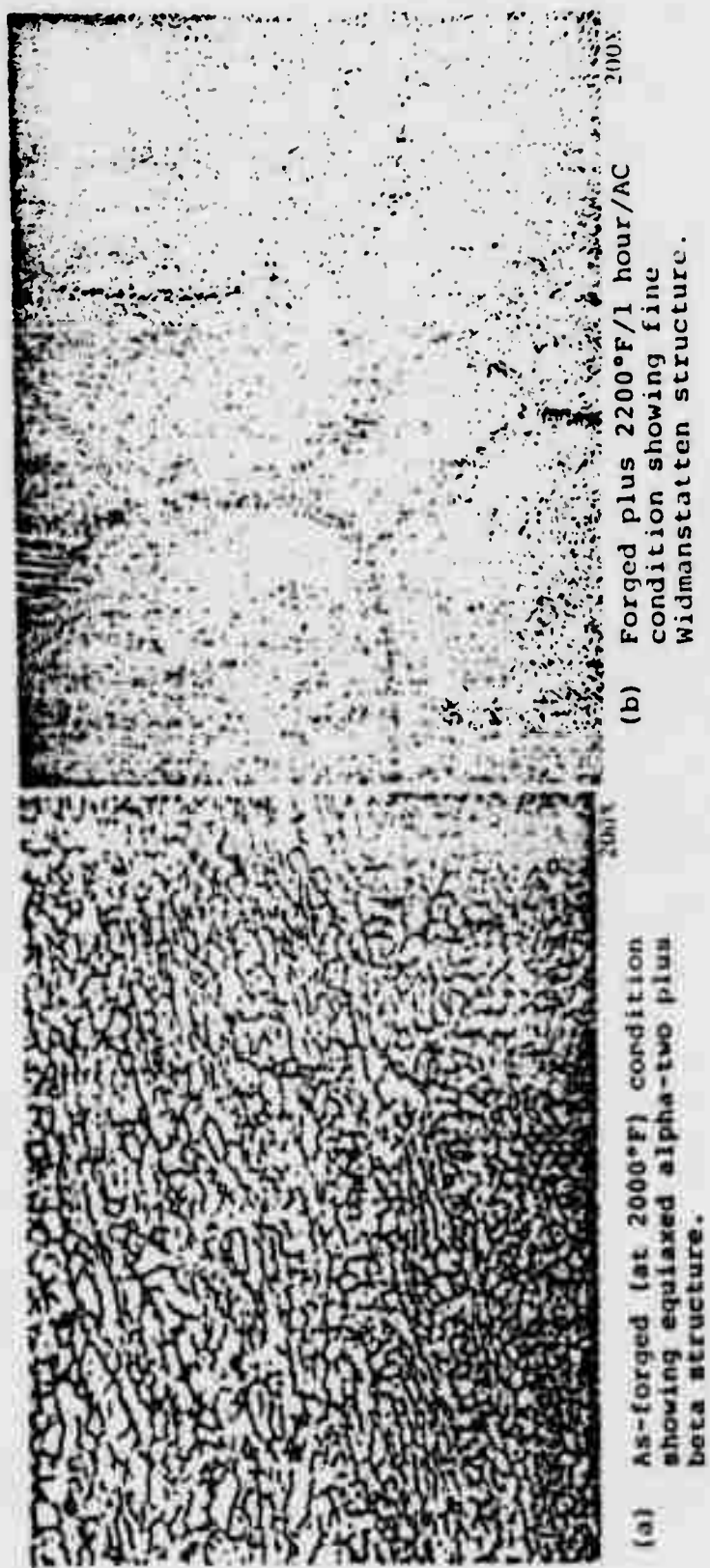


Figure 50. Microstructure of the 20-Pound Nominal Ti-13.5Al-21.5Nb Alloy

TABLE 26
Tensile Results for the Nominal Ti-13.5Al-21.5Nb
20-Pound Ingot

Heat Treatment/ Condition Temp. (°F)	Test Temp. (°F)	0.2% Offset Yield Strength ksi	Ultimate Tensile Strength (ksi)	Elongation %	Reduction of Area %
As-Forged	RT	73.7	73.7	7.0	7.0
As-Forged	250(500)	69.5	69.5	7.0	7.0
As-Forged	650(1200)	64.1	64.1	11.7	11.7
1200(2200)/2,50	RT	50.3	76.3	0.55	1.3
1200(2200)/2,50	RT	124.6	124.6	0.46	1.5
7	200(400)	123.6	123.9	0.49	1.5
	250(500)	123.4	123.8	2.1	1.5
	250(500)	123.0	122.5	1.9	1.5
	423(800)	126.1	122.1	3.5	1.5
	423(800)	121.1	124.0	3.1	1.5
	540(1000)	126.2	125.7	6.5	1.5
	540(1000)	121.5	125.0	7.7	1.5
	540(1000)	121.2	124.0	7.0	1.5
	650(1200)	121.9	120.0	5.2	1.5
	650(1200)	121.2	124.4	3.9	1.5
	650(1200)	121.2	121.1	6.0	1.5
	650(1200)	121.0	121.1	9.5	1.5
	650(1200)	121.0	121.1	9.7	1.5
1200(2200)/2,50	RT	74.1	74.1	0.35	1.5
As-Forged/1200(2200)/2,50	RT	74.2	74.9	0.50	1.5
As-Forged	250(500)	69.3	69.0	3.5	1.5
As-Forged	650(1200)	64.0	74.2	6.0	1.5

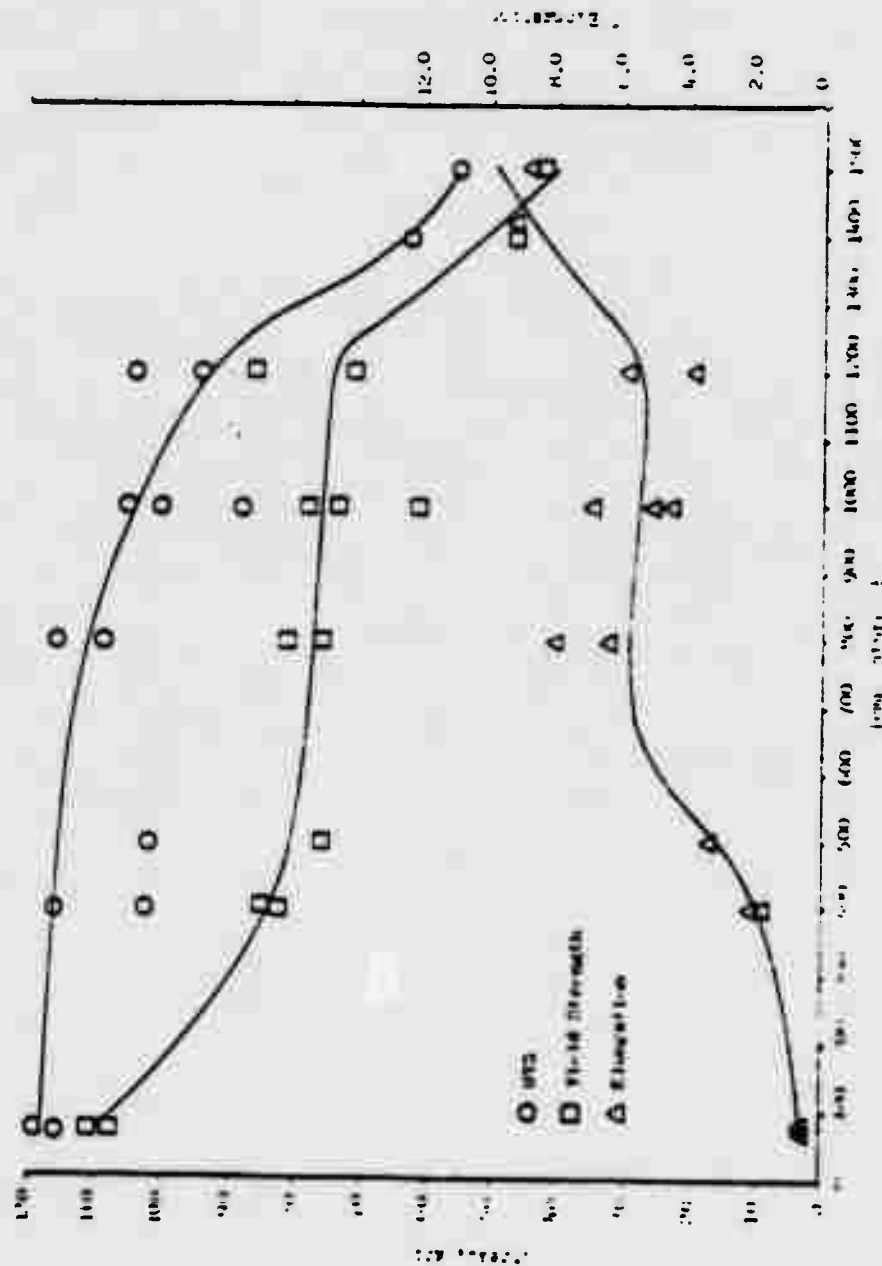


Figure 51. 0.2% Offset Yield Strength, Ultimate Tensile Strength and % Elongation vs. Temperature for the Nominal Ti-13.5Al-21.5Nb Ingot in the 2200°F (1200°C)/1 Hour/AC Condition

tensile strengths remain fairly constant between RT and about 800°F (425°C); above 800°F (425°C) ultimate strengths also decrease with increasing temperature. Although it is apparent that the data are rather variable, ductility levels can be seen to increase from a value of 0.65% at RT with increasing temperature. Considering the beta air cooled plus stabilized material, a decrease in both strength and ductility values is observed in the RT to 1200°F (650°C) temperature range compared to the unstabilized material. It can be noted that the furnace cooled and beta air cooled plus stabilized RT tensile results are quite comparable.

Creep rupture test results are presented in Table 27. As in the tensile evaluation, material has been screened in four heat treatment conditions. As-forged material was tested under conditions of 1300°F (700°C)/40 ksi and exhibited a poor rupture life of 0.4 hours, probably due in part to the low elevated strength of the material. The beta furnace cooled specimen exhibited a 1.3 hour rupture life under conditions of 1200°F (650°C)/55 ksi. This low value may also be attributed to a decline in the elevated temperature strength capability of the furnace cooled structure, although no data exists to substantiate this at the present time. The creep rupture capability of the ingot material appeared significantly improved subsequent to a 2200°F (1200°C)/1 hour/AC treatment. Material creep tested in this condition revealed a 1100°F (590°C)/60 ksi rupture life of 233.9 hours and a 1200°F (650°C)/55 ksi life of 44.7 hours. The former value is comparable to the Ti-16Al-10Nb alloy which exhibited a 1100°F (590°C)/60 ksi creep life of 235 hours, while the latter value is inferior to the first year program alloy which revealed a 92.2 hour creep life under condition of 1200°F (650°C)/55 ksi. These results may be rationalized by the fact that the strength

TABLE 27

Creep Results for the Nominal Ti-13.5Al-21.5Nb 20-Pound Ingot

Heat Treatment/ Condition C(F) 1 Hr.	Test Temper- ature C(F)	Stress (ksi)	Time To 1% Creep (Hrs.)	Time To Rupture (Hrs.)	Elongation (%)	Reduction in Area (%)
As-Forged	700(1300)	40	0.03	0.4	5.6	14.3
1200(2200)/1/TC	650(1200)	55	0.0	1.3	11.0	14.6
1200(2200)/1/AC	590(1100)	60	25.26	233.9	7.0	4.1
	650(1200)	55	2.94	44.7	14.5	4.3
1200(2200)/1/AC + 370(1600) 14/AC	590(1100)	60	21.55	605.9	3.6	5.7
	650(1200)	55	0.14	23.1	9.0	11.6

values of the Ti-13.5Al-21.5Nb 20-pound ingot decrease rapidly above 1000°F (540°C), as discussed above, in contrast to the rather flat strength curves (at least up to about 815°C) observed for the Ti-16Al-10Nb alloy, as may be seen from Figure 33. Specimens were also creep tested subsequent to a beta air cool stabilization treatment. An excellent rupture life of 605.9 hours was revealed under conditions of 1100°F (590°C)/60 ksi and a life of 23.1 hours was exhibited under conditions of 1200°F (650°C)/55 ksi.

The high cycle fatigue characteristics of the alloy were determined at 800°F (425°C). Smooth ($K_t = 1$) Westinghouse HCF specimens were tested in a reverse bend ($R = -1$) high cycle fatigue machine with test frequency maintained at 7200 cpm. Specimens were run until rupture or discontinued at 10^7 cycles with the results presented in Table 28 and illustrated in Figure 52. Material was solution treated at 2200°F followed by an air cool. The fatigue results indicate a runout stress (10^7 cycles) of 50 ksi. These properties are slightly superior to the Ti-16Al-10Nb alloy studied during the first year of this contract.

B. Additional Heat Treatment Studies

It has become clear during this investigation that microstructural control is a key to obtaining a balance of mechanical properties. In order to produce the required structures in a production situation more stringent control of cooling rate will be needed than available in air or furnace cooling. Therefore, a series of trials are in progress to evaluate the effectiveness of salt quenching in producing the necessary structures without any tendency to quench cracking. To date, three trials have been conducted and the resultant structures analyzed. The conditions

TABLE 28
High Cycle Fatigue Results for the Nominal Ti-13.5Al-21.5Nb
20-Pound Ingot

<u>Test Temperature C (F)</u>	<u>Kt</u>	<u>Cycle Rate CPM</u>	<u>Stress (ksi)</u>	<u>Cycles to Failure</u>
425(800)	1.0	7200	50	1.0×10^7 Runout
425(800)	1.0	7200	53	1.0×10^7 Runout
425(800)	1.0	7200	54	1.0×10^7 Runout
425(800)	1.0	7200	55	2.9×10^6
425(800)	1.0	7200	55	4.9×10^6
425(800)	1.0	7200	60	1.9×10^6
425(800)	1.0	7200	60	9.6×10^5
425(800)	1.0	7200	65	5.2×10^5

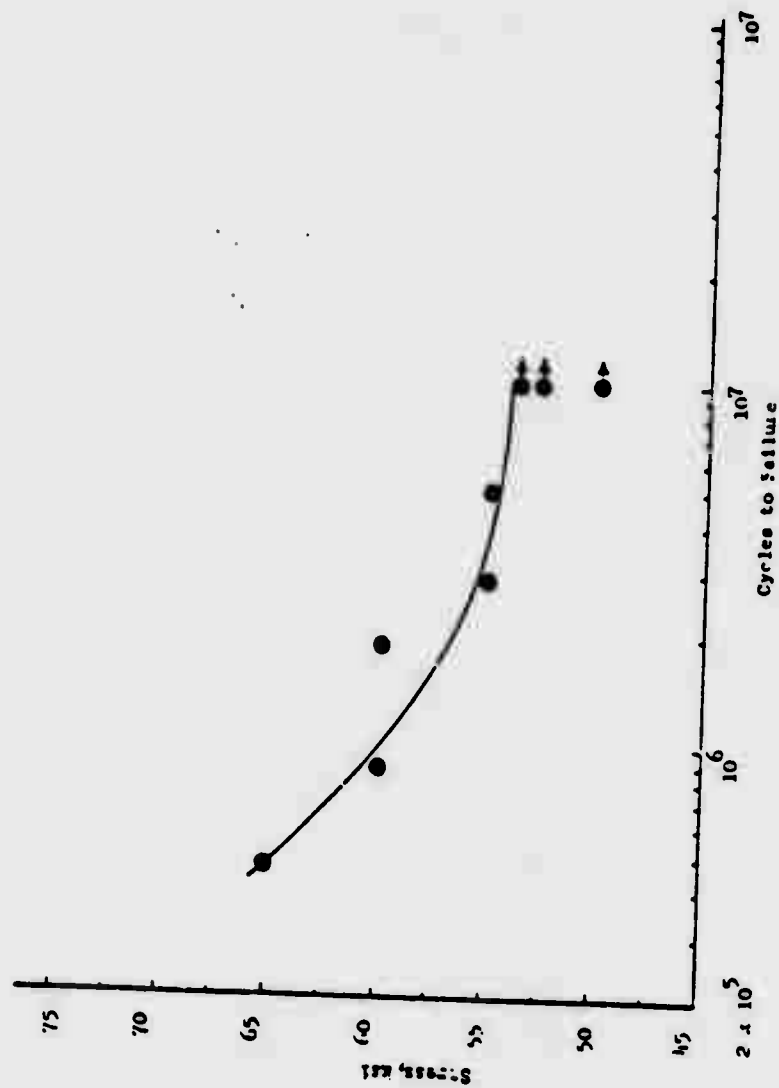


Figure 52. S-N Curve for Ti-13.5Al-21.5Nb at 800°F

were as follows:

- 1 2225°F Solution Treatment, quench into salt at 1400°F, hold for 15 minutes
- 2 2225°F Solution Treatment, quench into salt at 1000°F, hold for 15 minutes
- 3 2175°F Solution Treatment, quench into salt at 1400°F, hold for 15 minutes

Treatment 1 produced structures very similar to those observed in material forged above the beta transus. This indicates that the salt temperature must be decreased in order to produce the aim structure. Treatment 2 gave a structure virtually the same as that formed on air cooling from the beta phase field. Treatment 3, which was solution treated in the alpha plus beta phase field contains a uniform distribution of primary alpha in a relatively fine transformed beta structure.

3. Discussion

The program conducted on the Ti-16Al-10Nb alloy in the first year of this effort established process methods for handling reasonably large volumes of an aluminide alloy and generated extensive property data. The program demonstrated that powder metallurgical methods were applicable to this class of materials; consolidation by direct hot isostatic pressing yielded a sound product which was forged with no difficulty. Subsequent processing through heat treatment and the fabrication of a variety of specimens was also accomplished readily. However, closer examination of specimen surfaces prepared by conventional grinding and turning did reveal shallow surface cracks indicating that, at least in this alloy, not all finishing techniques could be used. In

addition, machining techniques that resulted in the retention of residual stresses in the material surface resulted in thermally induced instabilities. Thus, during exposure to elevated temperature, such as during a test, the surface layers tended to recrystallize resulting in a structural change from an acicular to an equiaxed grain configuration. Results of a more detailed study on such surface instabilities will be found in Section III which also indicates that the phenomenon is alloy dependent.

With the above two reservations, it is clear that this study showed that alpha two aluminide alloys can be processed and finished using many of the techniques used for conventional titanium alloys. This in turn means that the fabrication of components should be possible without the development of radically new methods.

Analysis of the mechanical and physical property data acquired indicates that the alloy investigated in the first year of the program, namely Ti-16Al-10Nb, is superior in elevated temperature capability to current conventional titanium alloy, such as Ti-6Al-2Sn-4Zr-2Mo, by 300 to 400°F and is fully competitive with nickel-base superalloys on a strength to density basis. The fatigue properties of the material are generally excellent over the investigated temperature range of 800 to 1200°F, although indication of increased scatter was found for lower temperature LCF; this was probably related to the limited low temperature ductility for this alloy as observed by tensile tests. The high cycle fatigue results for the material generally do not show a debit at the lower temperatures possibly because of the more limited strain exposure inherent in the high cycle fatigue results as compared to that of low cycle fatigue tests. Evidence of strain hardening behavior was

observed in the low cycle fatigue tests at both 900 and 1200°F, although it was more pronounced at the higher temperature. The Charpy impact data for this alloy are relatively low at room temperature, but a considerable increase in ductility observed above this temperature. At the potential operating temperature for most titanium aluminide gas turbine applications (1200-1600°F), the material is competitive with alternate nickel-base alloys such as INCO 713C.

The second year program scaled-up alloys chosen from the Alloy Development Program and generated mechanical property data. Conventional titanium alloy melting practice was used to produce 20-pound ingots of the selected material and ingots of good quality were produced. HIP consolidation of the ingots was shown to be an effective method of sealing porosity and improving product yield in the forging step of the process cycle. This methodology was used for two ingots, the third was forged in the as-cast condition and no difficulty was encountered. Thus, in addition to the P/M methodology demonstrated in the first year of the program, it has also been shown that consumable arc melting technology is a viable method for aluminide production.

Mechanical property testing has been completed for the Ti-13.5Al-21.5Nb alloy and is in progress for the other two alloys. The alloy showed a ductility improvement over the first year alloy, useful plasticity was measured at temperatures above 500°F and small but finite ductility occurs below that temperature. However, it is clear that the results are inferior to those obtained on laboratory size ingots; the differences may be due to either scale-up factors and/or compositional deviations. Another obvious difference between the two materials are in the oxygen

content which is ~0.05% in the laboratory material and ~0.2% in the 20-pound ingot. Further analysis is needed to pin down the reasons for the changes in plasticity observed.

The improved tensile ductility is accompanied by a reduction in the stress rupture capability of the material. Comparison of the present results with the first year alloy shows that the differences are slight at lower temperatures (~1100°F) but are quite marked at higher temperatures (~1500°F). It should be noted that a considerable advantage over conventional alloys is still apparent.

The improved ductility of the alloy leads to less scatter in HCF test results at 800°F and may also be responsible for the slight increase in runout stress value. It could be noted that the fatigue properties obtained at 800°F are rather similar to conventional high temperature titanium alloys, such as Ti-6Al-2Sn-4Zr-2Mo, and thus could be assumed to show no advantage. However, the critical point is that in these lower ductility materials, the properties at intermediate temperatures could act as a barrier to the material's use. Thus the fatigue results may be taken as a positive indication in the effort to apply these materials in gas turbine engines.

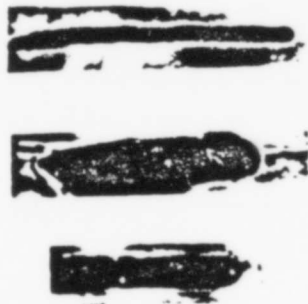
In summary, at this stage of the program the processing characteristics and the properties measured for alpha two type alloys can be considered encouraging. Scale-up to larger ingot sizes and continued evaluation of promising alloy compositions are planned for the future.

IV. MANUFACTURING FEASIBILITY STUDIES

1. Introduction

Broad acceptance of a new engineering material requires that it not only have attractive properties but that manufacturing techniques are available to produce a range of product forms. For the titanium aluminides in gas turbine engines, potential applications include components ranging from relatively small airfoils weighing less than a pound up to complex static structures, such as cases, which may weight over 100 pounds. Most components can be manufactured by alternative techniques; however, the cost and component capability resulting from various approaches are never equal. It is consequently highly desirable that a material's compatibility with a range of metal forming operations be understood.

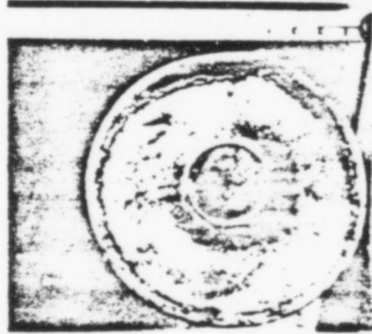
With each material system, a unique set of properties can dramatically affect the ease or complexity of a given manufacturing approach. For example, it was well known that the aluminides were subject to severe cracking during conventional forging operations when they were first evaluated during the 1950's. At that time, forging appeared nearly hopeless as a result of the material's limited plasticity and its relative strain rate sensitivity. With the development of isothermal techniques which allow excellent strain rate control, complex precision forgings were produced at Pratt & Whitney Aircraft with relative ease (Figure 53). The characteristics of this new manufacturing procedure allow even small pieces of metal to be maintained at high temperatures and within the plastic range of the aluminides, for the relatively long periods of time necessary to complete a forging at low strain rates.



TIG welded
plate



Isothermally
forged blade



Isothermally
forged P/M
pancake

Figure 53. Ti-16Al-10Nb Process Developments

The property characteristics of the material now fit the capability of the forging technique, and forging can be considered an acceptable metalworking approach. This new technique has overcome a manufacturing difficulty, but it has done so at considerable added cost as a result of increased equipment complexity and much slower forging cycle time. The forgings which have been produced to date have been done by procedures which work; however, much remains to be done to determine the feasibility of reducing their cost and improving their properties. Cost is in part a function of production rate or cycle time, and if it were feasible to increase strain rate by selecting a different forging temperature, cost could be reduced. Selection of new forging parameters can also affect properties since microstructure can be changed by both temperature and strain rate.

The feasibility of manufacture by other techniques, about which even less is known, also requires evaluation. Small high temperature components, such as low pressure turbine blades, are one of the most important areas where aluminides can be used since the lightweight strongly impacts inherent body stresses in rotating components. As a result, the payoff for the use of these materials in rotating structures as a percent of component weight is much higher than for static structures. In addition, the lightweight of aluminide turbine blades reduces the required weight of the supporting disk structure and of the associated static structures, such as struts, bearing supports and cases. If the aluminides are used to produce static structures, a large total weight savings as a percent of engine weight is possible but this results from the large number and great weight of static components.

Application of these materials in low turbine blades and static structures may require greatly different manufacturing procedures. For example, in the past, turbine blades have classically been produced by casting techniques since great precision is possible by investment casting and this minimizes high machining cost on complex curved airfoil surfaces. In addition, the important mechanical properties of creep and stress rupture are superior for current turbine blade materials in the cast, as compared to the forged condition. Preliminary evaluation of the Ti_3Al base aluminide (Ti-16Al-10Nb) characterized in the first year of this Air Force sponsored program at Pratt & Whitney Aircraft has indicated that this material exhibits superior creep rupture properties with the high temperature beta annealed microstructure. This type of structure is present for the cast material and, consequently, both cost and property considerations suggest that casting capability may be important for some aluminide materials.

In static structures such as cases, the large component size makes it desirable to have available joining techniques to assemble a complete structure using smaller cast or forged sections. The type of joining required may depend on local joint stresses and properties of the joint area, but, in addition, the cost of the joining operation is critically important. Classically, welding is widely used in such operations; however, restriction of geometrical access or property requirements can dictate the use of diffusion bonding to achieve high microstructural homogeneity, or the use of brazing in restricted access areas to reduce cost. The widest possible latitude in such manufacturing processes will result in optimum capability, and it is consequently important that the feasibility of a range of joining operations be defined.

Casting of titanium aluminides can be expected to differ considerably from casting of other materials since the primary elements present are highly reactive; this can affect the choice of casting environment (air, inert gas or vacuum) as well as the choice of mold material. In this area, some information is applicable from conventional titanium alloy casting experience, but the higher aluminum content may be expected to affect mold reactivity such that advanced low reactivity mold systems could be required.

Beyond these basic metal forging, casting and joining operations, it is critically important that the applicability of various metal finishing operations, such as machining, be defined. Virtually all components require some form of machining operation in areas where very critical dimensions must be maintained. The surface properties resulting from machining operations are often critical to satisfactory component performance in gas turbine engines. In the Ti_3Al alloy characterization phase of the first year of the Air Force program, it became apparent that the aluminides could be extremely sensitive to surface condition. Several specimens produced by conventional turning or grinding operations were found to have surface craze cracks in the as-machined condition, and this surface condition was found to decrease fatigue strength. Even when actual cracking was not present, tensile residual stresses reduced fatigue life so that stress relief improved specimen capability.

The aluminides are not basically different from conventional titanium base alloys in their surface sensitivity, although effects may vary in degree. Titanium base alloys, in general, have for some time required careful control of machining procedures to achieve satisfactory property capability. Parameters such as tool or grinding wheel

speed, depth of cut, type of lubricant and flow rate have all been defined for conventional titanium alloy and reproducible production results are achieved on a normal basis. Similar investigation of machining technique feasibility and definition of parameters were considered necessary for the titanium aluminides.

The various program elements described below were undertaken to provide some of the basic information and process development needed to fabricate titanium aluminide alloys. Much of the work was conducted with the alloy Ti-16Al-10Nb as a reasonably large amount of high quality material had been produced in the first year of this program. More recently, additional studies have been performed on the Ti-13.5Al-21.5Nb alloy.

2. Joining Studies

A. Brazing

Brazing feasibility was studied by producing approximately one-inch square joints using a range of selected filler materials. Braze alloys, such as aluminum, Ti-Cu-Ni and Ti-Zr-Be, were examined metallographically to determine wettability and filler flow; similar evaluations were conducted after long time exposure at 1650-1800°F (899-982°C) to determine base alloy/filler metal interaction, structural stability and oxidation effects.

The base-metal samples, which consisted of two sections (nominally 3/8" and 3/4" diameter x 1/4" thick), were centerless ground to rod configurations and sections on a precision cut-off wheel. The specimen faces were polished flat and parallel through 400 grit silicon-carbide paper

and vapor blasted. The Au-Ni, Al-Si, pure Al and Ti-Cu-Ni braze materials were obtained in the form of 2 mil thick sheet and cut to sections approximately 20 to 30 mils larger in diameter than the titanium aluminide disks. The Au-Ni and Al-Si braze materials were of eutectic composition, nominally 82Au-18Ni and 88Al-12Si, by weight. The Al sheet was C.P. Grade at least 95% pure. The Ti-Zr-Be-Al braze was obtained in the form of -120/+325 (10% maximum -325) powder. Prior to each brazing trial, the Ti-16Al-10Nb materials and braze filler to be evaluated were degreased and cleaned in a methyl alcohol solution. The braze material was assembled between two titanium aluminide sections and placed in a tantalum element, resistance heated, vacuum furnace equipped with a tungsten-rhenium thermocouple in close proximity to the sample.

The Al Si braze trial (#4) and the pure Al trial (#5) were conducted with a local oxygen protective getter of Mg powder in an attempt to improve the wetting characteristics of these two braze materials. A pure Mg powder was employed as a gettering agent and applied to the upper surface of the bottom disk adjacent to the circumference of the joint.

An acrylic cement was used as a binder for the Ti-Zr-Be-Al powder. The braze was applied in the form of paste only to the periphery of the joint. To maintain proper specimen spacing, four small 1 to 2 mil thick C.P. titanium spacers were placed at 90° intervals under the circumference of the top section. This technique maintained proper specimen spacing and allowed the braze material to flow into the joint at temperature. The previous trials were conducted between 1100°F to 1825°F from 7 to 10 minutes at 10^{-5} Torr. Both the Ti-Zr-Be-Al and Ti-Cu-Ni trials were conducted at 1750°F for 10 minutes at 10^{-5} Torr (Table 29).

TABLE 29
Parameters Used for the Titanium-Aluminide Brazing Study

<u>Trial</u>	<u>Base Material</u>	<u>Brazing Material</u>	<u>Temperature (F)</u>	<u>Time (Minutes)</u>	<u>Pressure mm Hg</u>	<u>Results/Comments</u>
1	Ti-16Al-10Nb w/o	82Au-18Ni (AMS 4787)	1825 \pm 25	7-15	10 ⁻⁵	Extensive wetting of both upper and lower disks.
2	Ti-16Al-10Nb w/o	88Al-12Si (Full made to AMS 4185 Specification)	1100-1110	7-15	10 ⁻⁵	Poor wetting. did not flow well.
3	Ti-16Al-10Nb w/o	C.P. Al AMS 4000	1220-1230	7-15	10 ⁻⁵	Irregular adhesion of Al braze to base metal.
4	Ti-16Al-10Nb w/o	Al-Si (see trial No. 2) with Mg Powder	1100-1110	7-15	10 ⁻⁵	About same result as No. 2.
5	Ti-16Al-10Nb w/o	C.P. Al with Mg Powder	1220-1230	7-15	10 ⁻⁵	Slightly better wetting than result for Trial No. 3.
6	Ti-16Al-10Nb w/o	Ti-15Cu-15Ni	1750	10	10 ⁻⁵	Extensive wetting of both disks.
7	Ti-16Al-10Nb w/o	Ti-47Zr-5Nb-5Al Solar Braze C-6604	1750	10	10 ⁻⁵	Extensive wetting of both disks.

Following visual inspection of the braze product to establish bond integrity, general reactivity and degree of wetting, the joint was inspected by means of fluorescent penetrant. The product was then sectioned longitudinally, Ni plated to maintain edge definition, mounted and polished. Examination of the polished and etched (Kroll's reagent) cross section by means of optical microscopy revealed the degree of braze wetting, braze-base interaction, erosion and porosity in the joint.

A total of seven brazing trials were carried out as listed in Table 29. Macro-analysis of the Au-Ni brazed product revealed extensive wetting of both the upper and lower titanium aluminide sections. Examination by means of fluorescent penetrant revealed an apparent small crack in the joint area. Microexamination of a longitudinal cross section confirmed the extensive wetting, as illustrated in the optical micrograph, Figure 54(a). It can also be seen in Figure 54(a) that approximately 1.5 mils of the base material has been eroded by braze. Examination of the joint at 500X also revealed a number of significant features. Three intermediate phases can be observed subsequent to brazing with a dark etching "needle-like" phase revealed in the braze/base metal interface. Voids and oxide particles are also observed in the center of the joint, as shown in Figure 54(b); the former the result of the extensive affinity of the braze alloy for the base material while the latter caused by oxides being "washed" from the material surface.

The results for the Al-Si trial and pure Al trial are tabulated in Table 29. In both cases, the upper and lower specimens were joined, however, macro-analysis indicated that the Al-Si filler did not flow well and revealed

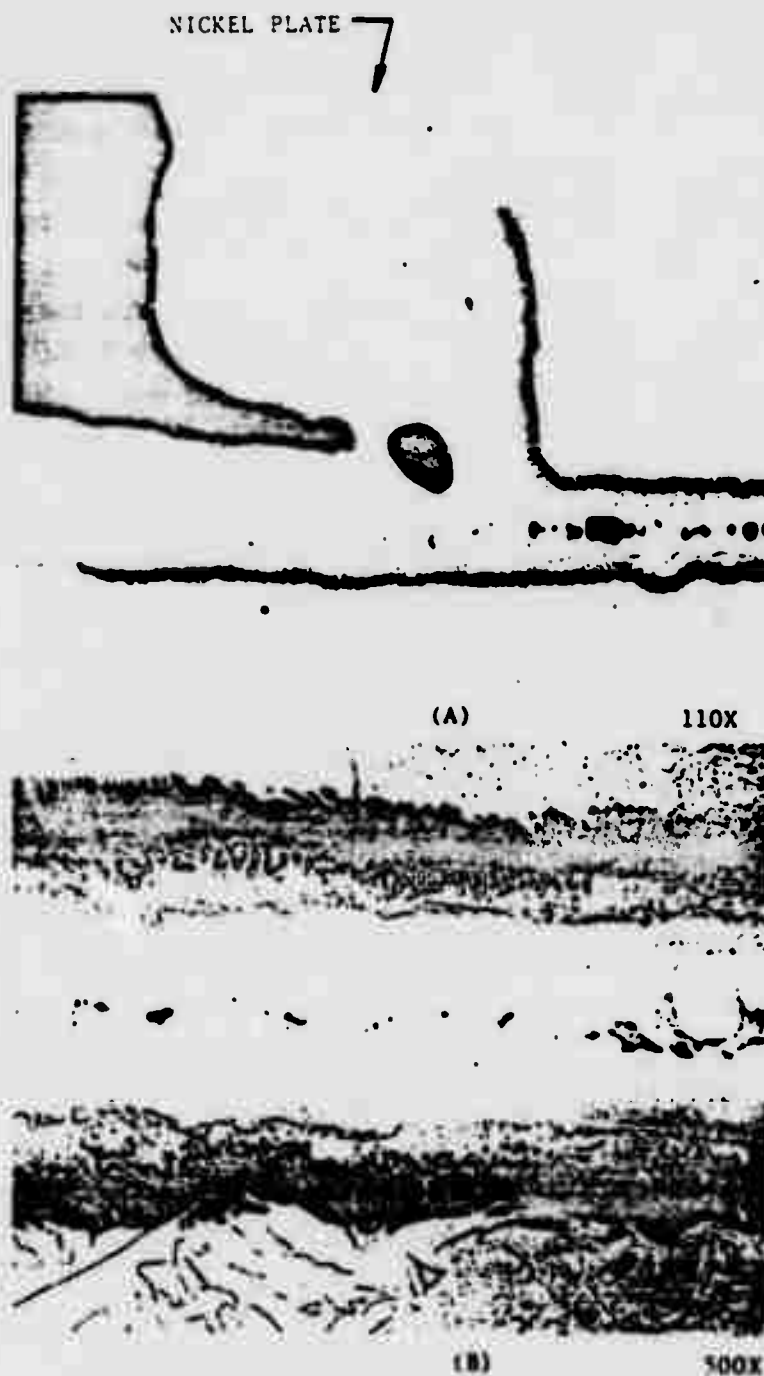


Figure 54. (a) Au-Ni Brazed Ti-16Al-10Nb Joint Showing Wetting and Erosion of Base Metal
 (b) Micrograph of Joint Showing Phases Formed During Brazing
 Note Porosity and Oxides in Joint

extremely poor wetting, Figure 55(a). The pure Al material exhibited only irregular adhesion to the base aluminide as illustrated in Figure 55(b). Microexamination of longitudinal sections confirmed the poor adhesion for both trials and only minor interaction was observed in either case. The poor brazing characteristics of the Al based materials could result from the formation of a strong adherent oxide film preventing filler/base wetting.

Thus, additional Al-Si braze and pure Al trials were conducted with a local oxygen protective Mg wetter in an attempt to improve wetting characteristics. Macroexamination of the gettered Al-Si trial (#4) revealed no apparent improvement in wetting characteristics compared to the ungettered trial (#2). However, the pure Al trial run with Mg powder adjacent to the braze exhibited a somewhat improved wetting appearance. Unfortunately, microexamination of the longitudinal cross sections revealed no significant improvement in base metal/braze interaction for either of the above two trials.

Macro-analysis of the Ti-15Cu-15Ni brazed product, Figure 56(a), revealed extensive wetting of both the upper and lower titanium aluminide sections. Examination by means of fluorescent penetrant revealed an apparent crack-free joint area. Microexamination of a longitudinal cross-section confirmed the extensive wetting, as illustrated in the optical micrograph, Figure 57(a). Note that the brazed specimen was nickel plated prior to sectioning, mounting and polishing to maintain edge definition. The original braze foil thickness (1.5 to 2 mils) is discernible in Figure 57(a) between an erosion zone of approximately 1 mil per side. Examination of the joint at 500X did not reveal the presence of voids, however, a phase was observed, which may be seen



4X

(a) Al-Si braze showing poor flow characteristics.



4X

(b) C.P. Al braze showing irregular wetting.

Figure 55. Results of Ti-16Al-1Nb Brazing Trials



4X

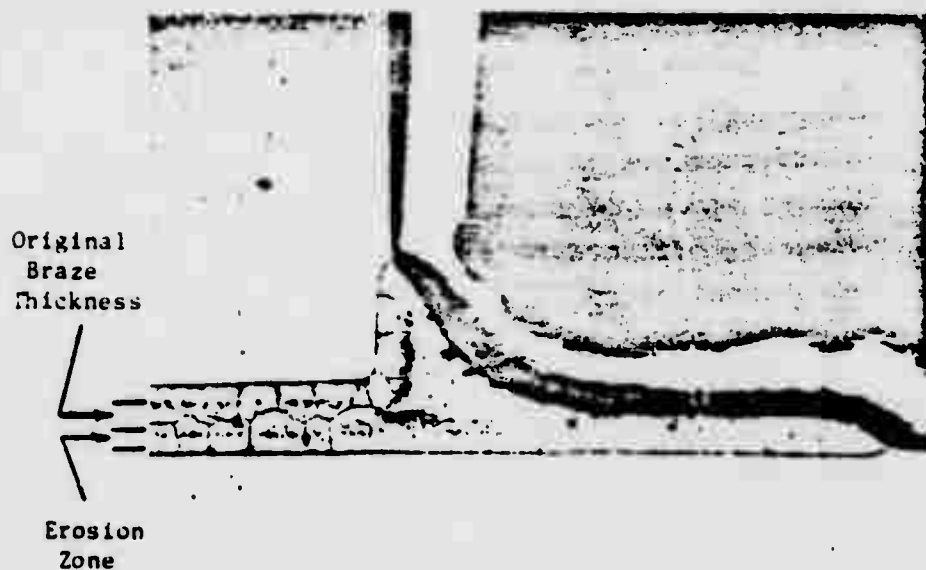
(a) Ti-15Cu-15 Ni braze.



4X

(b) Ti-47Zr-5Be-5Al braze.

Figure 56. Results of Ti-16Al-10Nb Brazing Trials



(A)

100X



(B)

50X

Figure 57. (a) Ti-15Cu-15Ni Brazed Ti-16Al-10Nb
 (b) Ti-47Zr-5Be-5Al Brazed Ti-16Al-10Nb
 Note Both Brazed Trials Conducted at 1750°F

in Figure 57(a), in the approximate center of the braze.

Macro-analysis of the Ti-47Zr-5Be-5Al braze trial revealed satisfactory wetting, Figure 56(b), although it is clear that an excess of braze material was applied. Inspection by means of fluorescent penetrant revealed a few pinpoint indications or voids in the joint region, however, it is felt that these voids are more related to the fact that the braze was applied as a paste as opposed to a chemical reaction. In contrast to the Ti-Cu-Ni braze trial, a diffusion zone (rather than erosion zone) slightly in excess of 1 mil may be observed in Figure 57(b), which were not observed in the braze at 500X; however, a number of phases were clearly revealed.

It was concluded on the basis of these trials that either the Ti-Cu-Ni or Ti-Zr-Be-Al braze alloys may be satisfactory for producing aluminide joints for use at low temperature. However, the interdiffusion and erosion characteristics indicate that either or both of the following methods would be preferred for use in high temperature structures.

B. Diffusion Bonding

The parameters for diffusion bonding the Ti-16Al-10Nb alloy were established on a laboratory scale. Sections of the alloy were prepared pending trials conducted in a vacuum press. Bonding variables studied were time, temperature and pressure. The bonded sections were evaluated by radiography and optical metallography to determine the extent of bonding and level of residual bond line porosity.

Specimens used for the diffusion trials were centerless ground to 0.4" diameter cylinders and sectioned to 0.25"

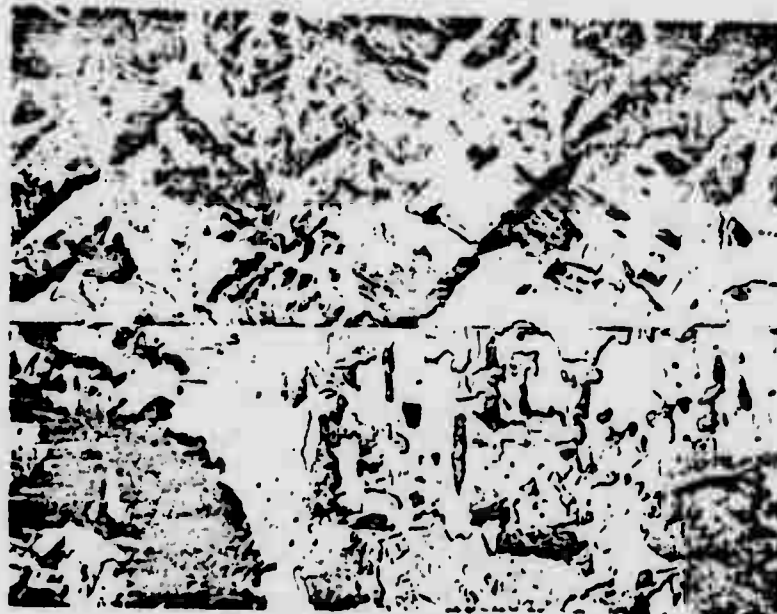
thick wafers on a precision cut-off wheel. Specimen faces were lapped flat and parallel in an alumina slurry to within 0.001". Final polishing was with 0.3 micron alumina powder on a felt cloth. Bonding experiments were carried out in a vacuum hot press equipped with an alumina die to maintain alignment of specimens; temperature was monitored with a Pt versus Pt - 10% rhodium thermocouple. Immediately prior to a diffusion bond trial, specimen faces to be bonded were etched (Kroll's reagent) and cleaned with a solution of methyl alcohol. The cylinders were diffusion bonded under vacuum of better than 10^{-5} mm Hg and under various pressure and time parameter conditions as presented in Table 30. Subsequent to each run, the joined samples were sectioned longitudinally, mounted and polished. Any microporosity in the bond line was established metallographically.

Eight diffusion bonding trials were run as listed in Table 30. A longitudinal cross section of the bond run at 1800°F/240 minutes/1,000 psi is shown in Figure 58(a), and indicates incomplete closure of bond surfaces with bond line porosity revealed, although a limited number of areas appear to be well bonded. The second bonding trial was run at 1900°F/240 minutes/3,000 psi. A longitudinal cross section of this bonded specimen appears in Figure 58(b). For these parameters it appears that complete closure of the bond surfaces has taken place and no microporosity was observed. Also of interest in this figure is the recrystallized layer of grains at the prior bond line.

Longitudinal cross sections of subsequent bond trials were examined metallographically for microporosity in the bond line. The specimen bonded at 1900°F/240 minutes/1,000 psi exhibited a bond line containing 20% voids. Each of the two bonds run at 1700°F also exhibited a degree of

TABLE 30
Parameters Used for the Titanium Aluminide Diffusion Bonding Study

<u>Trial</u>	<u>Material</u>	<u>Bond Temperature (F)</u>	<u>Bond Time (Minutes)</u>	<u>Bond Pressure (psi)</u>	<u>Surface Finish (Microns)</u>	<u>Results/Comments</u>
1	Ti-16Al-10Nb w/o	1800	240	1,000	0.3	Bond line observed.
2	Ti-16Al-10Nb w/o	1900	240	3,000	0.3	Sound bond, no micro-porosity observed.
3	Ti-15Al-10Nb w/o	1900	240	1,000	0.3	20% voids observed.
4	Ti-16Al-10Nb w/o	1700	180	5,800	0.3	Moderate porosity.
5	Ti-16Al-10Nb w/o	1700	300	7,000	0.3	Slight porosity.



(a) 1800°F/240 minutes/1,000 psi 100X



(b) 1900°F/240 minutes/3,000 psi 100X

Figure 58. Longitudinal Cross Section of Diffusion Bonded Ti-16Al-10Nb Specimens - Note Bond Line in (a) and Recrystallized Layer of Grains in (b) at Prior Bond Line

microporosity in the bond line as indicated in Table 30.

It can be seen from Table 30 that in order to achieve a complete bond, a temperature of 1900°F and a pressure of 3 ksi applied for four hours is required. Reducing any of the time, temperature, pressure parameters results in inadequate bonding, although high pressures and long times at 1700-1800°F probably could produce dense bonds. It would seem that the most effective approach would be to increase the bond temperature to 2000-2100°F, at which temperatures the flow stress is considerably reduced (see Forging results). In this temperature range, the time and pressure requirements could probably be reduced to relatively small values. However, these gains would be offset, from a practical viewpoint, by tooling and contamination problems.

C. Weldment Evaluation

Preliminary attempts to weld Ti₃Al based alloys conducted at P&WA indicated susceptibility to weld and heat-affected zone cracking. The cracks observed were somewhat similar in appearance to those observed in many nickel and iron based alloys. While the cause of this cracking behavior has been fairly well established for nickel base alloys, the knowledge was generally lacking for Ti₃Al. The only information that has been obtained to date is that cracking can be prevented, at least under conditions of low heat input and low restraint, by preheating the sections to 500-900°F (260-482°C). Further studies were initiated in the program to investigate the weldability of Ti₃Al base alloys, specifically Ti-16Al-10Nb.

Titanium aluminide panels were prepared by the following two methods: (1) one sheet was rolled directly from an

as-cast ingot section and (2) two sheets were rolled from HIP'ed powder. Gas tungsten arc (GTA) butt welding was the first method used in an effort to join these Ti-16Al-10Nb panels. Narrow strips cut from the panels were used as filler material.

Weldments were produced at preheat temperatures of 70, 300, 500 and 700°F, as shown in the following schedule.

<u>Sheet</u>	<u>Preheat</u>			
	<u>Ambient</u>	<u>300°F</u>	<u>500°F</u>	<u>700°F</u>
Ingot			X	X
HIP #1	X	X	X	X
HIP #2				X

Prior to welding, thermocouples were attached to the sheets to measure preheat temperature. Preheating was accomplished by feathering the welding arc on the panels until the selected temperatures were attained. Energy input was kept to a minimum but varied with the amount of preheat. One EB weld was run to join HIP #2 sheet panels. For this trial the panels were not preheated.

Large cracks were observed in all specimens except the HIP #2 specimen preheated to 700°F. This weld is illustrated in Figure 59(a). In all other samples, cracking occurred perpendicular to the weld and the appearance was typical of hot cracks, as shown in Figure 59(b). Apparently, HIP process parameters varied because a difference in weldability was observed between the two sheets produced from HIP'ed preforms. All HIP #1 specimens exhibited excessive weldment porosity, illustrated in Figure 59(c). Radiography revealed extensive networks of porosity throughout the weld beads. Porosity was not discovered in any of the other



(a) HIP'ed sheet, preheat temperature - 700°F.



(b) HIP'ed sheet, preheat temperature - 500°F, showing typical cracking pattern. 1.25X



(c) Longitudinal cross section of (b) showing porosity rim in weld bead.

Figure 59. Results of Ti-16Al-10Nb Welding Trials

specimens (e.g., HIP #2 or ingot).

More cracks were observed in the EB weld than in any of the GTA welds; however, the cracks were smaller, but the total length of cracks was about equal to that of the GTA welds.

The above experience may be attributable in part to the structure present in the sheet which was not optimum. Additional trials utilizing sections of the same thickness cut from forged and heat treated material did not show cracking after welding with a 700°F preheat temperature, examples are shown in Figure 53.

It is not clear if higher niobium content will make welding easier or more difficult. Improved ductility could lead to a reduction in cracking tendency and also in preheat required. However, the higher niobium content may increase the welding difficulty--at least by analogy with conventional titanium alloys in which high beta stabilizing element content usually results in poor welding characteristics.

D. Forging Studies

Forging of the Ti_3Al base titanium aluminide materials had not received a systematic evaluation, although it is obvious from previous sections that an empirical body of forging parameters exists. Prior in-house experience had shown isothermal forging to be a tractable approach to forming this class of materials. Therefore, the hot die, or more correctly, isothermal technique was studied in order to define the important process variables and explore their impact on subsequent flow stress, microstructure and properties. This aspect of the program investigated such variables as forging temperature, strain rate and reduction

ratios for titanium aluminide pancake forgings.

A 20-pound cast ingot of nominal Ti-16Al-10Nb, double consumably melted by Titanium Metals Corporation of America (TMCA), Henderson, Nevada, was procured for the forging evaluation. The chemical analysis of the ingot is given in Table 31. The ingot was hot isostatically pressed (HIP'ed) under conditions of 2200°F/15,000 psi argon pressure for three hours in order to close internal porosity. Subsequent to the HIP treatment, forging blanks nominally 1" diameter were EDM'ed from the ingot. The preforms were sections to about 2" lengths and the ends were machined flat and parallel prior to forging. Radiographic analysis revealed completely sound blanks free of any observable internal porosity.

Forging trials were conducted in the P&WA "Mini'Gator" isothermal forging press equipped with TZM molybdenum alloy tooling in vacuum and at controlled rates. The thermocoupled dies and billets were equilibrated at the forging temperature with induction heating coils for one-half hour prior to deformation. Also, prior to each forging run, the die surfaces and ingot were spray coated with boron nitride lubricant. Temperature and load were constantly monitored and recorded during deformation. Forged pancakes were furnace cooled subsequent to deformation.

Twelve subscale isothermal forgings were produced. Deformation parameters and the evaluation of these trials are summarized in Table 32 and photographs of the resulting pancake forgings are presented in Figure 60. Final forging thickness in each case was approximately 0.4", equivalent to about 80% reduction in height. The flow stress-reduction in height relationships for the various conditions are

TABLE 31
Chemical Composition of Titanium-Aluminide Alloy
TMCA Heat V-5123, Ti-16Al-10Nb

Element	TMCA*	Alm
Ti	Balance	Balance
Al	15.4	16.0
Nb	11.6	10.0
Fe	0.062	--
O	0.10	--
N	0.012	--

* Average of top and bottom analyses.

TABLE 3.2

3

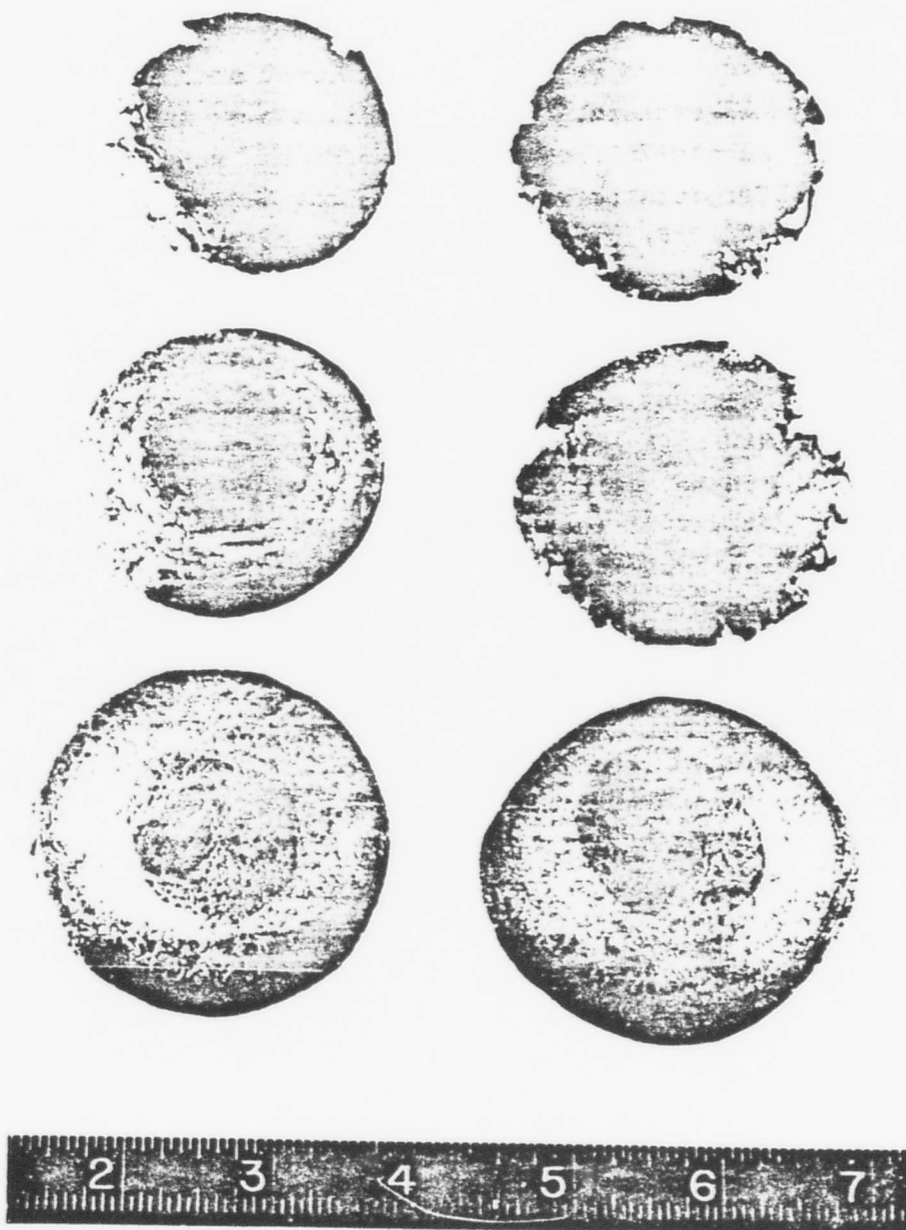


Figure 60. Ti-16Al-10Nb Forging Trials (Left to Right)

Top:	1900°F, 0.01 inch/inch/minute;
	1900°F, 0.05 inch/inch/minute
Middle:	2000°F, 0.1 inch/inch/minute;
	2000°F, 0.5 inch/inch/minute
Bottom:	2200°F, 0.1 inch/inch/minute;
	2200°F, 0.5 inch/inch/minute

shown in Figure 61. It is clear that a considerable reduction in flow stress is observed with increasing deformation temperature. Additionally, slower strain rates also result in flow stress reduction, particularly at lower forging temperatures. At the highest forging temperature (2200°F), a change in strain rate results in only a small effect on flow stress.

Visual examination indicated good results for forgings produced at 2200°F (above the beta transus of 2150-2175°F) for both low, 0.1 inch/inch/minute, and high, 0.5 inch/inch/minute, strain rates. Similar results were also obtained at 2100°F for low, 0.05 inch/inch/minute, intermediate, 0.1 inch/inch/minute, and high, 0.5 inch/inch/minute, strain rates. Good forgeability was obtained at 2050°F for both intermediate, 0.1 inch/inch/minute, and high, 0.5 inch/inch/minute strain rates, while the forging produced at 2000°F and a strain rate of 0.05 inch/inch/minute exhibited very slight cracking as can be seen in Figure 60.

Forgings produced at 1900°F exhibited considerable cracking while the billet run at 2000°F and 0.1 inch/inch/minute exhibited slight cracking compared to the extensively cracked pancake deformed at 2000°F and 0.5 inch/inch/minute. It is clear, at least at the 2000°F forging temperature, that the cracking tended to be more severe with increasing strain rate.

The Vickers hardness values and resulting microstructures for the twelve subscale forged products appear in Table 32. In almost every case, increasing strain rates tended to produce increased hardness values for a given forging temperature. The forgings produced at 2050°F appear to be the one exception to this trend. Additionally, increasing

2000 γ / δ =0.10
 2050 γ / δ =0.10
 2050 γ / δ =0.50
 2100 γ / δ =0.10
 2100 γ / δ =0.50

INCLUDES -

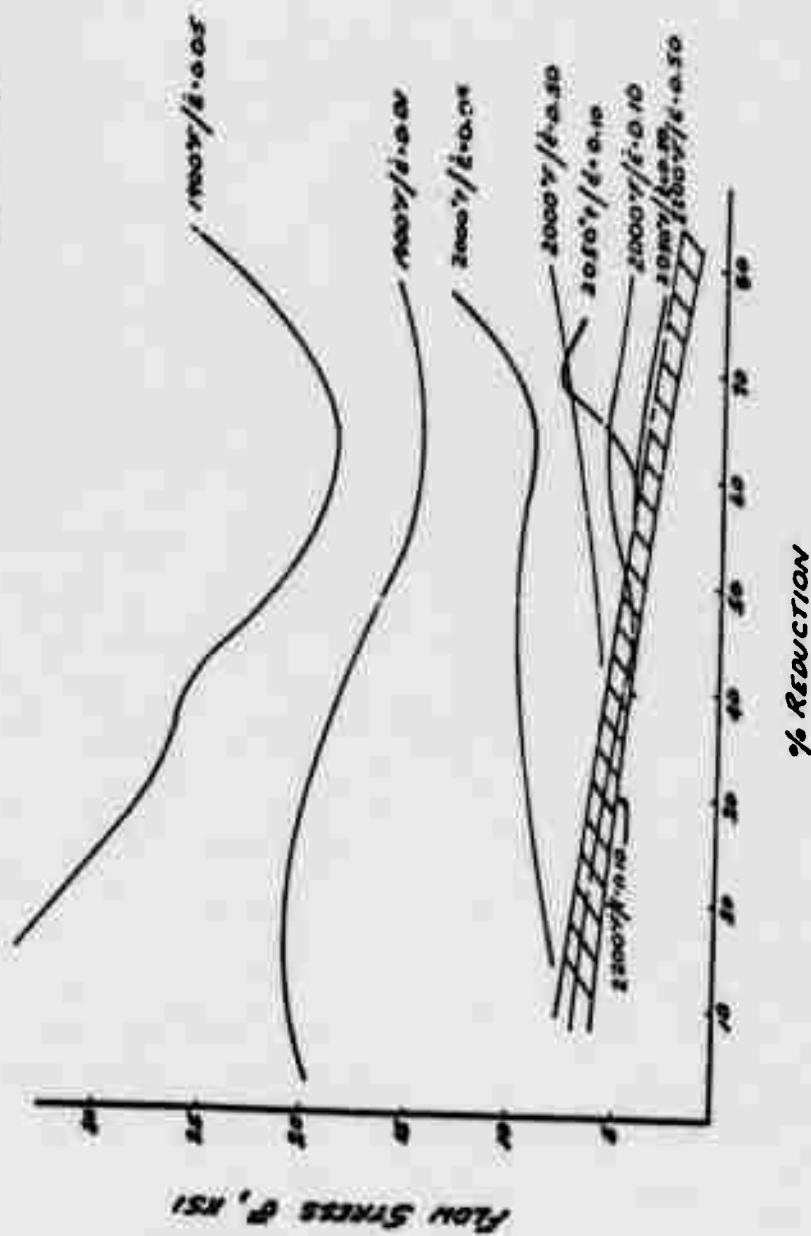


Figure 61. Flow Stress as a Function of Percent Reduction for Subscale Isothermal Forgings Produced from Ti-16Al-10Nb Ingot

forging temperatures, in general, yielded decreased hardness values; this trend is more obvious when the results for a specific strain rate are examined for a range of temperatures. Forgings produced at 1900°F yielded a fine equiaxed alpha two microstructure, while those produced at 2000°F and 2050°F yielded equiaxed alpha two plus intergranular beta (which transforms on cooling to room temperature) morphologies. Plate-like alpha two microstructures were observed for forging temperatures of 2100 and 2200°F (beta transus of approximately 2150°F) with an extremely coarse structure noted for the latter forging temperature.

Two tensile tests were performed for each of the forging trials produced at 800 and 1200°F with the results presented in Table 33. Although the data are limited, it can be seen that the trends discussed in the preceding paragraphs pertaining to hardness values are also observed in the tensile results. Increasing strain rates generally result in increased yield strengths for a given forging temperature. Low strength (and hardness values) are observed for forgings produced at temperatures above the beta transus, and in general, increasing forging temperatures resulted in reduced yield strength values for a given strain rate. Ductility values tend to be rather variable and show no clear-cut trend. From a practical viewpoint, a forging temperature in the alpha-beta phase field would seem the best selection as it will allow maximum flexibility and control in the selection of a subsequent heat treatment cycle.

E. Machining Studies

In spite of the extensive number of aluminide specimens produced to date, machining this class of materials continues

TABLE 33
Tensile Results for the Titanium Aluminide Isothermal Forging Study*

Material	Forging Temperature °F	Forging Strain Rate in/in/min	As-Forged Hardness HV-10	Test Temperature °F	0.2% Yield Strength (ksi)	Ultimate Tensile Strength (ksi)	Elongation (%)	Reduction-In-Area (%)
Ti-16Al-10Nb	1900	0.01	271	800	63.9	72.1	1.4	1.6
	1200			1200	50.4	50.8	0.8	1.6
	1900	0.05	294	800	65.5	68.5	0.65	-
	1200			1200	55.0	70.0	4.5	5.0
	2000	0.05	270	900	60.3	67.0	0.88	2.3
	2000	0.1	277	800	65.0	72.5	1.2	3.3
	1200			1200	51.2	65.8	5.2	5.8
	2000	0.5	288	800	76.2	80.5	0.90	2.4
	1200			1200	59.5	71.5	2.7	6.6
	2200	0.1	234	800	45.8	56.8	1.1	-
	1200			1200	38.4	58.4	5.0	5.7
	2200	0.5	248	800	42.8	54.3	1.0	-
				1200	36.7	55.4	4.4	7.5

*Note: All specimens tested in as-forged condition

to be based primarily on experience; machining variables have not been explored in detail. This effort attempts to examine in detail the impact of limited low temperature ductility on a number of processes currently employed in the machining of aluminide materials. Specifically, such processes as conventional grinding, single point tool machining (turning) and electrochemical grinding (ECG) were studied in terms of speeds and coolants on subsequent surface finish, surface stress state, material soundness (as determined by metallographic and mechanical property examination) and the economics of each approach.

The HCF specimen was selected to evaluate material for the machining program because of (1) the range of techniques which may be employed to produce the desired configuration and (2) the high sensitivity to small surface imperfections in this type of test. A total of ten MDL 2329 (Figure 62) Westinghouse High Cycle Fatigue (HCF) specimens were machined for evaluation. Table 34 summarizes the various machining parameters used in this program. One specimen (#1) was machined using single point tool techniques (lathe turned) at a cutting speed of 200 rpm. A tungsten carbide tool was employed with an oil-based coolant. Two specimens (#2 and 3) were prepared by conventional grinding techniques, with one machined at 6,000 surface feet per minute (SFPM) and the second at 3,000 SFPM. A water soluble coolant was used in the grinding operation. Several specimens were machined by the electrochemical grinding technique (ECG) with five specimens polished through 600 grit silicon-carbide paper after grinding. A sodium nitrate:sodium chloride water-based solution was used as the electrolyte with a copperdyne ($\text{Cu-Al}_2\text{O}_3$) wheel rotating 1,750 rpm. Total ECG time was about 10 minutes per specimen.

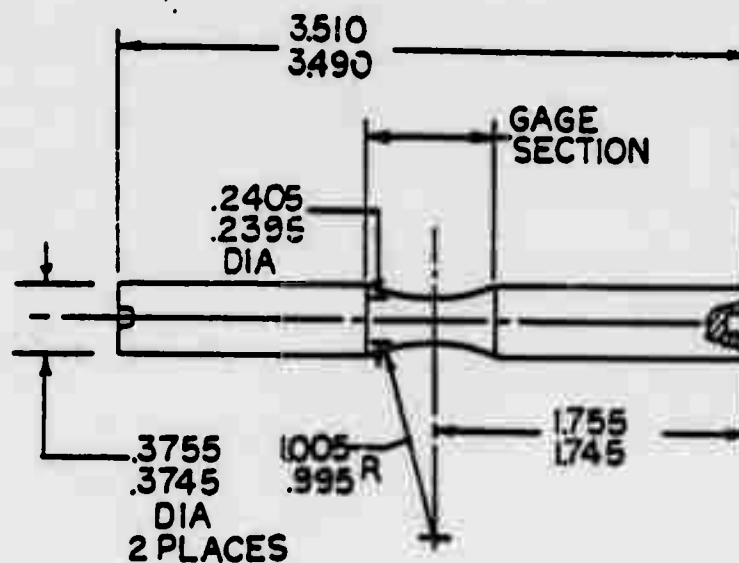


Figure 62. Smooth High Cycle Fatigue Specimen Used in Machining Studies Program (MDL 2329)

TABLE 34
Parameters Used for the Titanium-Aluminide Machining Study

WC7 Specimen Number	Material	Test Specimen	Machining Technique	Comments
1	Ti-16Al-10Nb	MDL 2329	Lathe Turning	200 rpm, tungsten carbide tool, oil base coolant
2			Conventional Grinding	6,000 SFPM, water soluble coolant
3			Conventional Grinding	2,000 SFPM, water soluble coolant
4			ECG + Polish	NaM:NaCl solution, Cu-Al ₂ O ₃ wheel rotating at 1,750 rpm, polished with silicon carbide 600 grit paper
5			ECG + Polish	
6			ECG + Polish	
7			ECG + Polish	
8			ECG + Polish	
9			ECG	NaM:NaCl solution, Cu-Al ₂ O ₃ wheel rotating at 1,750 rpm
10			ECG	

Subsequent to machining, all specimens were nondestructively inspected by means of zyglo fluorescent penetrant. In cases where zyglo indications were found, specimens were replicated to determine the exact nature of the indications.

Ancillary characterization tests were performed to determine the effect of peening the surface microstructure and subsequent high cycle fatigue life of Ti-16Al-10Nb. The basis of these experiments arose from the observation during the previous alloy characterization program of an equiaxed recrystallized layer approximately 2 mils thick in the notch of failed load controlled (cycled at 800°F and 1200°F) low cycle fatigue specimens. This condition was not present on K_t 1.0 specimens used for the strain controlled tests and apparently resulted from the rather severe conventional lathe turning operation used to produce the specimen notches.

In an effort to run a controlled experiment, circumferential sections of a Ti-16Al-10Nb rod were peened to known intensities. A section of the rod was left in the as-ground condition as a baseline. A total of four peening intensities were employed as follows--10N, 15N, 18N and 33N. The former two intensities were applied by means of glass bead peen while the latter two were applied by means of shot peening. Each of the peened sections (including the as-ground section) were divided into a number of sections by means of a precision cut-off wheel. Samples from each condition were thermally exposed at temperatures of 800 and 1200°F for 24 hours. Subsequent to treatment, the as-peened and peened plus exposed specimens were nickel plated to maintain edge definition and metallographically examined.

Typical as-peened (10N, 15N, 18N and 33N) surfaces are illustrated in Figure 63. Of significance in this figure is that for increasing peening intensities, the depth and concentration of slip bands appear to be increased. Also stronger peening has been observed to result in a deformed specimen surface and in occasional microcracking, Figure 63.

Figure 64 illustrated the effect of elevated temperature exposure (1200°F/24 hours) on the microstructure of peened (10N and 33N) Ti-16Al-10Nb. For each of the two examples illustrated, a recrystallized layer is revealed on the specimen surfaces. Of interest is the increased depth of the recrystallized zone as a function of increased peening intensity.

Based on the results of the peening and elevated temperature exposure study, it was decided to fabricate and test smooth Westinghouse high cycle fatigue (HCF) specimens employing three different fabrication techniques in order to determine the effect of surface condition on HCF properties. A total of ten smooth HCF specimens were prepared by the electrochemical grinding (ECG) technique. Six of the ten specimens were selected at random for glass bead peening to an approximately 13N intensity. Three of the peened specimens were then given an elevated temperature exposure of 1200°F/24 hours to produce a recrystallized layer of fine equiaxed grains on the specimen surface. The four remaining specimens were evaluated in the as-ECG'ed condition.

The ten smooth HCF samples were cycled at a temperature of 800°F. A reverse bend ($R = -1$) high cycle fatigue machine was used with test frequency maintained at 1,800 cpm; a stress of 55 ksi was employed for all tests. Specimens were run until rupture or discontinued at 10^7 cycles. The

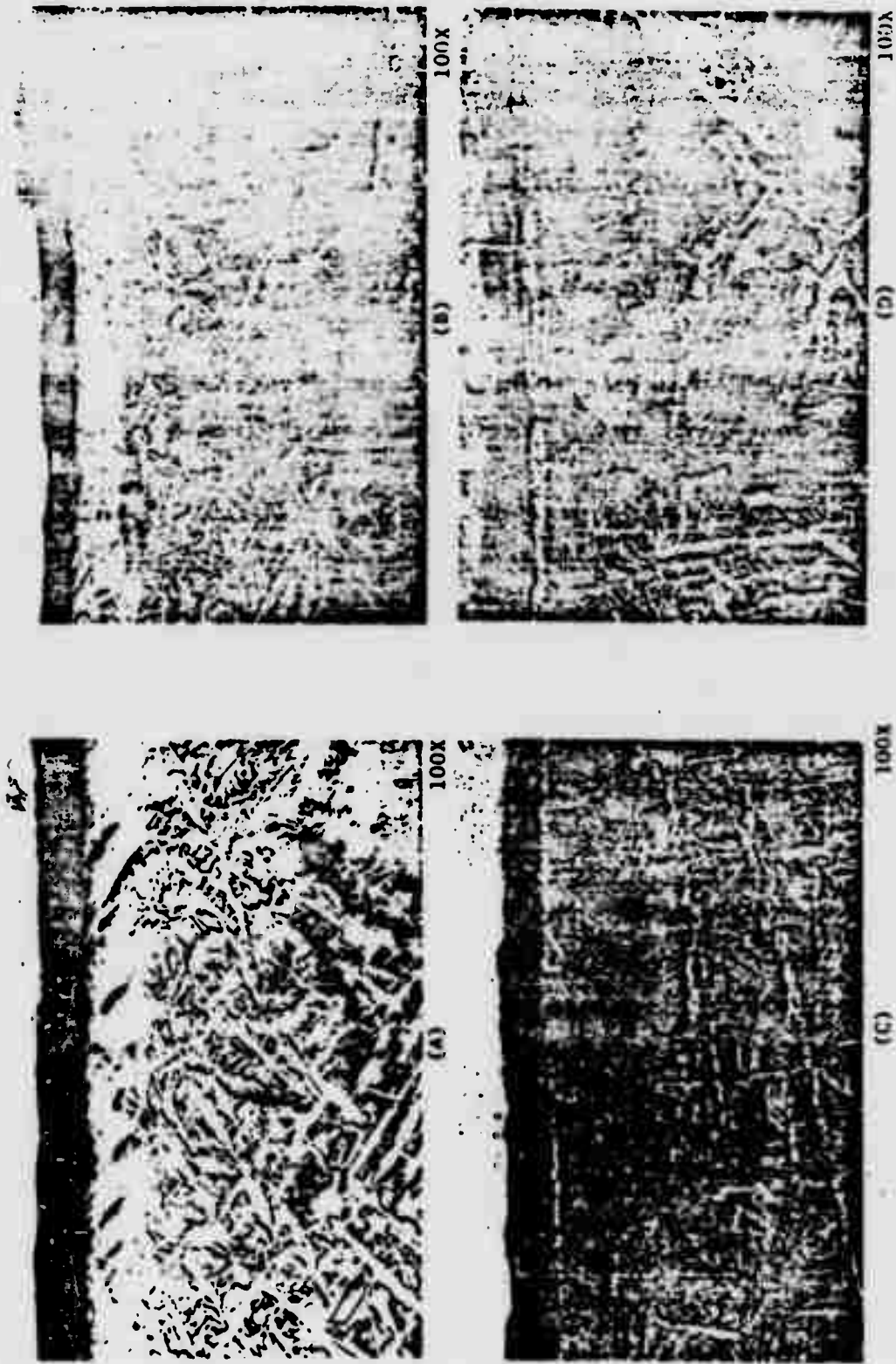


Figure 63. Effect of Peening on the Surface Condition and Microstructure of Ti-16Al-10Nb - (a) 10N, (b) 15N, (c) 18N and (d) 33N



(a) 10N - Exposed 1200°F/24 hours

200X



(b) 33N - Exposed 1200°F/24 hours

200X

Figure 64. Effect of Elevated Temperature Exposure on the Microstructure of Peened Ti-16Al-10Nb

results are presented in Table 35 and plotted in Figure 65, with the HCF results from the alloy characterization program. These results parallel the previous results (conventionally ground plus stress relieved) quite closely.

Fluorescent penetrant examination of as-machined trial specimens produced by various techniques revealed the following:

- 1) The lathe turned specimen exhibited an indication in the gage section which replication revealed to be a crack originating from a machining mark.
- 2) The specimen ground at 6,000 SFPM revealed a small indication in the gage section while the gage section of the specimen prepared at 3,000 SFPM appeared clean. The indication in the former specimen was apparently related to a deep grinding mark.
- 3) One specimen examined in the as-ECG'ed condition (#9) revealed pinpoint zygo indications in the gage section. Replication of this specimen revealed what appeared to be "pits" as opposed to cracks. All other specimens showed no indications of surface flaws.

Evaluation of failed low cycle fatigue specimen microstructure (#4) showed indications of surface recrystallization on lathe turned samples which could be correlated with variations in low cycle fatigue behavior at 800 and 1200°F. The recrystallization on lathe turned surfaces was postulated to occur as a result of the severe local deformation during the machining operation and exposure to elevated temperature, either as a direct result of machining during the stress relief treatment or during subsequent specimen test.

TABLE 35
Westinghouse Cycle Fatigue Data for Ti-16Al-10Nb

$r = -1$

<u>Machining Technique</u>	<u>Test Temperature (F)</u>	<u>K_t</u>	<u>Frequency (cpm)</u>	<u>Stress (ksi)</u>	<u>Cycles to Failure</u>
ECG + Polished	800	1	1800	40	7.0×10^6
				45	9.9×10^6
				50	1.0×10^6
				50	6.0×10^6
				55	3.0×10^5

O - 800°F, Kt=1
 □ - 1200°F, Kt=1
 ◇ - 800°F, Kt=38
 △ - 1200°F, Kt=38
 ⊙ 800°F, Kt=1
 ⊙ ECGe-1 plus
 polished

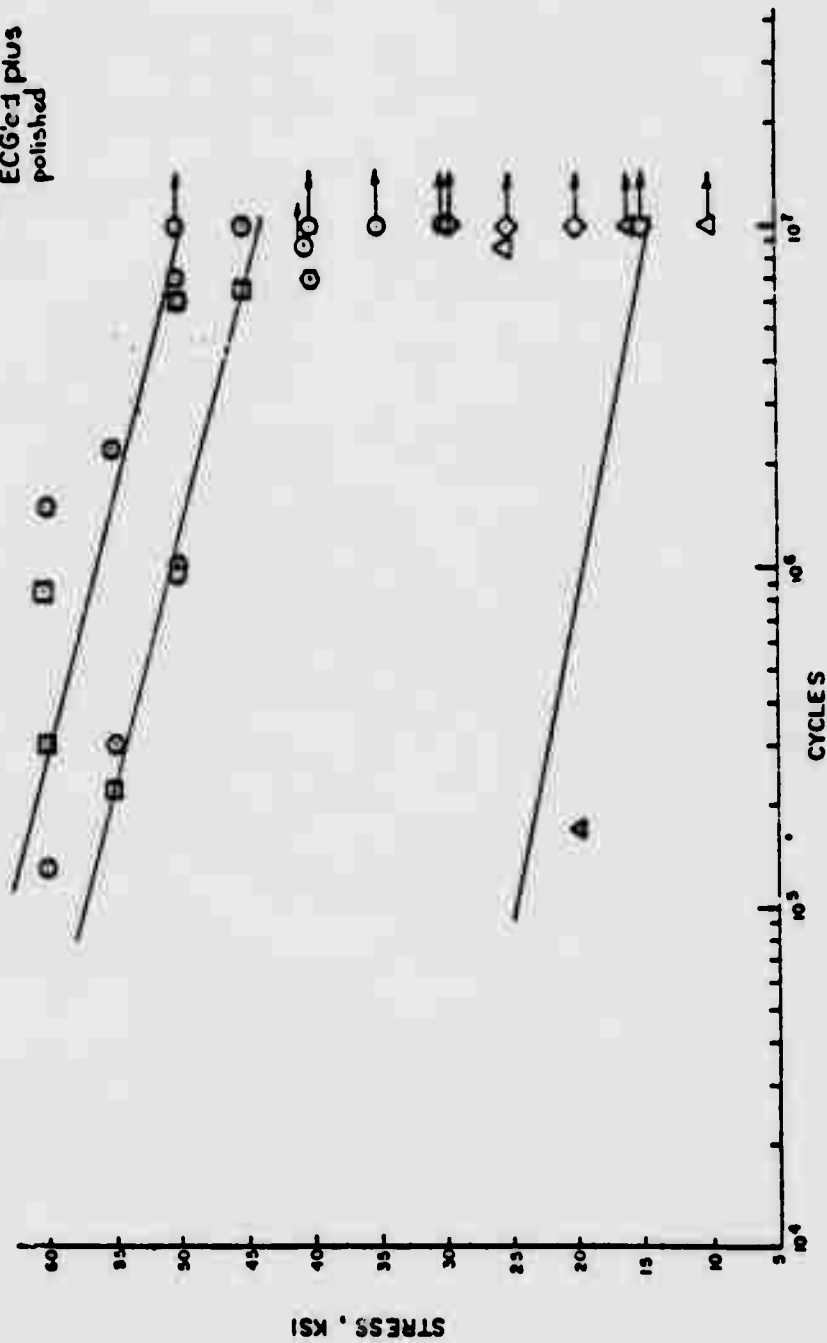


Figure 65. Westinghouse HCF Data for Ti-16Al-10Nb

The results of the ten Westinghouse HCF results are presented in Table 36. Although a significant amount of scatter is present in the data, it appears that the as-ECG'ed samples, taken as a group, may be slightly superior in comparison to the ECG + peened (13N) or ECG, peened (13N) plus thermally exposed (1200°F/24 hours) specimens. However, it is readily apparent that no significant differences exist between each of the three groupings.

Additional studies to more fully characterize turning characteristics of aluminide alloys have been performed. A set of Ti-16Al-10Nb bars fabricated by single point tool machining techniques were examined in both the as-machined and machined plus exposed for 24 hours at 1200°F conditions. All machining conditions examined revealed some degree of surface cracking. The best results appeared to be achieved using a small diameter tool, rotational speeds of 150-200 rpm and taking relatively heavy cuts. In several cases, the cracking present after machining was accentuated by the elevated temperature exposure. In no case did the exposure cause recrystallization, as had been previously observed in ground and peened surfaces.

Bars of Ti-13.5Al-21Nb and Ti-13.5Al-21Nb-0.15Si have been machined by single point turning using the parameters previously studied on the Ti-16Al-10Nb alloy. Ti-13.5Al-0.1Nb was machined with a rotational speed of 225 rpm and a 0.003" per pass feed, while Ti-24Al-11Nb-0.25Si was machined with a rotational speed of 357 rpm and the same feed. The surfaces of these two alloys were compared with the surface of Ti-16Al-10Nb which was machined under the same conditions. The Ti-13.5Al-21Nb and Ti-13.5Al-21Nb-0.1Si bars were inspected by zygo and in metallographic sections.

TABLE 36
Westinghouse High Cycle Fatigue Data for Ti-16Al-10Nb

Shot Peening Technique	Test Temperature (°F)	R_r	Frequency (cps)	Stress (ksi)	Cycles to Failure
As-ECG'ed	800	1.0	1800	75	6.3×10^6
As-ECG'ed					10^7 Disc.
As-ECG'ed					6.5×10^5
As-ECG'ed					1.7×10^5
ECG + Peen (13N)					9.5×10^5
ECG + Peen (13N)					2.2×10^6
ECG + Peen (13N)					2.2×10^5
ECG+Peen(13N)+1200°/24 hrs.					8.6×10^5
ECG+Peen(13N)+1200°/24 hrs.					1.3×10^6
ECG+Peen(13N)+1200°/24 hrs.					2.6×10^6

No crack indications have been found in either alloy, demonstrating a dramatic improvement in machinability over previous alloys such as Ti-16Al-10Nb, as illustrated in Figure 66. Sections of the machined bars were exposed at 1200°F to determine surface stability characteristics. The surface of the bars exposed at 1200°F exhibited essentially the same structure as the interior of the specimens and no cracks were formed as a result of exposure.

F. Casting Studies

Experiments designed to determine alpha two titanium aluminide casting fluidity relationships and metal-mold surface interaction have been performed. The fluidity experiments were conducted using a Leybold-Hereaus electron beam furnace with a vented, center pour spiral graphite mold maintained at room temperature. Length of pour into the spiral cavity was used as a measure of fluidity. The initial trial employed a Ti-6Al-4V alloy as a baseline in order to compare results with two subsequent Ti-16Al-10Nb runs. For comparison of cast structures and surface reactivity, melts were prepared in alumina and zirconia molds and sectioned.

Three melting trials have been run employing Ti-6Al-4V as a baseline trial and Ti-16Al-10Nb for the following two runs. The spirals for the three casting trials are illustrated in Figure 67. Chemical analysis of the solidified product for aluminum content gave the following results:

<u>Material</u>	<u>Weight of Aluminum</u>
Ti-6Al-4V	3.3
Ti-16Al-10Nb	13.9
Ti-16Al-10Nb (Increased EB Power)	7.5

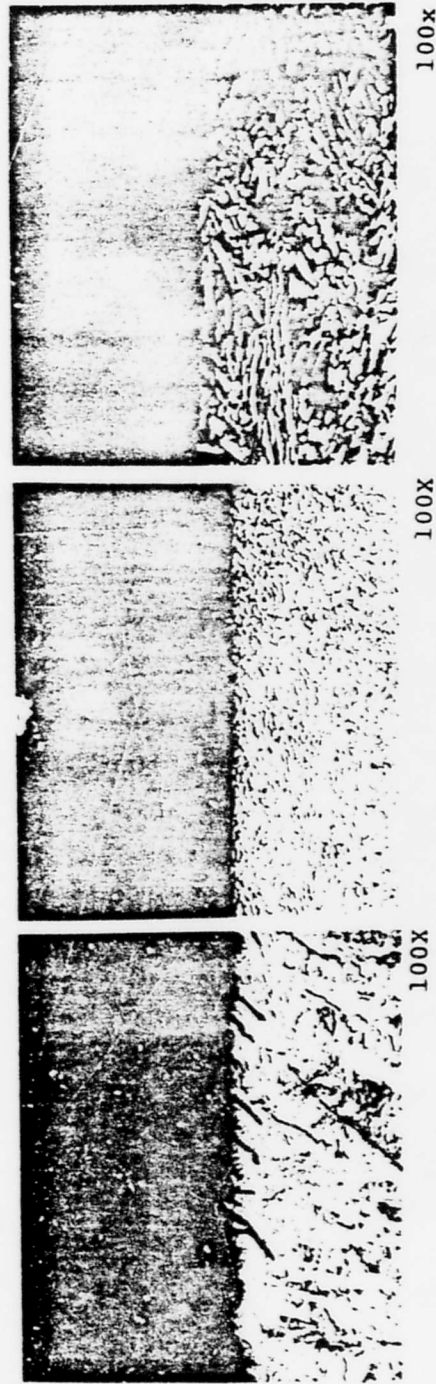


Figure 66. Surface Condition After Machining of Alloys

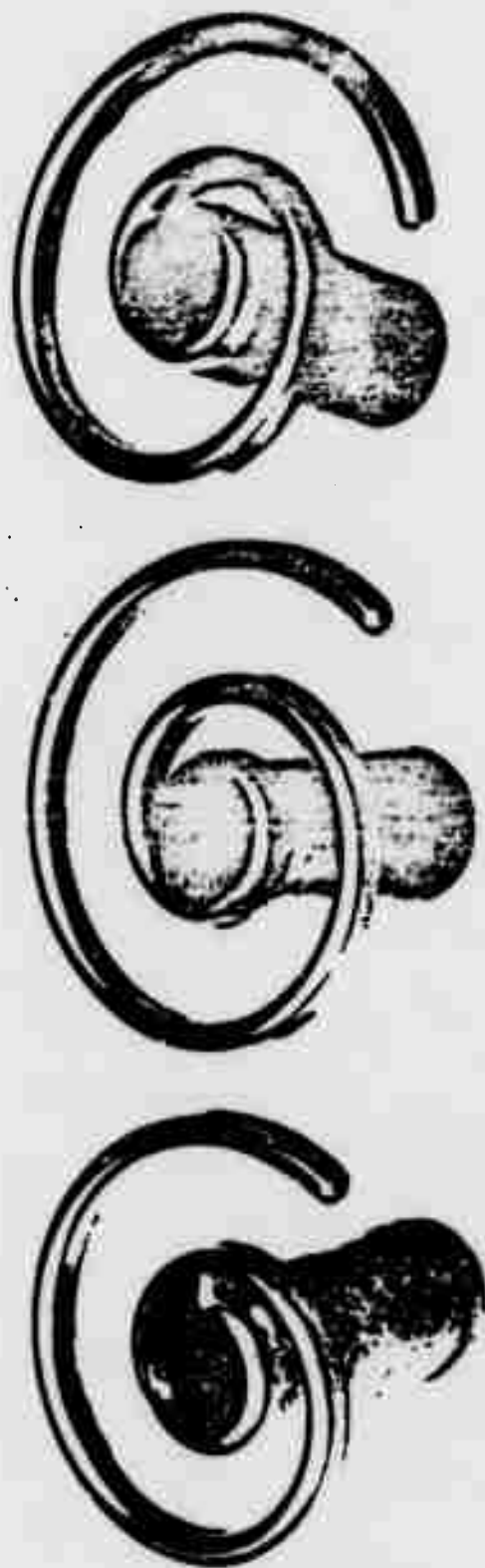


Figure 67. Results of Electron Beam Casting Experiments
Left : Ti-6Al-4V - Baseline Trial
Center: Ti-16Al-10Nb - Baseline Trial
Right : Ti-16Al-10Nb - Increased Electron Beam Power Compared to Center

The casting conditions for the Ti-6Al-4V casting and Ti-16Al-10Nb (a) were the same--the degree of superheat being controlled by the EB gun power setting and assessed by the temperature of the exit cooling water from the crucible. Increasing the power setting, as was done in the third trial, Figure 67, did not increase the penetration of the molten charge. In fact, the length of the spiral is virtually independent of alloy and EB gun power setting. Of more importance is the compositions of the castings. Problems with melting alloys with high aluminum content can arise due to the high vapor pressure of this element in the hard vacuum environment used for melting. It is of some importance, therefore, that using a low EB power setting results in the loss of only 2% aluminum, a value for which may be possible to compensate by using melt chemistries with a higher starting aluminum content.

Preliminary results of a surface evaluation of castings produced in various mold indicate that reaction is slight in both oxide and graphite molds. Alumina appears to be a superior mold material compared to zirconia (Figure 68).

3. Summary and Conclusions

This series of investigations of manufacturing techniques reflects clearly some of the problems in processing low ductility materials. The welding, machining and to some extent the forging results, all indicate cracking problems are associated with the processing of the Ti-16Al-10Nb alloy. There are indications that alloys with improved low temperature ductility can alleviate many of the undesirable characteristics. Conclusions that can be drawn at this stage of the investigation are as follows:

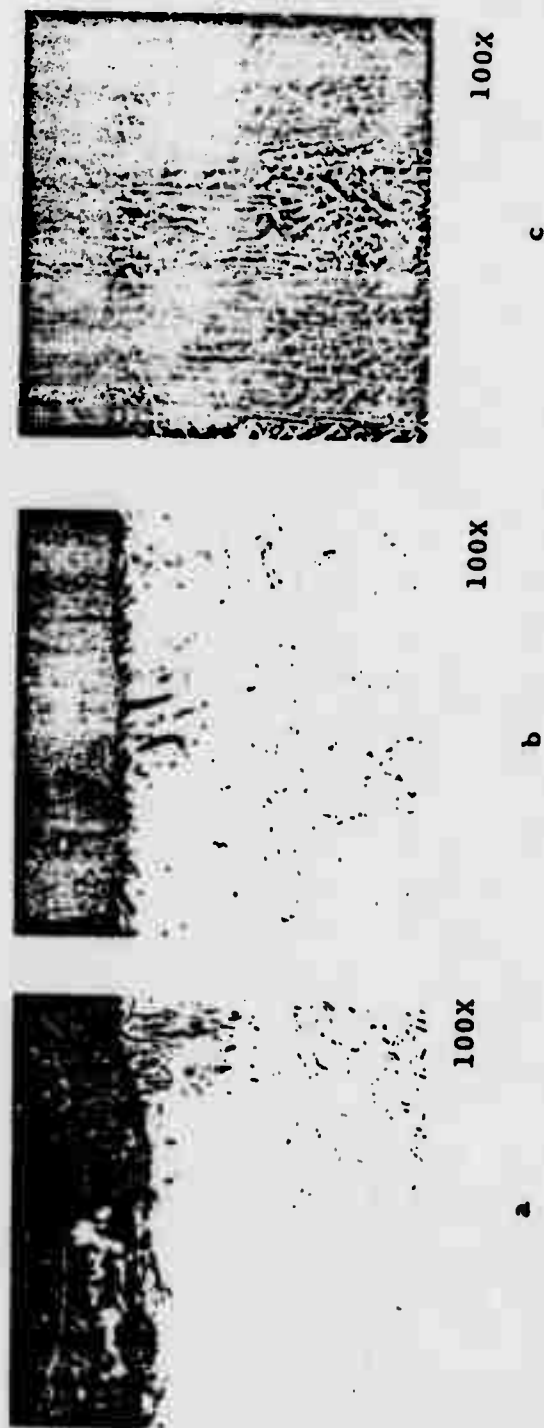


Figure 68. Surface Reaction of Alloy Ti-16Al-10Nb with (a) Zirconia, (b) Alumina and (c) Graphite Mold Materials

- Only electro-chemical methods are capable of producing a sound and stable condition in the alloy Ti-16Al-10Nb. More severe machining or finishing operations not only produce surface cracking but may also produce surface structural instabilities on exposure to elevated temperatures. Improved machinability and possibly surface stability are exhibited by alloys with improved ductility at low temperatures.
- Welding of the alloy Ti-16Al-10Nb is possible if sections are preheated to $\sim 700^{\circ}\text{F}$. The starting structure of the material may also be critical.
- Castability of aluminide alloys appears to be similar to conventional titanium alloys. Electron beam melting only offers minor advantages over conventional melting methods, low superheat is mandated by the loss of aluminum from melts.
- Although successful brazing methods have been established, it is considered that joining by diffusion bonding or welding are preferable joining methods, if the joint is to be exposed to elevated temperatures.

V. REFERENCES

1. Kornilov, I.I., Metallides, A New Base for Heat-Resistant Materials, Book: Structure and Properties of Heat Resistant Metal Materials (strukvura: Svoystba Zharo-prochynkh Metallicheskih Materialov), Moscow, Narka, 1967.
2. Nartova, T.T., Properties of Alloys Based on the Aluminide Ti_3Al , Poroshkovaya Metallurgiya, No. 8 (44), pp. 43-48, 1966.
3. McAndrew, J.B. and Kessler, H.D., Ti-36 Pct Al as a Base for High Temperature Alloys, Trans AIME: Volume 206, pp. 1348-1353, 1956.
4. Crossley, F.A., "Titanium-Rich End of the Titanium-Aluminum Equilibrium Diagram", Trans AIME, Volume 235, No. 8, p. 1174, 1966.
5. Blackburn, M.J., The Ordering Transformation in Titanium: Aluminum Alloys Containing up to 25 at. pct. Aluminum, Trans AIME, Volume 239, pp. 1200-1208, 1967.
6. Gehlen, P.C., The Crystallographic Structure of Ti_3Al , The Science of Technology and Application of Titanium, Eds. R.I. Jaffee and N.E. Promisel, Pergamon Press, pp. 349-357, 1970.
7. (a) Blackburn, M.J. and Williams, J.C., Transformation in Ti_3Al plus Niobium Alloys, Presented at Order Disorder Transformations in Alloys, Tabinger, Germany, September, 1973.
(b) Lipsitt, H.A. and Sastry, S.M.L., Ordering Transformation and Mechanical Properties of Ti_3Al and Ti_3Al-Nb Alloys, Met. Trans., Volume 8A, p. 1543, 1977.
8. Williams, J.C. and Blackburn, M.J., The Structure, Mechanical Properties and Deformation Behavior of Ti-Al and Ti-Al, Published in Ordered Alloys, F.D.B.H. Kear, C. Sims, N. Stoloff and H.H. Westbrook, Claistor Press, Baton Rouge, p.p. 425-445, 1970.
9. Lipsitt, H.A. and Shectman, D., Mechanical Properties of Ti_3Al , to be published in Met. Trans.
10. Hoch, M. and Gegel, H., Structure and Properties of Ti-Al-Ga Alloys, Paper presented at 1969 Fall Meeting AIME.

11. Godden, M.J. and Roberts, W.N., Ductility of Ti-Al-Ga Alloys, Second International Conference on Titanium, Cambridge, Massachusetts, May 2-5, 1972.
12. Prinzback, F. and Winter, H., Structure and Creep Properties of Ti-NbAl₃ Base Alloys, Titanium Alloys, Ed. Promisel and R.I. Jaffee, Pergamon Press, p. 875, 1970.
13. Nartova, T.T. and Sopochkin, G.G., Study of Phase Equilibrium of Alloys of the Ti-Al-Nb Ternary System, Novyy Konstruktivnyy Material-Titanium, pp. 19-23, 1972.
14. Hamajima, T., Luetjering, G. and Weissmann, S., Micro-Structure and Phase Relations for Ti-Mo-Al Alloys, Met. Trans., Volume 3, pp. 2805-2810, 1972.
15. Bohm, H. and Lahberg, K., The Ti-Al-Mo System, Z Metallk, Volume 49, p. 135, 1958.
16. Buehler, W.J. and Wiley, R.C., Trans ASM, Volume 55, p. 268, 1962.
17. Schulson, E.M., The Tensile and Corrosion Behavior of Ordered Zr₃Al-Base Alloys, Journal Nuclear Metals, Volume 20, p. 206, November, 1973.
18. Machlin, E.G., Pair Potential Model of Intermetallic Phases, ACTA Metallurgica, Volume 22, p. 109, 1974.